



UNIVERSITÀ  
DEGLI STUDI  
DI PADOVA

Sede Amministrativa: Università degli Studi di Padova

Dipartimento di Scienze del Farmaco

---

**SCUOLA DI DOTTORATO DI RICERCA IN SCIENZE FARMACOLOGICHE**  
**INDIRIZZO FARMACOLOGIA MOLECOLARE E CELLULARE**  
**CICLO XVIII**

**INNOVATIVE STRATEGIES FOR THE PERSONALIZATION  
OF THE THERAPY IN CANCER PATIENTS**

**FROM PHARMACOGENETICS TO THERAPEUTIC DRUG MONITORING: DIFFERENT  
APPROACHES FOR OPTIMIZING THE CHEMOTHERAPY DOSING**

**Direttore della Scuola:** Ch.mo Prof. Pietro Giusti

**Coordinatore d'indirizzo:** Ch.mo Prof. Pietro Giusti

**Supervisore:** Ch.mo Prof. Pietro Giusti

**Supervisore esterno:** Dott. Giuseppe Toffoli

**Dottoranda:** Luciana Giodini



*Alla mia famiglia*



*Questo lavoro di tesi è stato svolto presso la scuola di dottorato in Scienze Farmacologiche, indirizzo Farmacologia Cellulare e Molecolare dell'Università degli Studi di Padova, diretta dal Prof. Pietro Giusti in collaborazione con la Struttura Operativa Complessa di Farmacologia Sperimentale e Clinica del Centro di Riferimento Oncologico di Aviano (Istituto di ricerca e cura a carattere scientifico), diretta dal Dott. Giuseppe Toffoli.*



# CONTENTS

<b>ABSTRACT</b>	
<b>RIASSUNTO</b>	
<b>1.INTRODUCTION</b>	<b>1</b>
1.1.CHEMOTHERAPY: FROM CYTOTOXIC AGENTS TO TARGET THERAPY	1
1.2.CHEMOTHERAPY DOSING: THE CURRENT PRACTICE	2
1.3.CHEMOTHERAPY DOSING: THE INNOVATION OF THE PERSONALIZED THERAPY	5
1.4.INNOVATIVE APPROACHES FOR THE PERSONALIZATION OF THE CHEMOTHERAPY DOSING	9
1.4.1. PHARMACOGENETICS STRATEGY	10
1.4.1.1.PGx STRATEGY: THE CASE OF FLUOROPYRIMIDINE	14
1.4.1.2.PGx STRATEGY: THE CASE OF IRINOTECAN	20
1.4.2.THERAPEUTIC DRUG MONITORING STRATEGY	26
1.4.2.1.TDM STRATEGY: THE CASE OF SUNITINIB	27
<b>2.RATIONALE</b>	<b>32</b>
<b>3.AIMS</b>	<b>34</b>
<b>4.MATERIAL AND METHODS</b>	<b>36</b>
4.1.FLUOROPYRIMIDINE PROJECT	36
4.1.1.PATIENTS CHARACTERISTICS	36
4.1.2.MOLECULAR ANALYSES	37
4.1.3. METHODOLOGIES FOR POLYMORPHISMS ANALYSIS	40
4.1.4.CLINICAL DATA COLLECTION AND ELABORATION	50
4.1.5.STATISTICAL ANALYSIS	51
4.2. SUNITINIB PROJECT	53
4.2.1.HIGH PERFORMANCE LIQUID CHROMATOGRAPHY COUPLED WITH MASS SPECTROMETRY METHOD	53
4.2.2.DEVELOPMENT OF A BIOANALYTICAL METHOD	56
4.2.3.VALIDATION OF A BIOANALYTICAL METHOD	59
4.3. IRINOTECAN PROJECT	65
4.3.1. PATIENTS CHARACTERISTICS	65
4.3.2. DRUG ADMINISTRATION, DOSE ESCALATION AND DLT/MTD DEFINITIONS	66
4.3.3.PHARMACOKINETICS STUDIES	68
4.3.4.PHARMACOKINETICS PARAMETERS	69
<b>5.RESULTS</b>	<b>72</b>
5.1.FLUOROPYRIMIDINE PROJECT	72
5.1.1.PATIENTS CHARACTERISTICS	72
5.1.2.CLINICAL DATA MANAGEMENT	75
5.1.3.GENOTYPING RESULTS	76
5.1.4.CLINICAL VALIDITY OF <i>DPYD</i> SNPs FOR THE PREDICTION OF SEVERE TOXICITY	77
5.1.5.PREDICTIVE POWER OF THE PHARMACOGENETIC TESTS	81
5.2.SUNITINIB PROJECT	83
5.2.1-STUDY ON THE E/Z ISOMERIZATION	83
5.2.2.HPLC-MS/MS CONDITIONS	89
5.2.3. METHOD VALIDATION	92

5.3.IRINOTECAN PROJECT	97
5.3.1.PATIENTS CHARACTERISTICS	97
5.3.2. COLLECTION AND STORAGE OF THE SAMPLES	97
5.3.3.PHARMACOKINETICS ANALYSIS	98
<b>6.DISCUSSION</b>	<b>102</b>
6.1.FLUOROPIRIMIDINE PROJECT	103
6.2.SUNITINIB PROJECT	107
6.3.IRINOTECAN PROJECT	112
<b>7.REFERENCES</b>	<b>115</b>
<b>APPENDIX 1</b>	<b>127</b>
<b>APPENDIX 2</b>	<b>131</b>





# ABSTRACT

## Background

Most of the chemotherapeutic agents are characterized by a low therapeutic index and significant variability in therapeutic and toxic effects.

For this reason, many efforts have been made to optimize the dosage and the administration of antineoplastic drugs in order to obtain a maximal anti-tumor effect with acceptable levels of toxicity.

The recent progresses in the cancer field introduced the concept of personalized therapy with the aim of tailoring medical treatment to the individual characteristics and needs of the single patient.

The personalization of the dosage could be obtained with different approaches depending on the molecular peculiarities of each drug and on the genetic characteristics of the patients.

In particular, in this thesis two different strategies were applied to optimize the chemotherapeutic treatment with fluoropyrimidines, irinotecan, and sunitinib.

The first strategy concerns a pharmacogenetics approach with the purpose of optimizing the fluoropyrimidines and the irinotecan dosage based on genetic biomarkers predictive of severe toxicities.

Regarding the fluoropyrimidines, the aim of the study was to introduce, in the clinical practice, a pre-treatment test for polymorphisms (SNPs) within the *DYPD* gene, able to predict the development of severe toxicities related to these drugs.

Furthermore, a genotype-driven phase Ib study was designed to optimize the irinotecan dosage: according to *UGT1A1\*28* genotype, the dosage of irinotecan was chosen for metastatic colorectal cancer (mCRC) patients treated with FOLFIRI (fluorouracil in association with irinotecan) plus cetuximab regimen.

In addition to this, another treatment tailoring strategy was applied, that is the therapeutic drug monitoring (TDM) of sunitinib. This approach aimed to monitor the plasmatic drug concentration in order to maintain it within the therapeutic window.

## Aims

- ✓ **Fluoropyrimidines project:** a retrospective study was designed with the aim of validating the specificity of three *DYPD* SNPs in predicting the occurrence of severe toxicity events in a large set of oncological patients. The secondary aim of this study was to evaluate whether the additional testing of other investigational *DYPD* variants could increase the pharmacogenetic test

sensitivity.

- ✓ **Irinotecan project:** a phase 1b study was designed with three principal aims: 1) to define the Maximum Tolerated Dose (MTD), administered in the FOLFIRI regimen plus cetuximab in mCRC patients treated as first-line chemotherapy according to *UGT1A1\*28* genotype; 2) to evaluate the variability of irinotecan pharmacokinetics (PK), in combination with cetuximab, in patients with \*1/\*1 and \*1/\*28 genotype and the effect of the PK profile on toxicity and response rate; 3) to evaluate a possible effect of cetuximab on the PK of irinotecan.
- ✓ **Sunitinib project:** the project aimed to develop and validate, according to the FDA guidelines, an analytical method for the quantification of sunitinib and its main metabolite, N-desethyl sunitinib.

## **Methods**

Each project of this thesis considered the application of different methodologies depending on the characteristic of the study.

The methods for SNPs genotyping performed for the pharmacogenetic analysis were set up and developed using three different methodologies: Pyrosequencing, TaqMan® Allelic Discrimination Assay, and automated direct sequencing.

Regarding the PK analyses and the TDM approach, two HPLC-MS/MS methods were applied.

## **Results**

- ✓ **Fluoropyrimidines project:** data from this study demonstrated the clinical validity and specificity of the three *DPYD* SNPs genotyping test to prevent FL-related Grade ≥3 toxicity and to preserve treatment compliance, and support its introduction in the clinical practice.
- ✓ **Irinotecan project:** at the moment, one patient was enrolled in this study. The PK of the enrolled patient was followed during the days 1-3 and the days 15-17. The main PK parameters of CPT-11 and its metabolites of the first patient enrolled were calculated through a non-compartmental analysis.
- ✓ **Sunitinib project:** the method was setup and validated for the quantification of sunitinib and its main metabolite with a diagnostic perspective. The obtained method resulted easy, rapid and feasible for the clinical routine.

## **Conclusions:**

The different approaches described in this PhD thesis shared the same final aim: to translate the research results in the clinical practice and, consequently, to ameliorate cancer patients' life. In this perspective, the results of this thesis strongly encourage the introduction of the personalized therapy in the cancer field, where the optimization of the chemotherapy dosing is a compelling need.

# RIASSUNTO

## Introduzione

La maggior parte degli agenti chemioterapici è caratterizzata da un basso indice terapeutico e da una elevata variabilità inter paziente sia nella risposta alla terapia che nello sviluppo di tossicità.

Per questo motivo, la comunità scientifica ha investito molto nell'ottimizzazione del dosaggio dei chemioterapici con il fine ultimo di ottenerne la massima efficacia con accettabili livelli di tossicità.

A tal proposito, i recenti progressi nel campo della medicina oncologica hanno portato all'introduzione del concetto di terapia personalizzata. Tale approccio propone di individuare il giusto trattamento per ogni singolo individuo, basandosi sulle sue caratteristiche e necessità.

La personalizzazione della terapia chemioterapica può essere ottenuta tramite diversi approcci che dipendono sia dalle proprietà e caratteristiche molecolari del farmaco sia dalle peculiarità del singolo paziente. Questo lavoro di tesi si inserisce in questo filone di ricerca. In particolar modo, sono stati perseguiti due diversi approcci al fine di ottimizzare il trattamento con fluoropirimidine, irinotecano e sunitinib.

Il primo approccio selezionato si basa sull'applicazione delle conoscenze ottenute dalla farmacogenetica, disciplina che ha lo scopo di identificare il ruolo di varianti genetiche, polimorfismi (SNP), nella risposta al trattamento in termini sia di efficacia che di rischio di sviluppo di tossicità. In tale fase, la potenzialità dell'utilizzo di SNP predittivi di tossicità grave è stata studiata per migliorare il dosaggio di fluoropirimidine ed irinotecano.

Nel caso delle fluoropirimidine è stato disegnato uno studio retrospettivo con lo scopo di definire la validità clinica di un test genetico pre-trattamento per alcuni SNP nel gene della *DPYD* al fine di valutare la capacità di questo test di predire lo sviluppo di tossicità gravi correlate a tale tipo di trattamento. Lo scopo di questo studio è di introdurre nella pratica clinica tale test al fine di migliorare la qualità di vita dei pazienti cui vengono somministrati questi farmaci.

Un'altra applicazione delle conoscenze della farmacogenetica analizzata in questa tesi è rappresentata dagli studi di fase Ib basati sul genotipo, strategia che è stata perseguita per ottimizzare il dosaggio dell'irinotecano. Più in dettaglio, la massima dose tollerata (MTD) di tale farmaco è stata valutata in base al polimorfismo *UGT1A1\*28* in pazienti con cancro metastatico al colon retto trattati con il regime FOLFIRI (5-fluorouracile associato con irinotecano) e cetuximab.

Infine, un'altra strategia che riguarda la personalizzazione della terapia è rappresentata dal

monitoraggio terapeutico del farmaco (TDM). Questo approccio è stato applicato per il sunitinib in modo da monitorarne le concentrazioni plasmatiche e mantenerle all'interno di una finestra terapeutica.

## **Scopo**

- ✓ **Fluoropirimidine:** è stato disegnato uno studio retrospettivo con il fine ultimo di validare la specificità di tre SNP della *DPYD* nel predire l'insorgenza di tossicità grave in un'ampia casistica di pazienti oncologici. Scopo secondario di questo studio è stata quella di valutare se l'analisi di altre varianti del gene della *DPYD* possano migliorare la sensibilità del test farmacogenetico.
- ✓ **Irinotecano:** è stato disegnato uno studio di fase 1b con i seguenti scopi: 1) definire la MTD, in base al genotipo *UGT1A1\*28*, in pazienti metastatici con tumore al colon retto trattati con regime FOLFIRI associato a cetuximab; 2) valutare la variabilità dei parametri farmacocinetici dell'irinotecano, in combinazione con cetuximab, in pazienti con genotipo *UGT1A1\*1/\*1* e *UGT1A1\*1/\*28* e analizzare il possibile effetto del profilo farmacocinetico sulla tossicità e risposta; 3) stabilire se il cetuximab ha un effetto sulla farmacocinetica dell'irinotecano.
- ✓ **Sunitinib:** lo scopo di questo progetto è lo sviluppo e la validazione, in base alle linee guida rilasciate dalla *Food and Drug Administration* (FDA), di un metodo bioanalitico per quantificare sia il sunitinib sia il suo metabolita attivo, N-desetil sunitinib.

## **Materiali e metodi**

In base agli scopi e alle peculiarità dei singoli progetti di questa tesi sono state applicate specifiche metodiche.

I metodi messi a punto ed utilizzati per le analisi farmacogenetiche sono i seguenti: pyrosequencing, saggio Taqman per la discriminazione allelica e sequenziamento diretto automatizzato.

Per quanto riguarda invece le analisi di farmacocinetica sono stati utilizzati due metodi in HPLC-MS/MS, uno dei quali, il metodo del sunitinib, è stato messo a punto e validato secondo le linee guida FDA.

## **Risultati**

- ✓ **Fluoropirimidine:** i dati ottenuti da questo studio hanno dimostrato la validità clinica e la specificità del test farmaco genetico pre-trattamento basato sulla *DPYD* per prevenire l'insorgenza di tossicità gravi di grado  $\geq 3$ . Tali risultati incoraggiano l'introduzione di questo test nella pratica clinica.
- ✓ **Irinotecano:** al momento una sola paziente è stata ritenuta eleggibile secondo i criteri dello studio. La farmacocinetica di CPT-11 e dei suoi principali metaboliti è stata descritta grazie a prelievi ripetuti durante la prima (giorni 1-3) e la seconda (giorni 15-17) somministrazione. Sono stati inoltre calcolati i principali parametri farmacocinetici di CPT-11 e dei suoi metaboliti tramite l'applicazione di un'analisi non compartmentale.
- ✓ **Sunitinib:** il metodo per la quantificazione del sunitinib e del suo metabolita attivo è stato messo a punto e validato. Considerata la facilità e la rapidità di tale analisi , si può auspicare che tale metodo possa essere facilmente applicabile nella pratica clinica.

## **Conclusioni**

Gli approcci descritti in questa tesi condividono lo stesso scopo finale: traslare, cioè, i risultati della ricerca nella pratica clinica e, di conseguenza, migliorare la vita dei pazienti oncologici. In questa ottica, i risultati di questo lavoro incoraggiano fortemente l'introduzione di una terapia personalizzata nel campo oncologico, dove urge la necessità di nuovi approcci per ottimizzare il dosaggio dei farmaci.





# 1. INTRODUCTION

## 1.1. CHEMOTHERAPY: FROM CYTOTOXIC AGENTS TO TARGET THERAPY

Oncology has become one of the major focus area also for pharmaceutical and biotechnology companies. In 2009, about 16000 of the 40000 Phase I, II, III trials listed on ClinicalTrials.gov were related to cancer treatment ([www.clinicaltrials.gov](http://www.clinicaltrials.gov)). Such large interest stems from the need to improve treatments for multiple types of cancer. Although giant steps have been made from the first attempts with mustard compound of Alfred Gilman and Louis Goodman <sup>1</sup>, the scientific community has a long way to go in finding the right drugs to overwhelm this disease.

The early history of oncology was characterized by the development of cytotoxic drugs. Because of their promising results, drugs such as methotrexate and 5-fluorouracil (5-FU) triggered enthusiasm among clinicians in the post-war period and, up to these days, they still remain a pillar in the therapy of malignant diseases <sup>2,3</sup>. Even if more selective therapies have been developed (e.g. antibodies or molecular targeting agents), treatment schemes with some of these new drugs continue to be associated with classical cytotoxic agents <sup>4</sup>. Moreover, cytotoxic agents are also used as a support to either surgery or radiotherapy.

Even if nowadays the molecular targets of most of the drugs in clinical use have been clarified <sup>5</sup>, cytotoxic chemotherapy drugs damage proliferating cells and therefore the non-specificity of cytotoxic agents is their major drawback. Potential damage of normal tissues means that a cure with these chemotherapeutic agents is not often achieved <sup>6</sup>.

Over the last 10–30 years, new molecularly targeted agents have been discovered and showed great promise in the treatment of some diseases, such as gastrointestinal stromal tumors and chronic myeloid leukemia <sup>7</sup>. This new era of cancer therapy has emerged leading to treatment in association with cytotoxic agents for an improved effect and, for several cancers, even moving away from nonspecific chemotherapy to chronic oral treatment with targeted molecular therapies <sup>7</sup>. These treatments are characterized by unique mechanisms of action and are highly specific for single or multiple key cellular biological pathways implicated in the cancer process.

These therapeutic agents are now revolutionizing cancer treatment by transforming a few previously deadly malignancies into chronically manageable conditions.

However, these new molecules present new challenges represented, for example, by their oral administration<sup>8</sup>. In fact, whilst on the one hand the oral administration is certainly associated with a better patient's quality of life and compliance, on the other hand it generates a complex step in their pharmacokinetics (PK), especially in the phase of drug absorption<sup>8</sup>. In addition, poor tolerability and therapeutic failure are unfortunately common, and relapse is a nearly inevitable consequence of treatment interruption<sup>9,10</sup>. Moreover, this shift to targeted agents is creating new paradigms in cancer care, with drug adherence becoming a more critical issue with increased numbers of oral chemotherapeutics<sup>11</sup>.

Briefly analyzing the history of anticancer drugs discovery, many efforts have been made in order to obtain more efficient, compelling, and competitive molecules. However, both traditional cytotoxic drugs and new target therapy show, as aforementioned a complex PK profile, associated with an intrinsic difficulty in optimizing their dosage also due to the huge inter-patient variability. As cancer treatment has become increasingly complex, the challenge for clinicians and scientists now is to manipulate treatments to maximize benefit and minimize harm for the individual patient. For this reason, huge efforts have to be done in order to refine the treatments and to personalize the therapy.

## **1.2. CHEMOTHERAPY DOSING: THE CURRENT PRACTICE**

Most of the chemotherapeutic agents are characterized by a low therapeutic index and significant variability in therapeutic and toxic effects.

For this reason, many efforts have been made to optimize the dosage and the administration of antineoplastic drugs in order to obtain a maximal anti-tumor effect with acceptable levels of toxicity. In order to develop robust dose strategies, it is necessary to know tools able to predict clinical effects of a drug by direct or indirect measurements.

In the last 50 years, optimal chemotherapy dosing, established through clinical trials, has been generally calculated using a patient's body surface area (BSA), which takes into account body weight and height. The first scientific findings that validated this kind of practice was obtained in 1883 when it was discovered that small animals utilized relatively more oxygen and produced relatively more heat than larger animals. These findings could be explained because smaller animals have relatively larger surface areas per unit mass, when compared with larger animals<sup>12</sup>.

These observations were confirmed and applied to humans, giving rise to the practice of expressing human basal metabolism in terms of BSA rather than body weight (BW).

Prompted by publications by Pinkel<sup>13</sup> and Freireich and colleagues<sup>14</sup>, the scientific community allowed the incorporation of the BSA formula into allometric studies with animals. In the 1950s, BSA-based dosing was introduced to extrapolate human chemotherapy doses from animals studies in order to conduct phase I studies and to determine patients' dosing. After that, many pediatricians started using BSA for anti-cancer drug dosing, and medical oncologists followed them<sup>13</sup>.

By correcting for BSA, it was generally assumed that cancer patients would receive a dose of a particular cytotoxic drug associated with an acceptable degree of toxicities without reducing the agent's therapeutic effect.

The customary approach in clinical practice is to calculate BSA using Du Bois and Du Bois'<sup>15</sup> height-weight formula: Area (cm<sup>2</sup>) = BW (kg) 0.425 x height (cm) 0.725 x 71.84.

More recently, doubts have arisen to the real effects of BSA on the pharmacokinetics of antitumor agents.

In fact, except for the inherent inaccuracies inherent in methods for BSA calculation (Du Bois estimated the maximal error as 5%), there is a substantial risk of arithmetical errors: errors in the use of dosage equations have been found indeed to account for more than 15% of medication prescribing errors. Moreover, it is to be noticed that in BSA dosing there are two calculation steps that may introduce errors. First, the patient's BSA has to be calculated, that is dependent on the accuracy of weight and height measurements, and then the dose for the obtained BSA is to be determined. The first calculation is often avoided, as it is common to use nomograms to estimate the BSA. This kind of models, usually contain three parallel scales graduated for different variables (in this case height, weight, and BSA) so that when a straight line connects values of any two, the related value may be read directly from the third at the point intersected by the line. However, the reliability of these nomograms also tends to differ<sup>16</sup>.

Moreover, in clinical practice, the calculated anticancer drug doses are also frequently manipulated by rounding to the nearest convenient dose<sup>17</sup>. Finally, for many cancer patients, body size will probably vary during the course of the disease, due to conditions such as cachexia and anorexia. Despite this, BSA is not always re-calculated between treatment cycles, although there are recommendations that BSA should be re-calculated when BW has changed by more than 5-10%<sup>18</sup>.

Furthermore, given the complexity of drug clearance, drug-related toxicity and anti-tumor activity, it is unlikely that only one factor such as BSA can be used to adjust the dosage. A lot of other factors can indeed influence the PK and PD of anti-tumor drug such as the organ functions, the presence of SNPs that can affect the enzymatic activity, the gender, the age, and the comorbidities (Figure 1). The resulting marked interpatient variability caused by all these factors is not considered by the BSA-dosing approach (Gurney 2001).

In particular, the inaccuracy of this system is clear if we bearing in mind the cancer drug elimination. Typically, there is a 4-10 fold inter-patient variation in cytotoxic drug clearance, due to different activity of drug elimination processes related to genetic and environmental factors (Gurney, 1996).

BSA-dosing does not account for these variations so, one possible consequence, is unexpected underdosing which leads to reduce effectiveness of chemotherapy<sup>19</sup>.

In conclusion, in order to overcome the BSA approach, the recent progresses in the cancer field introduced the concept of personalized therapy with the aim of tailoring medical treatment to the individual characteristics and needs of the single patient.

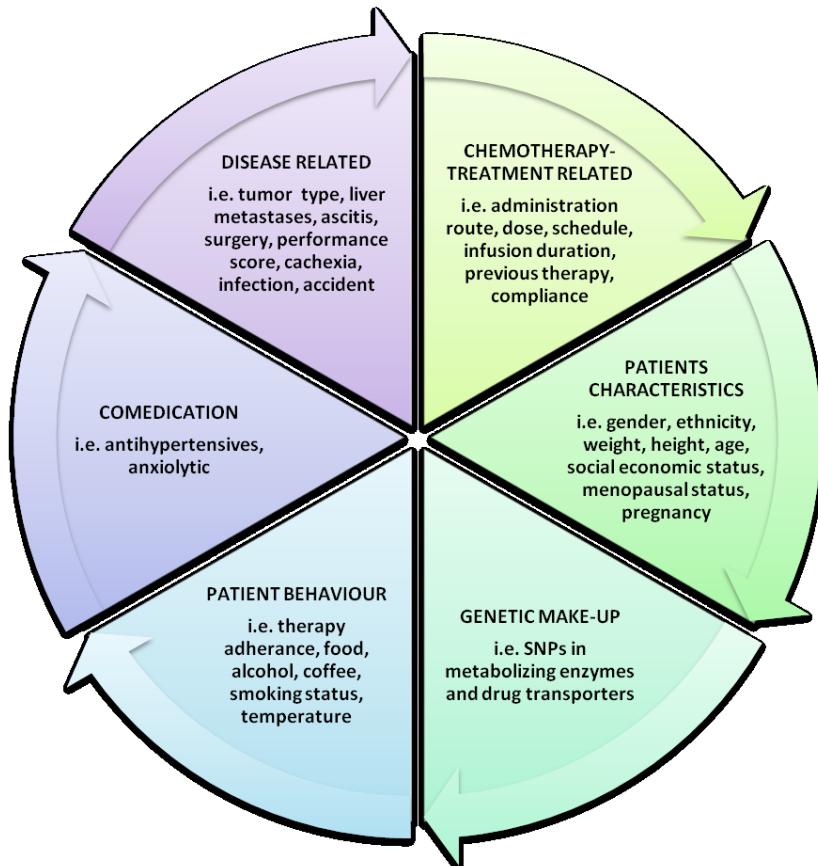


**Figure 1** Schematic summary of the main factors that can influence the systemic exposure to a drug.

### 1.3. CHEMOTHERAPY DOSING: THE INNOVATION OF THE PERSONALIZED THERAPY

*It is far more important to know what person the disease has than what disease the person has.* – Hippocrates

The clinical practice typical of the 20<sup>th</sup> century, based on the model “one dose fits all”, have shown, over the years, huge limitations that strongly compromised drug’s efficacy and dramatically underestimated the potentiality of several treatments.

In fact, every day millions of people take drugs that will not help them: numerous studies demonstrate that the obtained response rates can deeply vary among different therapeutic classes. For instance, the 75% of patients treated with anticancer drugs seems to have no benefits from the treatment and unfortunately for most of them it is caused by an unsuitable drug dosage (Figure 2). In addition, 2.2 millions adverse drug reactions occur each year in the US, including more than 100000 deaths.

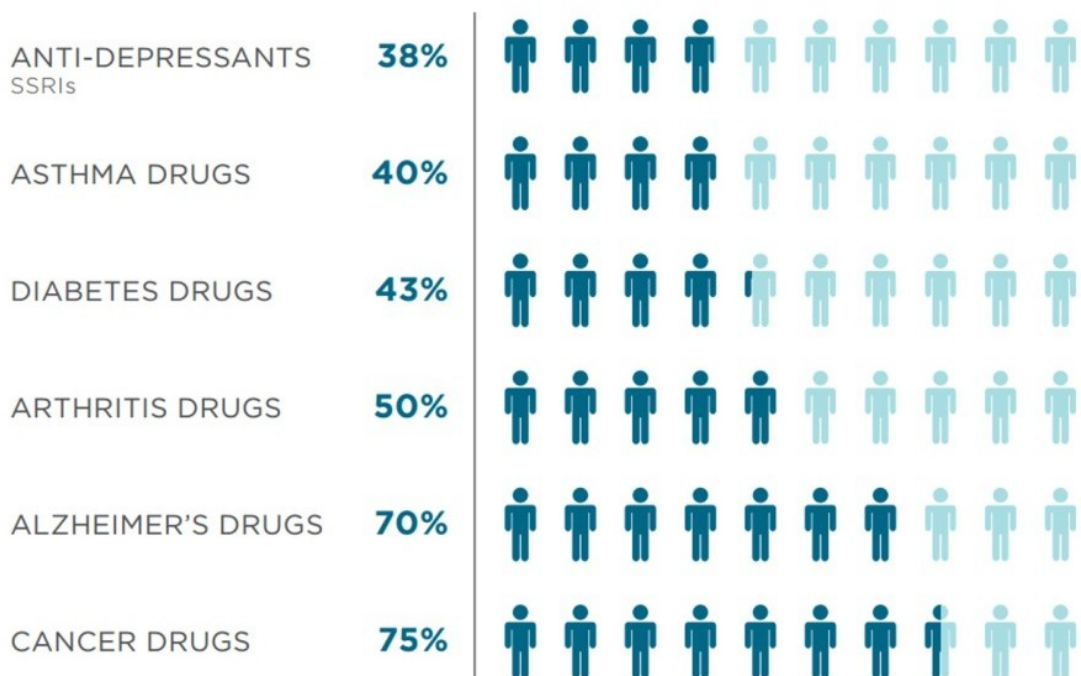


**Figure 2** Average percentage of the patient population for which a particular drug in a class is ineffective. From Spear et al., 2001 Clinical application of pharmacogenetics *Trends in Molecular Medicine*.

These data fuelled the discussion in the scientific community and dramatically changed the approach for the drug administration, moving from “one dose fits all” model and fostering the introduction of the “personalized medicine” model (Figure 3).

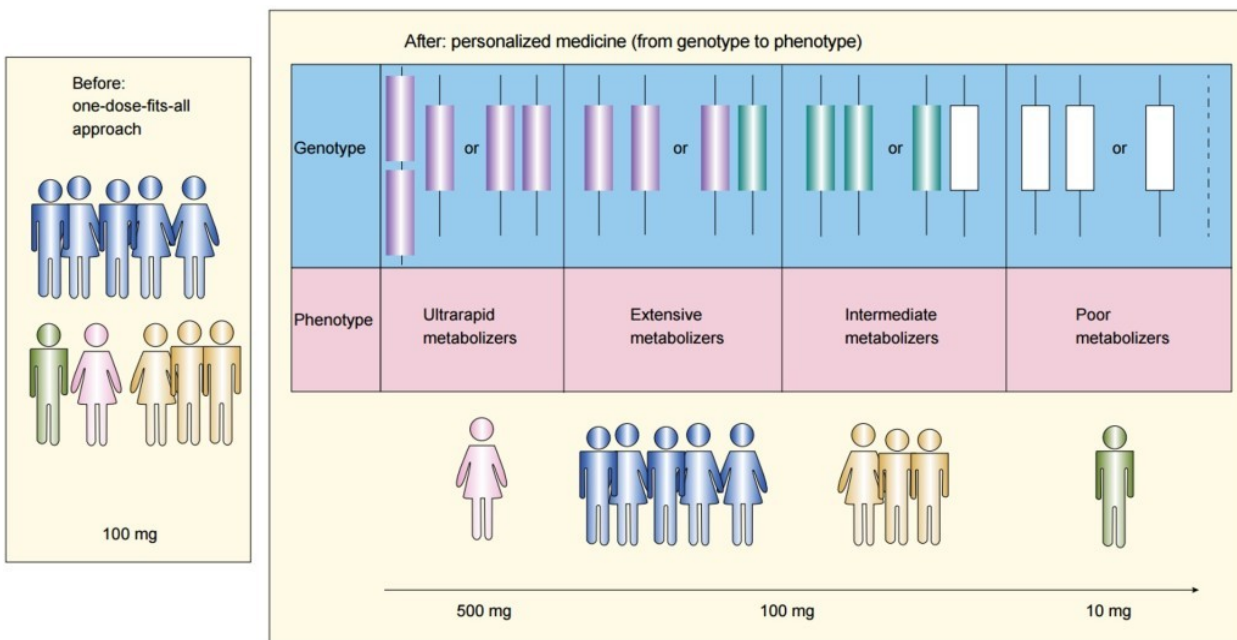


**Figure 3** Representation of the one-dose-fits-all approach versus personalized medicine. The left panel shows a situation in which everyone gets the same dose of a drug. The right panel shows a personalized medicine approach in which the dose of the drug is selected based upon the specific characteristics of the patients. (*Paving the Way for Personalized Medicine*, 2013).

In general, the term “personalized medicine” is often described as providing “the right patient with the right drug at the right dose at the right time.” More broadly, “personalized medicine” may be thought of as the tailoring of medical treatment to the individual characteristics, needs and preferences of a patient during all stages of care, including prevention, diagnosis, treatment and follow-up.

One of the earliest example of personalized therapy in the clinical practice could be found at the beginning of the 1900, when Reuben Ottenberg, for the first time, reported a blood compatibility test for transfusion using blood typing techniques and cross-matching between donors and patients to prevent hemolytic transfusion reactions.

Another famous example is the discovery, in 1956, of the genetic bases for the selective toxicity of fava beans (“favism”) and the antimalarial drug primaquine that could be led back to a deficiency in the metabolic enzyme, glucose-6-phosphate dehydrogenase (G6PD).

A more recent example is the finding that cytochrome P450 2D6, a polymorphic metabolizing enzyme, is identified as the culprit for causing some patients to experience an “overdose” or exaggeration of the duration and intensity of the effects of debrisoquine, a drug used for treating hypertension<sup>20</sup>.

From here, major advancements in science and technology have allowed healthcare decisions to move on the “trial-and-error” approach and to set in motion the transformation of personalized medicine from an idea to a practice.

Midway through the century, observations of individual differences in response to drugs gave rise to a body of research focused on identifying key enzymes that play a role in variation in drug handling and response and that served as the foundation for pharmacogenetics (PGx). More recently, rapid developments in genomics, together with advances in a number of other areas, such as computational biology, medical imaging, and regenerative medicine, are creating the possibility for scientists to develop tools to personalize diagnosis and treatment.

Several definitions of personalized therapy have been written with the purpose of describing such a complex and multidisciplinary field. The National Cancer Institute (NCI) has defined personalized medicine “[...] as a form of medicine that uses information about a person’s genes, proteins and environment to prevent, diagnose and treat disease”<sup>21</sup>. Another definition of personalized medicine has been described by the US President's Council of Advisors on Science and Technology as referring to “[...] the tailoring of medical treatment to the individual characteristics of each patient; to classify individuals into subpopulations that differ in their susceptibility to a particular disease or their response to a specific treatment so that preventive or therapeutic interventions can then be concentrated on those who will benefit, sparing expense and side effects for those who will not.”<sup>22</sup>.

As these definitions suggested, this issue is extremely wide and different points of view can highlight several facets of the same phenomenon.

In fact, several terms, including “precision medicine,” “stratified medicine,” “targeted medicine,” and “pharmacogenomics,” are used interchangeably and each of them better describe one particular aspect of the personalized medicine. The National Academy of Sciences (NAS) has defined “Precision medicine” as “the use of genomic, epigenomic, exposure and other data to define individual patterns of disease, potentially leading to better individual treatment.” “Stratification” refers to the division of patients with a particular disease into subgroups, based on a characteristic of some sort, who respond more frequently to a particular drug or, alternatively, are at decreased risk of side effects in response to a certain treatment. Stratification can be thought of as a core element of personalized medicine. PGx – the study of variations of DNA and

RNA characteristics as related to drug response – is a critically important area of personalized medicine where significant progresses have recently been made.

Oncology is one of the branches of medicine that strongly need the adoption of the personalized medicine due to the complexity of the disease and to its lethality. In 2016 about 1,685,210 new cancer cases are expected to be diagnosed in US and about 595,690 Americans are expected to die of cancer <sup>23</sup>. In January 2015, the American President Barack Obama launched a national Precision Medicine Initiative, founding it with 215 million dollars, aiming at promoting the introduction of personalized medicine concepts into the clinical practice, with a special focus on oncology and genetics.

In fact, cancer has been tackled for decades with cocktails of chemotherapeutic drugs that indiscriminately hit populations of rapidly growing cells. However, this strategy is effective only up to a point. A large part of patients' treatment is indeed not only toxic but also ineffective: it is estimated that in only 25% of patients a response is achieved <sup>24</sup>.

The new hurdle, in this century, is to find the key genetic mutations that drive specifically cancer growth in order to optimize the use of the therapies already used in the clinical practice and to develop new personalized drugs (Figure 4).

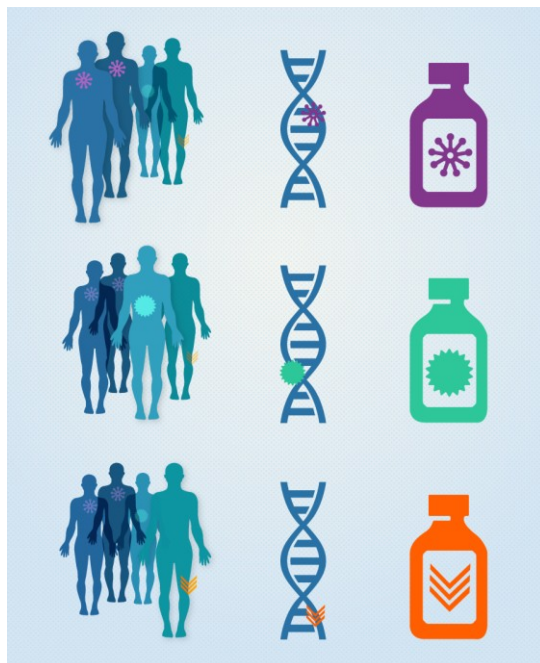


**Figure 4** Using the genetic changes in a patient's tumor to determine their treatment is known as precision medicine. ([www.cancer.gov.com](http://www.cancer.gov.com))

Genomic and proteomic technologies have made possible to subclassify different kinds of solid

tumors according to differences in gene sequence and/or expression patterns.

The development of imatinib against chronic myelocytic leukemia (CML) is the greatest success in the personalized cancer field so far<sup>25</sup>. In CML, a single molecular event, the 9:22 translocation, leads to expression of the Abelson proto-oncogene kinase ABL fused to BCR (breakpoint cluster region), yielding a constitutively activated protein kinase, BCR-ABL, and then the malignant phenotype. Imatinib attacks the unique and specific protein obtained with the BCR-ABL translocation, inducing clinical and molecular remissions in >90% of CML patients in the chronic phase of disease<sup>26</sup>.

Razelle Kurzrock, (the director of the Center for Personalized Cancer Therapy at the University of California, San Diego) has said about this discovery: "*In the 1980s, unless you got a bone-marrow transplant, the disease was an absolute death sentence in four to six years. Today, average survival is more than 20 years. And because the average age at diagnosis is 60, it's almost a normal life expectancy.*"

However, imatinib success has not been easy to duplicate and, despite the extraordinary advances that have been made till now, we have a long way to go in understanding why different individuals respond differently to treatment.

In fact, every tumor has a unique set of genetic mutations and this heterogeneity, which is found even among cells in a single tumor, means that matching a patient with the appropriate therapy can be a complex proposition.

## **1.4. INNOVATIVE APPROACHES FOR THE PERSONALIZATION OF THE CHEMOTHERAPY DOSING**

In this thesis, different innovative approaches were studied in order to obtain a personalized cancer therapy.

1. The first strategy concerns a PGx approach with the purpose to validate a personalized drug dosing based on specific patient genetic polymorphisms (SNPs) for two drugs.
  - i. The SNPs in *DPYD* will be validated in a retrospective large group of patients as predictive markers of severe **fluoropyrimidines (FLs)** related toxicity, to support current guidelines suggesting a dose reduction in variant alleles carriers.

ii. The analysis of *UGT1A1\*28* will be adopted to stratify patients in a genotype-driven phase Ib study to define, according to patient' genotype, the correct **irinotecan (CPT11)** dose to minimize the risk of treatment related toxicity.

The study described in this thesis is a genotype-driven phase Ib study: metastatic colorectal cancer (mCRC) patients treated with FOLFIRI regimen (5-FU in association with CPT-11) plus cetuximab will be stratified in subgroups associated with a personalized dosage according to *UGT1A1\*28* genotype.

2. The second strategy concerns the therapeutic drug monitoring (TDM) approach.

i. The TDM of **sunitinib** will be used for dose optimization in solid tumor patients. Specifically, drug plasmatic concentration will be supervised during the treatment in order to optimize the clinical outcome and minimize side effects .

#### **1.4.1. PHARMACOGENETICS STRATEGY**

PGx, the study of variations of DNA and RNA characteristics as related to drug response, is one of the most interesting areas of personalized medicine today. The field arises from the convergence of advances in pharmacology (the science of drugs) and genomics (the study of genes and their functions) and seeks to understand how differences in genes and their expression affect the body's response to medications. More specifically, PGx uses genetic information (such as DNA sequence, gene expression, and copy number variations) to explain interindividual differences in pharmacokinetics (PK)- and pharmacodynamics (PD) parameters, identifying responders and non-responders, and predicting the efficacy and/or toxicity of a drug.

Physiological variations within the human genome have a frequency of about 1 every 500±1000 bases. These affect the interindividual variability that is observed also in drug response and are the object of PGx. Although there are a number of different types of polymorphic markers, over the last years, the scientific community has focused on SNPs, and on the potentiality they offer in determining the individual drug response profile. Conventionally, a SNP is defined as a nucleotide variation having an allele frequency greater than 1%, whereas, when the frequency is lower, the genetic variation is indicated as mutation or as rare variant.

The 1.42 million known SNPs are found at a density of one SNP per 1.91 kilobases. This means that more than 90% of any stretches of 20 kilobases long sequence will contain one or more SNPs. The

density is even higher in gene containing regions<sup>27</sup>. In 2001, the International SNP Map Working Group estimated that they have identified 60,000 SNPs within genes ('coding' SNPs), or one coding SNP per 1.08 kilobases of gene sequence. Moreover, they have evaluated that 93% of genes contain SNPs, and 98% are located within 5 kilobases of a SNP. For the first time, nearly every human gene and genomic region was marked by a sequence variation<sup>27</sup>. After that, the National Center for Biotechnology Information (NCBI) established in 1998 the Single Nucleotide Polymorphism Database (dbSNP) (<http://www.ncbi.nlm.nih.gov/SNP>) in collaboration with the National Human Genome Research Institute (NHGRI). Since its inception in September 1998, dbSNP has served as a central, public repository for genetic variation.

The last update of the dbSNP website was in November 2015 and referred to 316,710,573 registered SNPs, 150,482,731 of them were found in *Homo Sapiens* ([http://www.ncbi.nlm.nih.gov/SNP/snp\\_summary.cgi](http://www.ncbi.nlm.nih.gov/SNP/snp_summary.cgi)). These projects (beyond dbSNP we can enumerate also 1Kgenome project, UCSC, ensemble among the most important ones) could lead to an innovative way to conceive drug administration. Using SNPs as predictive and prognostic biomarkers, it may possible to tailor drug prescription and drug dosage, with a great potential clinical impact in case of drugs characterized by a low therapeutic index such as those administered in oncology<sup>28-30</sup>.

Furthermore, the introduction of predictive and prognostic biomarkers in the clinical practice, enables to enhance quality of life for patients and to decrease overall health care costs<sup>31</sup>.

On one hand, predictive PGx biomarkers are usually SNPs located in genes that are direct targets of drugs, molecules involved in DNA repair, or in drug metabolism, and are specifically associated with the response to a therapy, that can be defined as the probability to have a response or as the risk to develop toxicities. Prognostic PGx biomarkers, on the other hand, predict the natural course of a specific disease and patients' outcome<sup>32</sup>. Examples of prognostic oncology markers are SNPs located in proteins involved in tumor cell proliferation, dedifferentiation, angiogenesis, invasion or metastasis.

Genetic testing represents one method to define these biomarkers. Typically, genetic testing will fall into one of three categories:

1. diagnostics: the evaluation of genetic sequences to confirm the presence of disease (often used for oncology monitoring);
2. prognostics: the evaluation of genetic mutations to determine susceptibility to a future

- condition (for example, cystic fibrosis genotype testing);
3. pharmacogenomics: the evaluation of genetic variations to identify patients likely to respond to a particular therapy (for example the mutations within *RAS* gene in colorectal cancer patients).

Although there has been substantial hype over the potential of genetic testing to improve medication use, the American Food and Drug Administration (FDA) has recommended only a few of them for therapeutic optimization and this provides valuable lessons as to the barriers to implementing “individualized” medicine. Several important PGx tests have been available from “Clinical Laboratory Improvement Amendments-approved laboratories” for many years, and yet their adoption in the clinic remains uncommon. Although there is a scarcity of evidence of clinical utility and cost-effectiveness with respect to many of the PGx tests, the evidence for a few of them is quite strong.

Surely, one barrier to clinical implementation of PGx is the lack of freely available, peer-reviewed, updatable, and detailed information about PGx biomarkers to be introduced into drug guidelines. For this reason, several international and national consortiums dedicated to PGx have risen and published drug dosing guidelines with indications and recommendations about drug-related genetic tests and their integration in the clinical routine.

Regarding the oncologic field, the main international consortiums that participated to the implementation of the dosing guidelines with PGx information are the Clinical Pharmacogenetics Implementation Consortium (CPIC) and the Dutch Pharmacogenetics Working Group of the Royal Dutch Association for the Advancement of Pharmacy (DPWG) that have published drug-specific guidelines based on patient genotype.

CPIC was formed in 2011 as a shared project between PharmGKB and the Pharmacogenomics Research Network, while The Royal Dutch Pharmacist’s Association (KNMP) established the DPWG in 2005. The DPWG is formed by a multidisciplinary team that includes clinical pharmacists, physicians, clinical pharmacologists, clinical chemists, epidemiologists, and toxicologists.

These consortiums provide guidelines that enable the translation of genetic laboratory test results into actionable prescribing decisions for specific drugs. These guidelines, indeed, were designed to help clinicians in understanding how available genetic test results should be used to optimize drug therapy. In the future, it is plausible that clinical high-throughput and pre-emptive genotyping could become more widespread.

Each guideline adheres to a standard format. Genes, drugs, and dosing recommendations are

categorized in each document. Specifically, each guideline contains an introduction summarizing the drug dosing that is addressed as a result of specific genotyping tests, a focused literature review, gene based information, and drug-based information. Table 1 provides an example of key data needed by clinicians: the assignment of likely phenotypes based on genotypes. Each guideline also includes dosing recommendations for drugs based on genotype/phenotype, along with a strength for each dosing recommendation, based on detailed levels of evidence graded as to its quality.

<b>Likely phenotype</b>	<b>Genotype</b>	<b>Examples of diplotypes</b>
<i>Homozygous wild type or normal, high activity (~ % of patients)</i>	An individual carrying two or more functional (*1) alleles	*1/*1
<i>Heterozygous or intermediate activity (~ % of patients)</i>	An individual carrying one functional allele (*1) plus one non-functional allele (*2, *_, *_)	*1/*2, *1/*2A, *1/*28
<i>Homozygous variant or deficient activity (~ % of patients)</i>	An individual carrying two non-functional alleles (*2, *_, *_)	*2/*2, *2A/*2A, *28/*28

**Table 1** Example of assignment of likely phenotype based on genotype.

The PGx guidelines available nowadays in the oncologic field regard 5-FU and its oral prodrug capecitabine (CAPE), CPT-11, mercaptopurine, tegafur, thioguanine, and tamoxifen (Table 2). The most updated information related to PGx dosing guidelines can be found on PharmGKB- The Pharmacogenomics Knowledgebase ([www.pharmgkb.org](http://www.pharmgkb.org))

<b>Drug</b>	<b>Consortium</b>	<b>Gene</b>	<b>Last update</b>
<i>capecitabine</i>	CPIC	<i>DPYD</i>	18/09/2015
	DPWG	<i>DPYD</i>	10/08/2011
<i>5-fluorouracil</i>	CPIC	<i>DPYD</i>	18/09/2015
	DPWG	<i>DPYD</i>	10/08/2011
<i>irinotecan</i>	PRO	<i>UGT</i>	03/06/2015
	DPWG	<i>UGT</i>	10/08/2011
<i>mercaptopurine</i>	CPIC	<i>TPMT</i>	18/09/2015
	DPWG	<i>TPMT</i>	10/08/2011
<i>tamoxifen</i>	DPWG	<i>CYP2D6</i>	10/08/2011
<i>tegafur</i>	CPIC	<i>DPYD</i>	18/09/2015
	DPWG	<i>DPYD</i>	10/08/2011
<i>thioguanine</i>	CPIC	<i>TPMT</i>	18/09/2015
	DPWG	<i>TPMT</i>	10/08/2011

**Table 2** List of the main anticancer drugs with PGx dosing guidelines (PharmGKB).

#### 1.4.1.1. PGx STRATEGY: THE CASE OF FLUOROPYRIMIDINE

FLs are antimetabolite drugs able both to inhibit biosynthetic processes and to be incorporated into macromolecules, such as DNA and RNA, hindering their normal function.

In particular, FLs are analogues of the uracil base and they cause the inhibition of the nucleotide synthetic enzyme thymidylate synthase (TS), responsible of the *de novo* synthesis of thymidylate, which is necessary for DNA replication and repair<sup>33</sup>.

FLs include 5-FU, CAPE, and tegafur. CAPE is an oral FL that is absorbed unchanged through the gastrointestinal wall and is converted to 5'-deoxy-5-fluorouridine (5'-dFUR) in the liver by the sequential action of carboxylesterase and cytidine deaminase. Tegafur is another prodrug administered *per os* that is enzymatically activated in the liver to 5'-hydroxytegafur and subsequently to 5-FU (Figure 5).

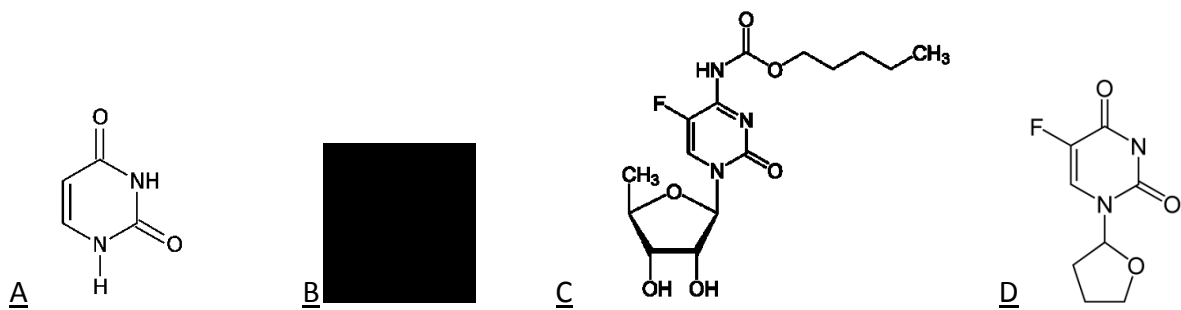


**Figure 5** Chemical structures of uracil (A), 5-fluorouracil (B), capecitabine (C), and tegafur (D).

Regarding the mechanism of action of 5-FU, it is an analogue of uracil with a fluorine atom at the C-5 position in place of hydrogen. For this reason, it can rapidly enter the cells using the same facilitated transport mechanism of uracil <sup>34</sup>. 5-FU is converted intracellularly into several active metabolites such as fluorodeoxyuridine monophosphate (FdUMP), fluorodeoxyuridine triphosphate (FdUTP), and fluorouridine triphosphate (FUTP), which lead to RNA synthesis disruption and the inhibition of the TS (Figure 6).

In fact, the 5-FU metabolite FdUMP binds to the nucleotide-binding site of TS, forming a stable ternary complex with the enzyme and CH<sub>2</sub>THF, thereby blocking binding of the normal substrate dUMP and inhibiting dTMP synthesis <sup>35</sup>.

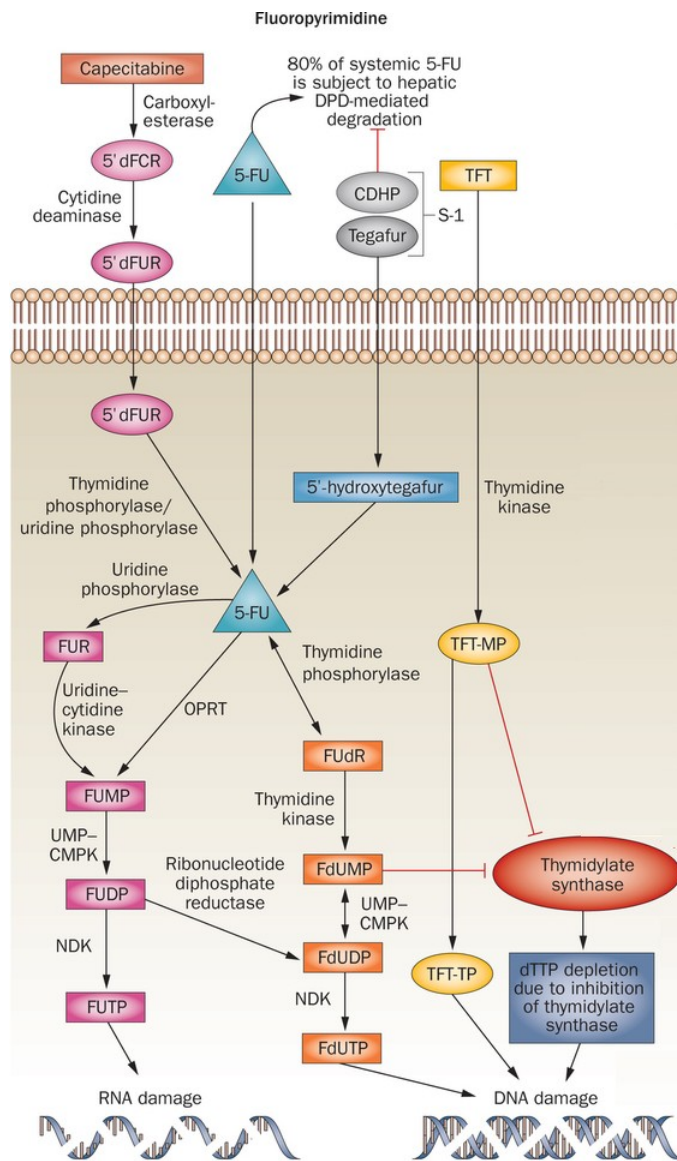


**Figure 6** Metabolic pathway of FLs. Modified from Wilson, et al., 2014 Standing the test of time: targeting thymidylate biosynthesis in cancer therapy *Nat. Rev. Clin. Oncol.*

Nowadays, these drugs are widely used in the treatment of a range of cancers, including colorectal-, breast-, head and neck-, and stomach cancer.

However, despite the acknowledged efficacy of these drugs in the treatment of different solid tumors, FL treatment remains challenging as a result of a considerable inter-patient variability in terms of efficacy and toxicity.

The PGx research, aimed at defining predictive markers of FL response, mainly focused on the dihydropyrimidine dehydrogenase (DPD), encoded by the gene *DPYD*, which is the first and rate-limiting enzyme of FL catabolic pathway<sup>36</sup>.

DPD deficiency occurs in 4–5% of the population and results in decreased inactivation of 5-FU. This can lead to an increase in active metabolites of 5-FU, which is associated with a higher risk of

severe and even fatal toxicity<sup>37</sup>. Toxicity could be limited by exposing DPD-deficient patients to a decreased dose of FL, and by keeping plasma levels of 5-FU and its metabolites at therapeutic levels.

Up to date, 167 SNPs altering the DPD aminoacidic sequence have been identified and many clinical studies have investigated their association with FL-related severe toxicities.

SNPs can appear in heterozygous form (one SNP on one allele), homozygous form (two identical SNPs on two alleles) or double heterozygous form (two different SNPs on either one or two alleles, the latter is also called compound heterozygous). Two SNPs on two alleles lead to a larger decrease in DPD enzyme activity, compared with the heterozygous form.

Among the most studied *DYPD* SNPs, *DYPD-rs3918290* (*DYPD\*2A*, *DYPD IVS1411G>A* or *c.190511G>A*) is surely one of the most well-known.

It was first described by Vreken in a case report of two unrelated patients<sup>38</sup> and McLeod named it *DYPD\*2A* in an article in which the nomenclature for a series of *DYPD* SNPs was defined<sup>39</sup>. Variant allele frequencies have been reported to vary between ~0.1 and 1.0% in African-American and Caucasian populations, respectively<sup>40</sup>. *DYPD-rs3918290* is located at the intron boundary of exon 14 that results in a splicing defect, leading to the skipping of the entire exon. The mature mRNA lacks a 165bp segment and the DPD mutant protein shows a very little residual activity. This was recently confirmed in a study by Offer et al. that analyzed in mammalian cells in the expression of several *DYPD* homozygous variants. The enzymatic activity of the protein codified by the gene with *DYPD-rs3918290* was completely absent<sup>41</sup>. This indicates that in heterozygous carriers, who have one dysfunctional - and one functional allele, ~50% of the normal DPD enzyme activity is maintained.

Several papers<sup>42-46</sup> have confirmed the importance of this SNP both for its clinical impact and for its deleterious effect on the mature protein.

Another well studied SNP is *DYPD-rs67376798* (*DYPD 2846 A>T*), that has also been reported as a plausible candidate for predictive pharmacogenetic test.

The variant allele of this SNP was first described by van Kuilenburg in 2000<sup>47</sup>. *DYPD-rs67376798* results in a Asp949Val amino acid change localized near an iron-sulfur motif and leads to a structural change in the DPD that interferes with cofactor binding or electron transport<sup>48</sup>. Reported variant allele frequencies vary from 0.1 to 1.1% in African-Americans and Caucasians, respectively<sup>40</sup>. *In vitro* data show that homozygous expression of the *DYPD-rs67376798* variant

allele results in an activity of 59% compared with wild-type ( $p = 0.0031$ )<sup>41</sup>. Although the enzyme activity of *DYPD*-rs67376798 is significantly impaired, it is not comparable to the extent observed for *DYPD*-rs3918290, where homozygous expression resulted in a completely nonfunctional enzyme<sup>49</sup>. This finding suggests that a heterozygous carrier would have around 25% reduction in DPD activity.

The group of Morel<sup>50</sup> has found strong associations with both *DYPD*-rs3918290 and *DYPD*-rs67376798 and severe 5-FU toxicity in a cohort of 487 patients receiving FL-based therapy. The same SNPs reported in the study of Morel were also associated with toxicity due to CAPE treatment at high significance levels<sup>42</sup>.

Terrazzino and his colleagues<sup>51</sup> in their meta-analysis further strengthened these associations. They presented pooled data from PGx studies and investigated the association between both *DYPD*-rs3918290 and *DYPD*-rs67376798 and the risk of grade more or equal than 3 toxicity following FL treatment. Their results are consistent with the evidence of an increased risk of overall severe toxicity.

Moreover, in the largest study published to date (2886 stage III colon cancer patients), statistically significant associations were found between *DYPD*-rs3918290, *DYPD*-rs67376798 and increased incidence of grade 3 or greater 5FU-adverse reaction in patients treated with adjuvant 5-FU-based combination chemotherapy<sup>45</sup>.

Recent studies analyzed also *DYPD*-rs55886062 (*DYPD*\*13 or *DYPD* 1679 T>G) as a candidate for predicting FL-toxicities.

*DYPD*-rs55886062 was first described by Collie-Duguid et al. as ‘T1679G’<sup>52</sup>. This SNP causes Ile560Ser amino acid change in a flavine mononucleotide binding domain and the allele frequency was found to vary from 0.07 to 0.1% in Caucasians<sup>40</sup>.

The precise functional consequences of the *DYPD*-rs55886062 variant have not yet been unraveled, but are thought to be related to destabilization of a sensitive region of the protein<sup>48</sup>. This hypothesis is reinforced by the observation that the heterozygous form of this SNP has been found only in patients with decreased enzyme activity<sup>53</sup>. From the aforementioned study of Offer, it was demonstrated that the homozygous expression of the variant allele of this SNP resulted in a 75% reduction of DPD enzyme activity compared with the wild-type<sup>49</sup>, suggesting that this variant inactivates almost completely the protein.

Patients with allele variants of *DYPD*-rs55886062 showed severe toxic side effects in several

studies<sup>43,46,52</sup>. Moreover, Morel et al. described a heterozygous patient that experienced severe grade 4 toxicity. After a 6-week treatment interruption, 5-FU was safely reintroduced with individual PK adjustment, based on 5-FU plasma levels<sup>50</sup>.

This huge amount of information about the clinical impact of these SNPs fueled the discussion in the scientific community and gave rise to the publication of PGx FL dosing guidelines. In particular, the Clinical Pharmacogenetics Implementation Consortium (CPIC) and the Dutch Pharmacogenetics Working Group of the Royal Dutch Association for the Advancement of Pharmacy (DPWG) have published FL-specific guidelines with indications and recommendations about drug-related genetic tests and their integration in the clinical routine<sup>54,55</sup>. Nowadays, personalization of the FL treatment can be performed with the pre-therapeutic test of three aforementioned genetic variants: *DPYD*-rs3918290, *DPYD*-rs55886062, and *DPYD*-rs67376798. In the CPIC guidelines patients heterozygous for at least one of these three SNPs are considered to have intermediate or partial DPD enzyme activity and a reduction of at least 50% of the initial dose for these patients is recommended.

In addition, also the DPWG provides evidence-based guidelines and recommendations about dose adjustments to apply in *DPYD* variant allele carriers. Regarding this, the Dutch group recently updated<sup>40</sup> their online guidelines for FLs dose adjustments accordingly with the “gene activity score”. This method is based on the principle that variant alleles can differ in the extent to which they influence enzyme activity. Consequently, following the calculated gene activity scores for *DPYD*, an individualized dose recommendation for FLs can be given, as is shown in Table 3.

<b>Gene activity score</b>	<b>% of standard dose</b>
0	Alternative drug
0.5	25
1	50
1.5	75
2	100

**Table 3** Initial dose recommendation for *DPYD* gene activity score.

After initial reduction, dosages can be further titrated based on clinical tolerance. Dose reductions are 75, 50 or 25% for gene activity scores of 0.5, 1, and 1.5, respectively. The gene activity score varies from 0 (no DPD activity) to 2 (normal DPD activity).

Clues that other *DYPD* SNPs (e.g. *DYPD-rs2297595*, *DYPD-rs1801160*, *DYPD-rs1801158*, *DYPD-rs1801159*, and *DYPD-rs17376848*) could have a role in the development of FL-related toxicities came from international guidelines<sup>55</sup> and looking at the most recent literature<sup>43,46,56</sup>. These SNPs have been previously observed in patients with low DPD enzymatic activity<sup>41</sup>, however there is no final proofs that promote them as possible predictive biomarker of FL-related toxicity.

#### **1.4.1.2. PGx STRATEGY: THE CASE OF IRINOTECAN**

CPT-11 (7-ethyl-10-[4-(1-piperidino)-1-piperidino] carbonyloxy camptothecin) is a semisynthetic derivative of the natural alkaloid camptothecin, an extract from the Chinese tree *Camptotheca acuminata*<sup>5</sup>.

It was introduced into the clinics in the late 1980s and it received accelerated approval by FDA in 1996 and the full approval in 1998 ([http://www.accessdata.fda.gov/drugsatfda\\_docs/appletter/1998/20571s8ltr.pdf](http://www.accessdata.fda.gov/drugsatfda_docs/appletter/1998/20571s8ltr.pdf)). Nowadays it is one of the most active drugs in the first- and second-line treatment of this malignancy<sup>57,58</sup>.

Regarding the mechanism of action, in the liver CPT-11 is enzymatically converted by carboxylesterase to its most active cytotoxic metabolite, 7-ethyl-10hydroxy-camptothecin (SN-38) (Figure 7), which establishes an equilibrium between the pharmacologically active closed lactone ring and the inactive open ring hydroxy acid form by reversible pH-dependent hydrolysis. SN-38 is responsible for CPT-11 biologic effects, including efficacy and toxicity since compared with the parent drug, SN-38 is 100- to 1000-times more cytotoxic<sup>59</sup>.

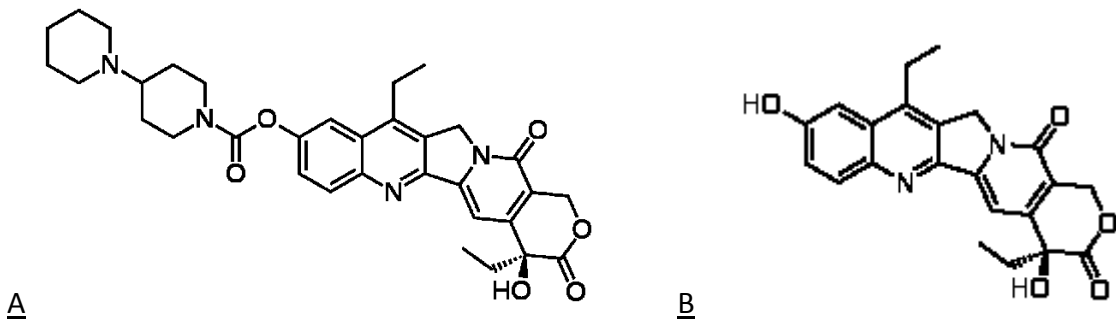


**Figure 7** Chemical structures of CPT-11 (A) and its main metabolite SN-38 (B)

SN-38 is then glucuronized to SN-38 glucoronic acid and detoxified in the liver via conjugation by the *UGT1A1* family, which releases SN-38G into the intestines for elimination. Approximately 70% of SN-38 becomes SN-38G, which has 1/100 of the antitumor activity and is virtually inactive. Simultaneously, and competing with the activation and detoxification pathways of irinotecan, the SN-38 oxidation pathway is mediated by the P450 *CYP3A* genes. Oxidation of CPT11 results in the inactive metabolites APC (7-ethyl-10-[4-N-(5-aminopentanoic acid)-1-piperidino] carboxyloxycamptothecin) and NPC (7-ethyl-10-[4-(1-piperidino)-1-amino] carboxyloxycamptothecin) (Figure 8).

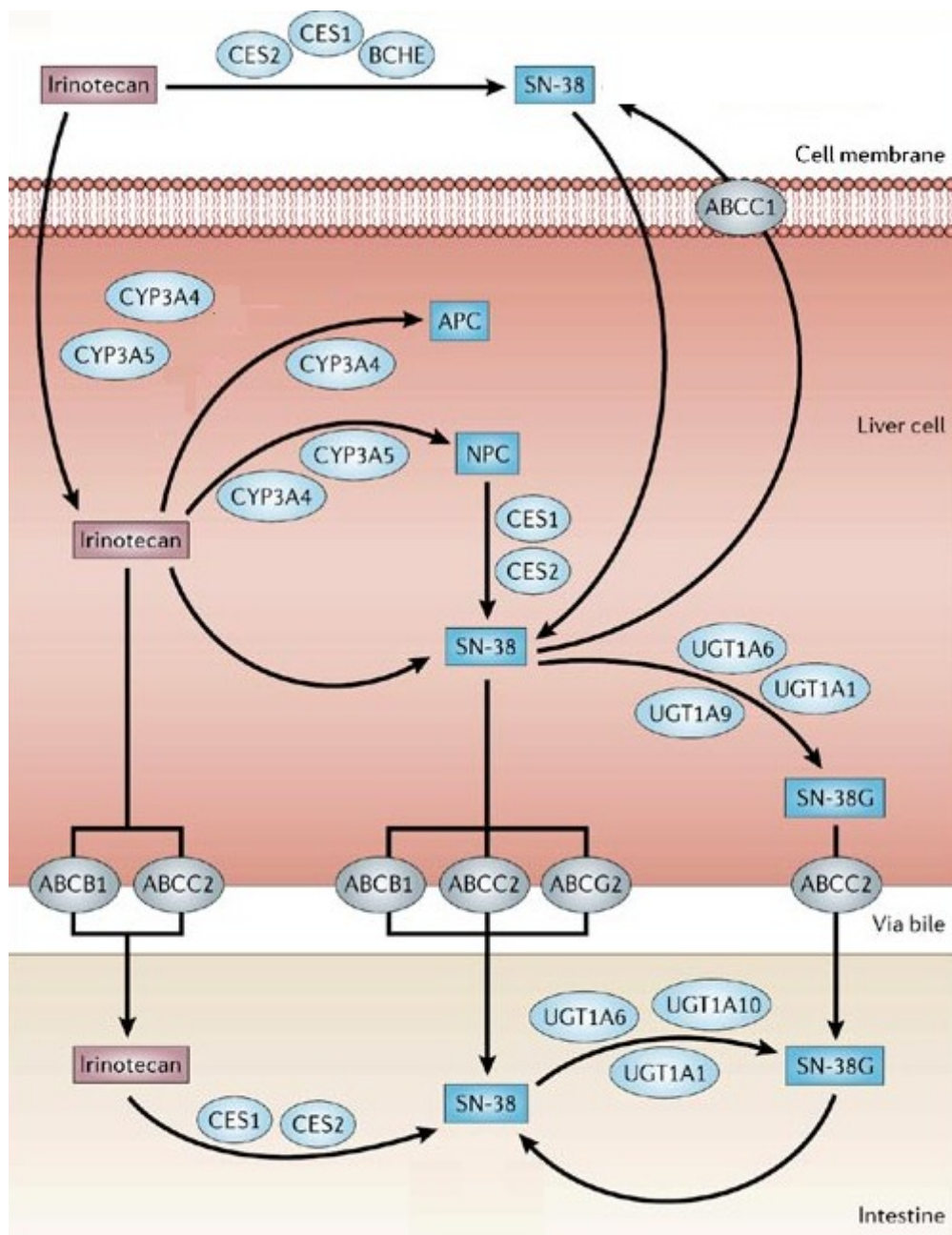


**Figure 8** Mechanism of action of CPT-11. Modified from Scripture et al., 2006 Drug interaction in cancer therapy *Nature Reviews Cancer*

CPT-11 is one of the chemotherapeutic drug, together with FLs, that is listed among the drug with PGx warning.

In particular, the PGx research mainly focused on the *UGT1A* family, responsible for conjugation of the active SN-38 to inactive SN-38G.

Among the most studied SNPs within these genes, *UGT1A1\*28* (rs81753479) SNP is surely one of the most well-known.

The *UGT1A1\*28* allele is characterized by seven thymine-adenine (TA) repeats within the

promoter region, as opposed to six that characterizes the wild-type allele (*UGT1A1\*1*). These extra repeats impair proper gene transcription, resulting in decreased gene expression by approximately 70%<sup>60,61</sup>. Moreover, the increased number of repeats results in decreased rates of transcription, initiation, expression, and enzyme activity, that result in a reduced SN-38 detoxification and a prolonged exposure time of active SN-38 in the intestines. Thus, patients homozygous or heterozygous for the *UGT1A1\*28* commonly develop dose limiting severe neutropenia and late diarrhea and the current US package insert includes homozygosity of *UGT1A1\*28* as a risk factor for

severe

neutropenia

(<http://www.fda.gov/Safety/MedWatch/SafetyInformation/ucm215480.htm>).

*UGT1A1\*28* is prevalent within the Caucasian and African-American populations with frequencies of 0.26-0.31 and 0.42-0.56 respectively<sup>62</sup>.

Since 2011 the DPWG has evaluated therapeutic dose recommendations for CPT-11 based on *UGT1A1* genotype: a reduction of the 30% of the standard dose was suggested for patients homozygous for the *UGT1A1\*28* allele and treated with doses higher than 250 mg/m<sup>2</sup><sup>55</sup>.

More recently, a French joint working group comprising the National Pharmacogenetics Network (RNPGx) and the Group of Clinical Onco-pharmacology (GPOO-Unicancer) have published more complex guidelines for the use of *UGT1A1\*28* genotype when prescribing CPT-11<sup>63</sup>. In summary, for initially scheduled doses between 180 and 230 mg/m<sup>2</sup> every 2-3 weeks, *UGT1A1\*28/\*28* patients are at increased risk of developing hematological and/or digestive toxicity as compared to other genotypes and a 25-30% dose reduction at the first cycle is recommended, particularly in cases of associated risk factors (performance status >3). For initially scheduled doses ≥240 mg/m<sup>2</sup> every 2-3 weeks, *UGT1A1\*28/\*28* patients are at a much higher risk of hematological toxicity (neutropenia) as compared to other genotypes. The guidelines thus recommend the administration of an intensified dose (240 mg/m<sup>2</sup>) only in *UGT1A1\*1/\*1* patients, as well as in *UGT1A1\*1/\*28* patients. The administration of an intensified dose (240 mg/m<sup>2</sup>) is only possible in *UGT1A1\*1/\*1* patients, as well as in *UGT1A1\*1/\*28* patients, in the absence of additional risk factors and under strict medical surveillance (Figure 9).

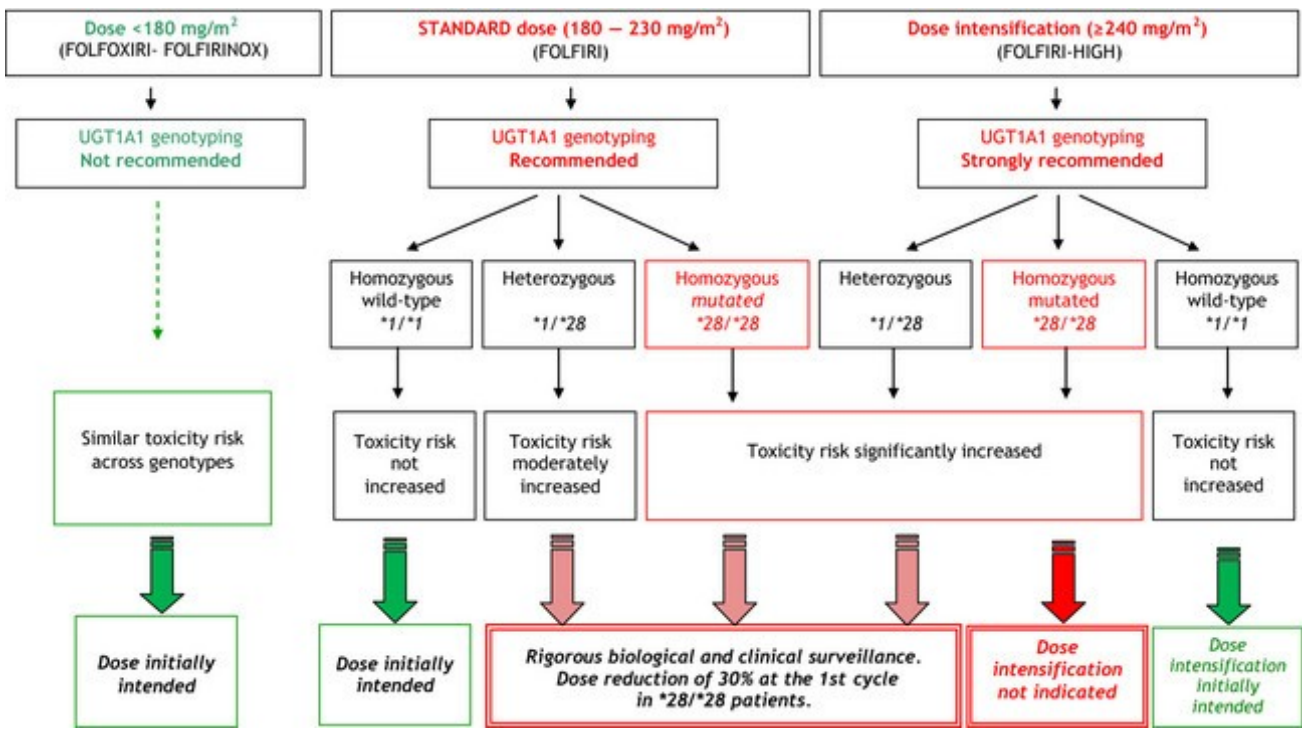


**Figure 9** Scheme of the guidelines for the use of *UGT1A1\*28* genotype when prescribing CPT-11.

On the background of the CPT-11 PGx dosing guidelines described above, this drug is a perfect candidate for genotype-driven phase Ib studies (Box 1).

In particular, the group of Toffoli performed a dose-finding study in mCRC patients treated with FOLFIRI regimen and with the *UGT1A1\*1/\*1* and *UGT1A1\*1/\*28* genotypes. By dose escalating CPT-11 only in patients without the high-risk *UGT1A1\*28/\*28* genotype (10% on average in patients of European descent), they demonstrated that the recommended dose of 180 mg/m<sup>2</sup> for CPT-11 in FOLFIRI is considerably lower than the dose that can be tolerated by the non-*UGT1A1\*28/\*28* patients. In particular, patients with *UGT1A1\*1/\*1* genotype can safely be treated with dose of 370 mg/m<sup>2</sup>, while the maximum tolerated dose for *UGT1A1\*1/\*28* is assessed at 310 mg/m<sup>2</sup><sup>64</sup>.

The same group, to better deepen the issue for the correct CPT-11 dosage, began another phase 1b study, “A genotype-guided phase I study of CPT-11 administered in combination with 5-fluorouracil/leucovorin (FOLFIRI) and bevacizumab as first-line therapy in metastatic colorectal cancer patients”. Patients enrolment began in 2009. The study was conducted in three centers (University of Chicago, Chicago, IL, USA; Centro di Riferimento Oncologico, Aviano, Italy; San Filippo Neri, Rome, Italy), and the protocol was approved by the Institutional Review Board of each participating site. All patients signed a written informed consent before entering the study

(EudraCT 2009-012227-28; Protocol code CRO-2009-25, NCT01183494).

The primary objective of this study was to determine the MTD of CPT-11 in FOLFIRI plus bevacizumab regimen during cycle 1 in *UGT1A1\*1/\*1* and *UGT1A1\*1/\*28* genotype patients. Secondary objectives included: 1) the evaluation of PK of CPT-11 and SN-38 with and without bevacizumab during cycle 1; and 2) the effect of higher doses of CPT-11 and genotype on the efficacy of FOLFIRI plus bevacizumab as determined by objective response rate (ORR) and progression-free survival (PFS).

The MTD of genotype-directed CPT-11 was assessed at 260 mg/m<sup>2</sup> for *UGT1A1\*1/\*28* patients, and 310 mg/m<sup>2</sup> for *UGT1A1\*1/\*1* patients. Although these doses were still higher than the standard ones, they did not reach the level of the previous phase Ib study with FOLFIRI alone. Furthermore, in a preliminary analysis of 22 patients, bevacizumab decreased the area under curve (AUC) of SN-38 ( $p = 0.026$  by Wilcoxon matched pairs signed rank test), suggesting a role of this monoclonal antibody in the pharmacokinetic of CPT-11<sup>65</sup>.

### **BOX 1: Genotype-driven Phase Ib studies**

According to the Italian legislation (DPR n°439/2001, art.3), it is necessary to design a Phase 1 study with:

- ✓ New pharmaceutical products never tested in human subjects
- ✓ Pharmaceutical products resulted from a new association of already registered agents
- ✓ Pharmaceutical products already registered in other countries but declared new by the Italian Ministry of Health
- ✓ Pharmaceutical agents already registered but for which new pharmaceutical forms, excipients, recommendations, dosages, administration routes are proposed.

The genotype-drive phase IB studies fall into the last category.

Patients are indeed treated with drugs already used in the clinical practice but, according to PGx determinants, they are stratified and treated with specific drug dosages.

## **1.4.2. THERAPEUTIC DRUG MONITORING STRATEGY**

The interpatient variability in PK leads to plasma concentration fluctuation that may vary over 10-fold range when fixed doses of chemotherapeutic agents are administered (Bardin 2014). For example, patients with a low clearance receive a relative overdose and will be at increased risk of toxicity. These patients may benefit from a lower dose than the standard one.

TDM has been introduced in the clinical care from the early 1960s. It involves the measurement and interpretation of drug concentrations in biological fluids and the individualization of drug dosages or schedules to maximize therapeutic outcomes or to minimize toxicities, or both <sup>66</sup>.

In order to apply TDM in the clinical practice, the drug under investigation has to fulfil the following criteria: presence of considerable inter- or intra-individual PK variability, existence of a defined and ascertainable relationship between concentration and pharmacological effects, narrow therapeutic window, absence of a simple accessible parameter to evaluate clinical efficacy, and the availability of a defined and accurate method for drug quantification in biological fluids <sup>67</sup>. This method is broadly applied to drugs from different therapeutic classes, such as cardiovascular agents, antiepileptics, antibiotics, respiratory smooth muscle relaxants, anti-inflammatory agents, some cancer agents, immunosuppressants, and antidepressants <sup>68</sup>.

Anticancer drugs fit many of the criteria commonly defined as prerequisites for utilizing TDM approaches. Firstly, the extent of inter-individual PK variability exhibited is large in the majority of cases, with coefficients of clearance variation of more than 50%. This large inter-individual PK variability is likely to be related to genetic differences as well as variations in the functional status of cancer patients <sup>66</sup>.

Secondly, relationships have been described between drug plasma concentrations and PD endpoints such as percentage decrease in neutrophil counts between pretreatment and nadir values <sup>69</sup>.

In addition, when treating cancer patients, the determination of the highest efficacy from chemotherapy is an important principle because of the magnitude of the possible side effects, like myelosuppression, which can be even life-threatening and may be related to higher than optimal therapy. Nevertheless, sub-optimal therapy can greatly reduce the probability to defeat curable cancers. Consequently, a therapeutic range that defines efficacy concentrations as well as toxicity concentrations would have enormous clinical utility <sup>70</sup>.

Many clinical cancer trials <sup>71,72</sup> showed the benefits of maximum chemotherapy intensity underscoring the need to treat patients with doses that will produce concentrations in the upper

end of the nontoxic range to increase likelihood of response or cure. If toxic plasma concentrations can be defined for each agent, then TDM could be useful in identifying which agents are being overdosed or underdosed in any given regimen. TDM in cancer chemotherapy has additional advantages like enhancement of compliance, minimization of PK variability among patients, dose adjustment in patients with hepatic and renal dysfunction, and detection of drug interactions<sup>73</sup>.

Given the great potentialities associated to TDM, a sensitive, precise and reproducible assay available for the clinical use is required in order to implement its use in daily practice. The gold standard assay for determining the drug plasma concentration in human samples is represented by high-performance liquid chromatography coupled with mass spectrometry (HPLC-MS/MS).

To apply these methods to patients' samples, they need not only to be setup to detect the drug of interest but also to be validated according to international guidelines such as those of FDA, "Guidance for Industry Bioanalytical Method Validation", and the European equivalent ones published by EMA (European Medicines Agency), "Guideline on bioanalytical method validation"<sup>74,75</sup>.

#### **1.4.2.1. TDM STRATEGY: THE CASE OF SUNITINIB**

Sunitinib malate is an oral multi-targeted tyrosine kinase inhibitor that selectively inhibits class III, V, and XII split-kinase domain of receptor tyrosine kinases (RTKs)<sup>76</sup>. Most of the small number of kinase inhibitors that have been approved so far were developed with the aim of selectively inhibiting a particular kinase involved in cancer, like the BCR-ABL kinase that is recognized by imatinib. In part, this was due to concern that less-selective kinase inhibition would cause problems with toxicity. However, evidence shows that drugs that inhibit multiple kinases can have acceptable toxicity profiles and potentially enhance antitumor activity relative to more selective kinase inhibitors<sup>77</sup>.

In particular, data from preclinical studies and animal models suggested that simultaneous inhibition of the vascular endothelial growth factor receptor (VEGFR2) and the platelet-derived growth factor receptor (PDGFR $\beta$ ) might produce greater antitumor effects than inhibition of either RTK alone<sup>78,79</sup>.

From these efforts, a rational design identified sunitinib as a potent inhibitor of VEGFR2 and PDGFR $\beta$  that had good solubility, bioavailability and protein-binding characteristics<sup>80</sup>. In addition,

it inhibits also other proteins like PDGFR $\alpha$ , VEGFR1, fetal liver tyrosine kinase receptor 3 (FLT3), colony-stimulating factor receptor type 1 (CSF1R), neutrophic factor receptor (RET), and stem-cell factor receptor (KIT)<sup>81</sup>.

Sunitinib inhibits the phosphorylation of these receptors and consequently block the RTKs initiate downstream signaling affecting many of the processes involved in tumor growth, progression, and metastases.<sup>82,83</sup> (Figure 10).

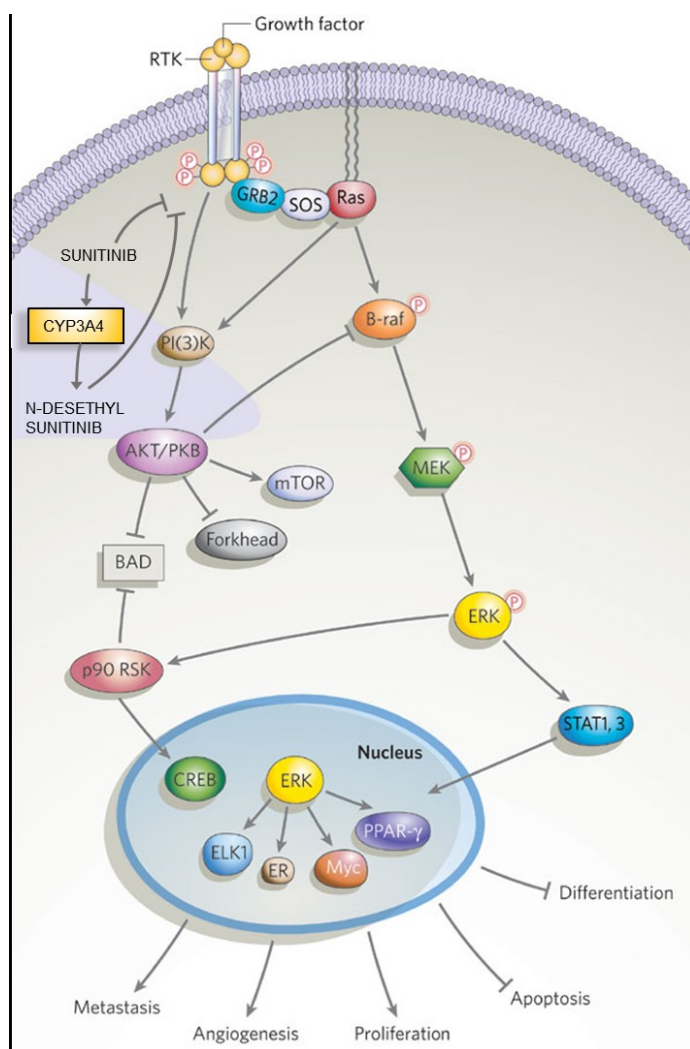


**Figure 10** Mechanism of action of sunitinib. Modified from Sebolt-Leopold et al., 2006 Mechanisms of drug inhibition of signaling molecules *Nature*.

Sunitinib is primarily metabolized by CYP3A4 to an equipotent N-desethyl metabolite, that also contributes to the inhibition of these receptors (Figure 11).

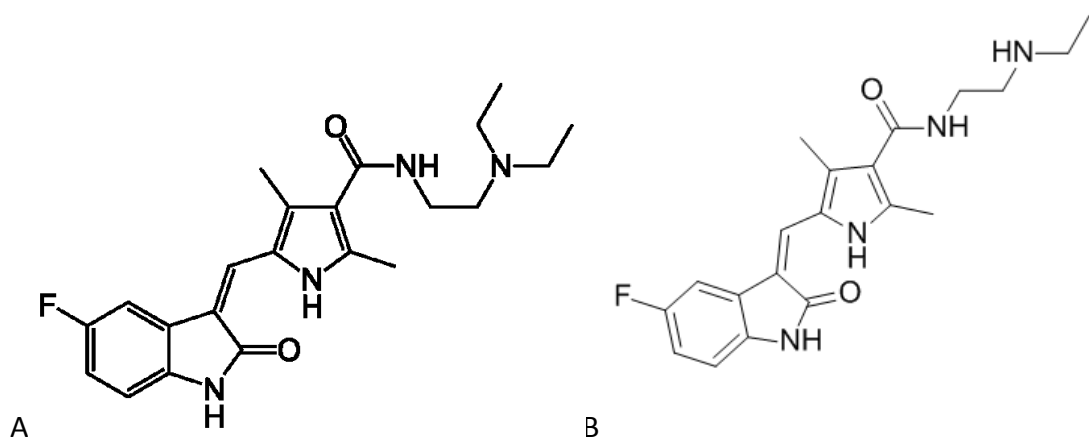


**Figure 11** Chemical structure of sunitinib (A) and N-desethyl sunitinib (B)

The antitumor activity of sunitinib has been shown in a number of preclinical tumor models, and its clinical efficacy has been demonstrated in patients with metastatic renal cell carcinoma (mRCC) (with FDA approval in 2006), gastrointestinal stromal tumor (GIST), metastatic breast cancer, and a variety of other solid tumors (e.g. neuroendocrine tumors). Moreover, sunitinib was approved by FDA also for the treatment of GIST in patients who have failed to respond to imatinib or were unable to tolerate it<sup>84,85</sup>.

Small molecules like sunitinib are mainly used at a fixed dose ignoring the possible need for dose individualization. Fixed dosing may indeed result in suboptimal treatment or excessive toxicity considering the high inter-individual variability in the PK of these therapies<sup>8</sup>.

The appropriate management of cancer patients thus requires careful monitoring of newer targeted therapies and the development of innovative approaches to treatment individualization. TDM may thus provide additional information on efficacy, adherence, and safety compared to clinical evaluation alone. This would contribute to increase the probability of efficient, long-lasting, therapeutic responses in patients and minimizing the risk of major adverse reactions<sup>86</sup>. Finally, as these new treatments are expensive, a precise piloting of the most appropriate approach to dose them might represent a benefit for public health systems.

However, only for imatinib the concentration thresholds have currently been suggested to guide treatment. To date, the European Society for Medical Oncology suggests indeed that "*measuring imatinib blood concentrations may be important in all patients and is recommended in case of sub-optimal response, failure, dose-limiting toxicity or adverse events*"<sup>87</sup>.

However, recent studies suggested sunitinib as another candidate for a TDM program. In fact,

increased exposure to sunitinib in patients with advanced solid tumors is associated with improved clinical outcomes (longer time to tumor progression, longer overall survival, a higher probability of a response and greater tumor-size decreases), as well as some increased risks of adverse effects (incidence of fatigue, increase of diastolic blood pressure, decrease of absolute neutrophil count)<sup>88</sup>. Additionally, a recent retrospective analysis of 521 patients with mRCC has shown that plasma concentration might be better correlated to PFS than to the administered dose of drug<sup>89</sup>. Thus, based on preclinical data<sup>90</sup> and on a phase I study<sup>77</sup>, a target plasma concentration of sunitinib and active metabolite (N-desethyl-sunitinib) in the range of 50–100 ng/mL has been suggested.

Despite this information, in order to introduce the TDM of the sunitinib in the clinical practice it is necessary also to have a rapid, specific, sensitive and reproducible method.

One of the most challenging peculiarity of sunitinib for the setup of an analytical method is represent by its isomerization in presence of light. More in detail, it has an exocyclic alkenyl group and is capable of showing Z-E isomerism. In the solid state sunitinib exists as the Z-isomer, which is the stable form of this isomer. Preliminary studies indicated that in solution sunitinib shows the presence of an unstable E-isomer when exposed to light. Similar photo-induced isomerism of molecules with double bonds has already been reported in literature<sup>91,92</sup> and has shown to result in the formation of the less stable isomer<sup>92</sup>.

When the light-exposed solutions of sunitinib are placed in the dark, the E-isomer reverts back to the Z-isomer, which is consistent with other molecules containing C=C or N=N bonds<sup>93</sup>. In solution sunitinib converts to the E-isomer following light exposure and reverts to the Z-isomer in the dark. The group of Sistla demonstrated that while light protection minimizes the photoinduced formation of the E-isomer, storage in the dark can result in a decrease in the already formed E-isomer. To determine the reversion kinetics, the analytical solution of sunitinib was first exposed to light for 23 hours to attain equilibrium. This solution was then protected from light at different temperatures to study the E- to Z-isomer conversion. The E-isomer was observed to revert to the Z-isomer following storage in the dark with an increase in the reconversion rate at higher temperatures. This observation indicates that the reversion of E- to Z- isomer is a thermal reversion<sup>93</sup> (Figure 12).

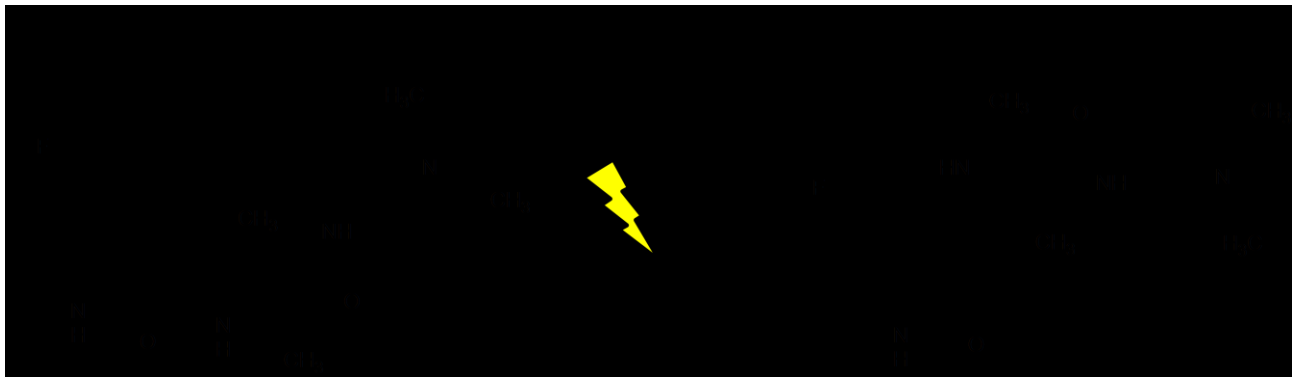


**Figure 12** Interconversion of Z-E isomers of sunitinib

## 2. RATIONALE

The great inter-variability in the PK and PD of the anticancer drugs and their low therapeutic index dramatically complicate the dosing of these drugs. Moreover, the traditional methods based on the measurement of the BSA do not account for the complex processes of anticancer drug metabolism and elimination and, over the years, the need for a new dosing approach has become increasingly evident. The giant steps made in the PGx field paved the way for a tailoring therapy leading to the publications of international, peer-reviewed guidelines that recommend a personalized dose based on the patient genotype. These PGx dosing guidelines referred, in particular, to cytotoxic drugs: over 40 years of experience in the clinical practice, indeed, has defined the right background to identify clearly the molecular and genetic bases of their pathway. For these drugs, several published data underlined a sharp PGx profile that led to the determination of genetic biomarker useful for optimize their dosage.

Unfortunately, only for few anticancer drugs there is a clear defined biomarker, an available and feasible PGx test, and, consequently, peer-reviewed guidelines that help the clinicians in the definition of the right dosage for each patient. FLs and CPT-11 are among them and represent the most explicative examples of PGx implementation in the daily clinical practice.

Regarding FLs, different international working groups, as described in section 1.4.1.1., strongly recommended the introduction of a pre-emptive PGx test for three *DPYD* SNPs. Despite the published guidelines and the vast amount of literature assessing the associations between *DPYD* variant alleles and the occurrence of severe toxicity related to FLs, the genotyping test is still scarcely widespread among clinicians. Moreover, the low frequencies of these variant alleles (around 1%) do not permit the design of prospective phase Ib dose escalation trials to define the MTD for each *DPYD* genotype. In order to overtake this hurdle, the real clinical validity of the pre-treatment PGx test needs to be assessed in large sets of cancer patients and, consequently, the *DPYD* pre-emptive genotyping test should be implemented in the clinical practice with health technology assessment and cost-effectiveness monitoring.

Regarding CPT-11, although the scientific community focused the attention on several *UGT1A1* SNPs<sup>94,95</sup>, only *UGT1A1\*28* became part of the international PGx dosing guidelines, whereas, for the other SNPs, the evidences are still considered too weak. Due to the relatively high frequency

(about 10%) of *UGT1A1\*28* variant alleles in Caucasians, CPT-11 is a perfect candidate for genotype-driven phase 1b studies, in order to optimize its dosage in both mono- and association-therapy. This represents a compelling need, considering that this drug was introduced into the clinics in the late 1980s and dose-finding analyses were conducted before the genetic basis of severe toxicity was established. Previous studies of our group, as described in section 1.4.1.2., have already demonstrated that the stratification of patients in FOLFIRI or FOLFIRI plus bevacizumab regimens according to *UGT1A1\*28* genotype led to a higher MTD both in *UGT1A1\*1/\*28* and *UGT1A1\*1/\*1* patients. These interesting results gave a strong rational to further examine the issue and, based on the genotype profile of the patients, determined the CPT-11 MTD in other administration settings.

For drugs such as targeted anti-cancer agents, which are only recently introduced in the clinical practice, no PGx biomarkers are known up-to-date for dosage optimization.

In these cases there is the necessity to apply other methods to personalize the therapy. One of the most important drug in this class is sunitinib, an oral multi-targeted tyrosine kinase inhibitor, approved only in 2006.

Evidences in literature defined the TDM as the best approach to monitor the sunitinib plasma concentration and, consequently, to obtain the best therapeutic effect with low adverse reactions. The limits of this approach regard, in a large part, the use of HPLC-MS/MS for the quantification of this drug. Although this instrument is the gold-standard for TDM, the methods are often laborious, time-consuming and not feasible for the application in the clinical routine. Moreover, as described in detail in section 1.4.2.1, one of the most challenging peculiarity of sunitinib for the set-up of an analytical method is represented by its isomerization in presence of light. The major part of the methods already published in literature takes into account this phenomenon and the design of all sample handling procedures under strict light protection strongly complicate the process. For this reason, it is necessary to develop and validate a specific, sensitive and reproducible method that overcomes the complex step due to the isomerization of the analyte and can be introduced in the clinical routine of a hospital.

### **3. AIMS**

The principal aim of this PhD thesis was to apply different approaches to optimize the dosing of anticancer drugs. This project has taken advantage of the molecular and bioanalytical background of each analyzed drug, with the common purpose of translating the best approach in the clinical practice. Thus, the ultimate aim is to have a real impact on the cancer patients and ameliorate their quality of life.

The study design and the analytical approaches used to reach these goals are listed below:

✓ **Fluoropyrimidine project:**

Regarding the FLs, a retrospective study was designed with the aim of validating the specificity of three *DPYD* SNPs recommended by international guidelines (i.e. *DPYD-rs3918290*, *DPYD-rs55886062*, and *DPYD-rs67376798*) in predicting the occurrence of severe toxicity events in a large set of cancer patients. This study included a broad range of FL-based regimens and cancer types representative of common clinical practice, assessing the clinical relevance of *DPYD* variants in a “real world” clinical setting. The secondary aim of this study was to evaluate whether the additional testing of other investigational *DPYD* variants (*DPYD-rs2297595*, *DPYD-rs1801160*, *DPYD-rs1801158*, *DPYD-rs1801159*, and *DPYD-rs17376848*) could increase the pharmacogenetic test sensitivity and it is worthy to be integrated in the FL dosing guidelines.

✓ **Irinotecan project:**

A phase 1b study called “*A genotype-guided phase I study of irinotecan administered in combination with 5-fluorouracil/leucovorin (FOLFIRI) and cetuximab as first-line therapy in metastatic colorectal cancer patients*”, was approved by the competent authorities in December 2014 (EudraCT 2013-005618-37 Protocol code CRO-2014-01). The aims of this study were: 1) to define the MTD, the Dose limiting toxicity (DLT), and the phase II recommended dosage of CPT-11 administered in the FOLFIRI regimen plus cetuximab in mCRC patients treated as first-line chemotherapy according to *UGT1A1\*28* genotype; 2) to evaluate the variability of CPT-11 PK, in combination with cetuximab, in patients with *UGT1A \*1/\*1* and *UGT1A \*1/\*28* genotype and the effect of the PK profile on toxicity and response rate; 3) to evaluate the PK profile of CPT-11 and its major metabolites in absence and in presence of cetuximab administration, in order to define the effect of the chimeric monoclonal antibody on CPT-11 PK properties.

✓ **Sunitinib project:**

This project aimed at developing and validating, according to the FDA and EMA guidelines, an analytical method for the quantification of sunitinib and its main metabolite (N-desethyl sunitinib) without any limitations in terms of light protection in order to strongly facilitate sample handling.

## **4. MATERIAL AND METHODS**

### **4.1. FLUOROPYRIMIDINE PROJECT**

#### **4.1.1. PATIENTS ENROLMENT AND TREATMENT**

This retrospective study, sponsored by the CRO-National Cancer Institute of Aviano, Italy, included patients with different solid tumors and treated with FL-based chemotherapeutic regimen.

The inclusion criteria for this study were:

- ✓ histologically confirmed diagnosis of solid cancer;
- ✓ available peripheral blood biological sample;
- ✓ signed written informed consent approved by the local Ethical Committee;
- ✓ assumption of a FL-based treatment for at least three cycles unless interrupted due to a severe treatment-related toxicity occurrence;
- ✓ Caucasian origins.

Based on the these criteria, a set of 603 patients treated with a FL-based chemotherapeutic regimen was selected from a prospective patients' collection of 5,126 clinical cases of the Experimental and Clinical Pharmacology Unit of Centro di Riferimento Oncologico (CRO)-National Cancer Institute, Aviano.

Patients' medical records were examined to collect the following clinical information:

- ✓ baseline patient assessment;
- ✓ chemotherapy information
- ✓ toxicity data related to the first three therapy cycles (classified according to NCI—Common Toxicity Criteria version 3).

Dosage, schedule, and duration of treatment were based on FL current clinical setting.

#### **4.1.2. MOLECULAR ANALYSES**

##### **Sample collection and storage**

For PGx analyses, a 3mL whole blood sample was collected from each patient, and stored in freezer at -80° C. Blood specimens were collected in sterile tubes with any anticoagulant agent but heparin was not admitted.

##### **Genomic DNA extraction**

The extraction of genomic DNA from whole blood was performed with the automated extractor BioRobot EZ1 (Qiagen SPA, Milano, Italy). The Card “EZ1 DNA Blood”, in association with the Kit “EZ1 DNA Blood Kit 350 µL”, was used for the extraction of genomic DNA from 350 µl of whole blood obtaining 200 µL as final volume. Once introduced the appropriate card and start the program, the BioRobot allows to process 6 samples simultaneously, without any intervention by the operator.

This technology is based on the use of silica-coated magnetic particles. DNA is isolated from lysates in one step through its binding to the silica surface of the particles in the presence of a chaotropic salt. The particles then are separated from the lysates using a magnet and the DNA is efficiently washed and eluted in a buffer. DNA yields depend on the sample type, number of nucleated cells in the sample, and the protocol used for purification of DNA. For the protocol applied in this thesis, the yield should be approximately of 5-12 µg of DNA in 200 µL.

The extracted DNA is stored at 2-8° C and its purity is determined by calculating the ratio of corrected absorbance at 260 nm to corrected absorbance at 280 nm, i.e.,  $(A_{260} - A_{320})/(A_{280} - A_{320})$ . Pure DNA has an A260/A280 ratio of 1.7–1.9.

##### **Polymerase chain reaction**

The technique of DNA polymerase chain reaction (PCR) was invented in 1983 by K. Mullis and allows the production of a large number of copies of a specific DNA sequence *in vitro*. It also permits to isolate and amplify any gene from any organism and then analyze the sequence, to perform cloning or mutagenesis procedures, or even to establish diagnostic tests that detect the presence of mutated forms of the gene. In the *in vitro* process, DNA is initially heated to temperatures close to boiling, in order to denature it and thus obtain single-stranded mold, then

*Taq* polymerase is used to catalyze the duplication of the parental strand. To start the synthesis reaction, this enzyme requires a primer represented by a small sequence of single-stranded DNA. In the reaction tube two primers are added, one to allow the synthesis of the sense strand (sense or forward primer) and one for the synthesis of the antisense (antisense or reverse primer). The two primers define the target region to be amplified.

PCR requires several reagents and reaction conditions that vary with the time. In particular, the samples are subjected to a series of thermal cycles that are summarized below:

- ✓ An initial period at elevated temperature (94-95°C) that allows the DNA denaturation, in order to separate the template strands that act as a mold.
- ✓ A variable number of consecutive cycles of amplification, each of which consists of three phases corresponding to three different temperatures:
  1. complete DNA denaturation, carried out by heating at elevated temperature (94-95° C);
  2. pairing (annealing) of sense and antisense primers with complementary sequences on the DNA template. In this phase the temperature is lowered to values which may vary from 50° C to 65° C according to the specific characteristics of the primers used;
  3. extension (elongation) of the primers and synthesis of new strands by the *Taq* polymerase, at a temperature of 72°C optimum for the enzyme activity.

To obtain the amplification of the desired DNA sequence, this cycle of three steps must be repeated several times, typically from 25 to 40 times. A final period at 72°C to complete the elongation.

This series of thermal cycles is carried out thanks to a programmable instrument, the thermal cycler, capable of changing the temperature very quickly and keep it constant for a given period. The result of a PCR is that, at the end of  $n$  cycles of amplification, the reaction mixture contains a theoretical maximum number of double-stranded DNA equal to  $2^n$  (where " $n$ " represents the number of amplification cycles). In the first cycle of PCR, the two primers anneal with the two strands of the denatured template, thus providing the trigger for the polymerase that synthesizes complementary strands. As result of this cycle, two new strands, longer than the region to be amplified, whose end parts correspond to the sequence of the primers used to identify the target sequence, are created. In the second cycle, the primers anneal to the original template again and so it produces other new strands of undefined length. In subsequent cycles only fragments of the desired length are formed and they contain the specific region you want to amplify (Figure 13).

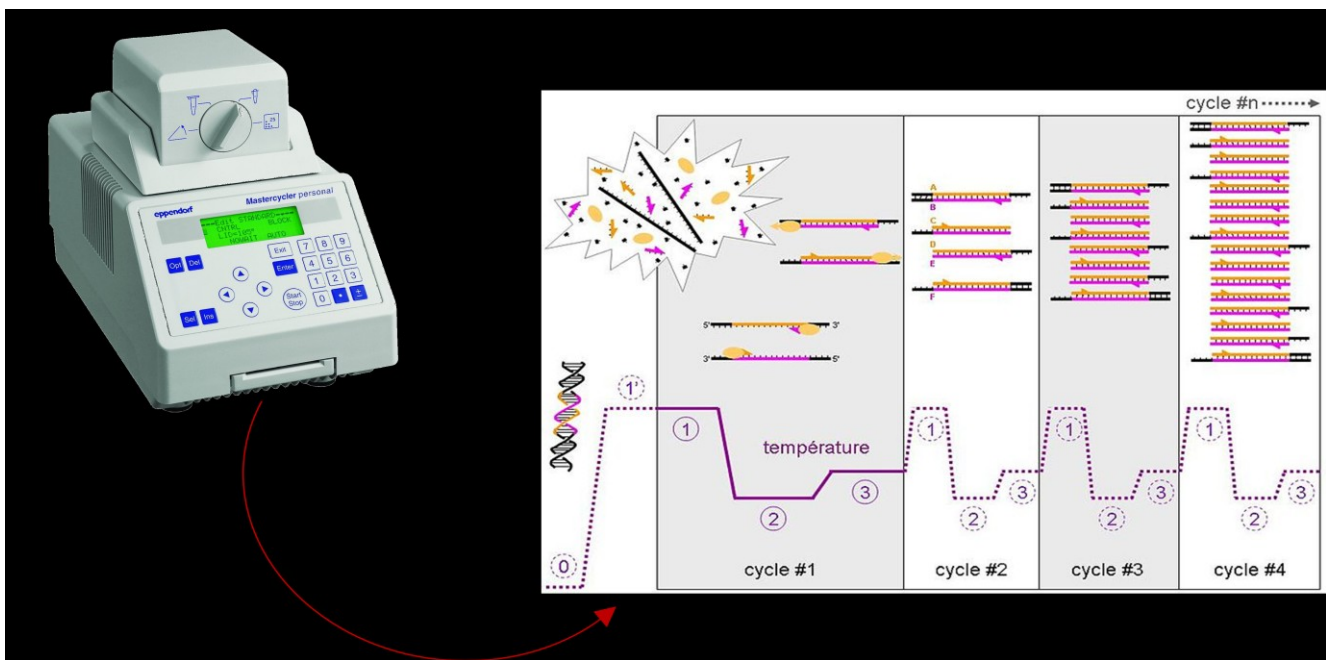


**Figure 13** Polymerase Chain Reaction (PCR).

The reagents used in a PCR are listed above:

### 1) Reaction Buffer

It is a Tris-HCl and KCl based buffer necessary to reproduce the optimal conditions for the activity of the polymerase thus increasing the throughput or the number of nucleotides that the enzyme can insert in succession before separating from the template strand.

### 2) $Mg^{2+}$

It is essential for the activity of *Taq* polymerase as its bond with the enzyme stabilizes it in a three-dimensional conformation that facilitates its activities. The *Taq* polymerase shows its highest activity around a concentration of free  $Mg^{2+}$  equal to 1.2-1.3 mM. However, this value is influenced also by the concentration of nucleotides, as there is a link between equimolar  $Mg^{2+}$  and dNTPs. For this reason, some methods consider  $Mg^{2+}$  concentrations higher than those indicated above, although this could lead to an incorrect incorporation of the nucleotides.

### 3) dNTPs

The solutions of dNTPs contain the four nitrogenous bases of DNA: dATP, dGTP, dTTP and dCTP. For a good efficiency of the PCR the four nucleotides must be present in equimolar around 50-200

$\mu\text{M}$ . A too high concentration may increase the incorrect rate of incorporation, while a too low concentration may reduce the efficiency of the reaction.

#### **4) Primers**

Primers design can be performed manually, or more frequently with software that facilitate the choice such as "Primer3Plus" (<http://www.bioinformatics.nl/cgi-bin/primer3plus/primer3plus.cgi/>). The aim of primer design is to obtain a balance between two goals: efficiency and specificity of amplification. Given a target DNA sequence, primer design software attempts to strike a balance between these two goals by using pre-selected default values for each of the primer design available. In particular, optimal primer pairs should be closely matched in Melting Temperature (Tm) and must not be able to form loops and primer dimers. Primer length (about 20-base pairs), sequence and GC contents are taken into account to select proper primers sequences.

#### **5) DNA polymerase**

The Taq polimerase is derived from the *Thermophilus aquaticus* bacterium, it is stable at high temperatures and works with maximum efficiency between 72°-75°C. The thermal stability is a critical feature of this enzyme. Taq polymerase at 72°C has an enzymatic activity that allows the incorporation of 50-60 nucleotides per second, which corresponds, approximately, to 3 Kb per minute. The optimal concentration of Taq DNA polymerase ranges from 0.5 to 2.5 U. A too high concentration may decrease the specificity of the reaction, while a too low concentration may not enable the conclusion of all cycles.

### **4.1.3. METHODOLOGIES FOR POLYMORPHISMS ANALYSIS**

NCBI (National Center for Biotechnology Information) databases and tools were used to select the analyzed SNPs. The NCBI presents a web site showing links to databases containing information about genes (Gene), polymorphisms (dbSNP), scientific literature (PubMed), besides search and analysis tools. These and other additional databases (SNP500, PharmGKB, and 1000 Genomes Browser) were consulted for assay design (genetic sequences, SNPs description, primer design), during this work of thesis. Subsequently, according to the type of the selected SNP and to the specific characteristics of the surrounding nucleotide sequence, the most suitable method of genotyping has been chosen.

In particular, in this PhD thesis, semi-automated, recently developed genotyping methods have been used. They are based on PCR reactions and allow the identification of genetic SNPs in a very simple and easy way: pyrosequencing (PSQ), allelic discrimination based on TaqMan chemistry, and direct sequencing.

## Pyrosequencing

Pyrosequencing is an analytical technology for SNP identification consisting of a real-time pyrophosphate detection method (Fakhrai-Rad *et al.*, 2002; Ronaghi *et al.*, 2001).

This technique is based on indirect bioluminometric assay of the pyrophosphate (PPi) that is released from each dNTP upon DNA chain elongation. Klenow polymerase mediated the base incorporation, PPi is released and used as substrate, together with adenosine 5'-phosphosulfate, for the ATP sulfurylase, which results in the formation of ATP. Subsequently, the ATP accomplishes the conversion of luciferin to its oxi-derivative by luciferase. The ensuing light output is proportional to the number of added bases, up to about four bases. To allow processivity of the method, dNTPs in excess are degraded by apyrase, which is also present in the starting reaction mixture and continuously degrades ATP and unincorporated dNTPs. This switches off the light and regenerates the reaction solution. The dNTPs are added one by one to the template during sequencing procedure. It should be noted that deoxyadenosine alfa-thio triphosphate is used as a substitute for the natural dATP since it is used efficiently by the DNA polymerase, but not recognized by the luciferase (Figure 14). The process is fully automated and adapted to a 96-well format, which allows rapid screening of large panel of samples.

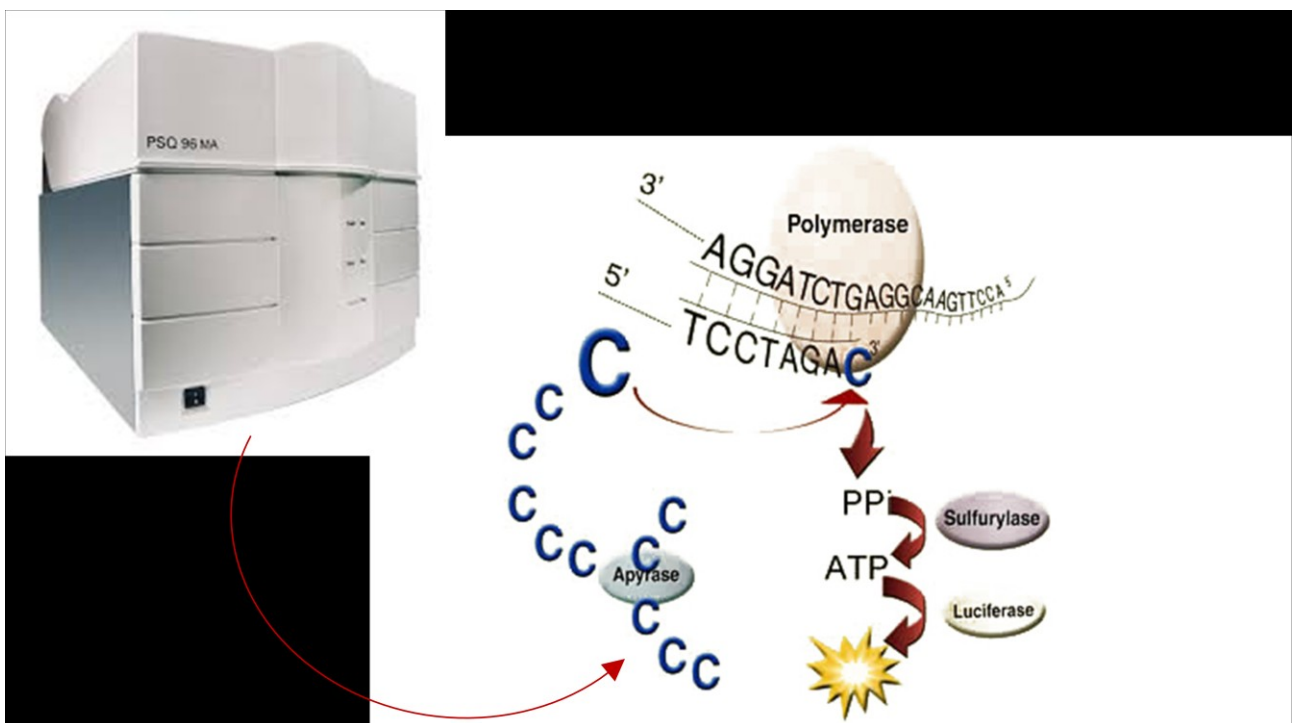


**Figure 14** Pyrosequencing chemistry: biochemical reactions and enzymes involved in the generation of light signals by DNA pyrosequencing.

Following a first phase of sample preparation, the plate is loaded on an instrument, the PSQ 96MA Pyrosequencing, which determines and provides directly the genotype at the level of the analyzed SNP.

Pyrosequencing analysis is performed on PCR-amplified DNA. One of the PCR primers must be biotin-labeled for immobilization to streptavidin coated sepharose beads. This allows the separation of the two DNA strands produced by PCR, since the assay must be carried out on single stranded DNA. If reverse primer is biotynilated the assay is called forward, otherwise, if the forward primer is biotin-labeled, the assay is called reverse.

PCR reaction product is mixed with streptavidin coated High Performance Sepharose beads (Amersham Biosciences, Uppsala, Sweden) in the presence of a binding buffer (Tris 10 mM, Sodium Chloride 2 M, EDTA 1 mM and Tween 20 0.1%, pH 7.6). The mixture is allowed to shake for 10 min at room temperature. The samples are subsequently transferred to a 96-well filter plate and vacuum (vacuum manifold for 96 well filter plate, Millipore) is applied to remove all liquid. Denaturating solution (Sodium Hydroxide 0.2 M) is added to denature double stranded PCR product DNA. After 1 minute incubation, vacuum is applied to remove the solution and the non immobilized DNA. The beads are washed twice with a washing buffer (Tris 10 mM, pH 7.6) in the presence of the vacuum. The beads with the immobilized template are resuspended by adding 45

$\mu$ l annealing buffer (Tris 20 mM, Magnesium Acetate Tetra-Hydrate 2 mM, pH 7.6) and sequencing primer (2  $\mu$ M) is added to each sample. Design of sequencing primers for pyrosequencing follows the same criteria as for the PCR primers, except that the Tm of these primers may, if necessary, be lowered. The sequencing primer could thus be shorter than the PCR primers, typically 15 bp. The position of the primer is flexible within 5 bases from the SNP and can be designed on both the positive (reverse assay) or on the negative (forward assay) strand. Thirty-five  $\mu$ l of this mixture is transferred to a Pyrosequencing 96 wells plate (PSQ 96 Plate Low).

The plate is incubated for 5 min at 60° C to allow the complete sequencing primer annealing on the template DNA. After samples cooling, the plate is transferred on the pyrosequencing instrument. The biotin labeled DNA template, annealed to the sequencing primer, is incubated with enzymes (DNA polymerase, ATP sulfurylase, luciferase, and apyrase) and the substrates (adenosine 5'phosphosulfate and luciferin). The first of the four dNTPs is added to the reaction. DNA polymerase catalyzes the incorporation of the dNTP into the DNA strand, complementary to the base in the template strand. Each incorporation event is followed by the previously described reaction cascade, leading to the generation of visible light in amount that is proportional to the number of nucleotide added. The light produced in the luciferase-catalyzed reaction is detected by a charge coupled device (CCD) camera and seen as peak in a pyrogram. The height of each peak (light signal) is proportional to the number of incorporated nucleotides.

As the process continues, the complementary DNA strand is built up and the nucleotide sequence is determined from the signal peaks in the pyrogram.

"PSQ Assay Design" software was used for the planning of the described assays: it allows to easily choose the set of primers (sense and antisense primers for PCR and sequencing primer for subsequent analysis at PSQ) most suitable for the study of each SNP. The analysis of the results is accomplished with the "PSQTM 96 MA software".

In this thesis *DPYD*-rs3918290 was genotyped using a pyrosequencing analysis. The region of interest was amplified using primers forward 5'- CGGCTGCATATTGGTGTCAA-3' and reverse 5'-[Btn]CACCAACTTATGCCAATTCTCTTG-3'. The PCR products were amplified using AmpliTaq Gold® DNA Polymerase.

PCR conditions were: 5 min denaturation at 95°C then 35 cycles of 30 s denaturation at 95°C, 30 s annealing 60°C and 1 min extension at 72°C and a last cycle consisting of 5 min extension at 72°C.

## Taqman® Assay

The allelic discrimination consists in the determination of the two variants of a single nucleic acid sequence by means of the "5' fluorogenic nuclease assay". In particular, this technique exploits the exonuclease property in the direction 5'→3' of the Taq polymerase when it encounters, during its activity of DNA fragment elongation, an oligonucleotide perfectly matched with the DNA template used for the elongation. Through this method, it is possible to investigate SNPs.

TaqMan® allelic discrimination is based on a Real Time PCR (RT PCR) that involves the sense and antisense primers needed for the amplification of the SNP containing fragment but also an oligonucleotide (probe) able to pairing with the template. The probe pairs in an intermediate position between the sense and the antisense primer and it is functionalized at the two ends. At one part there is a "quencher" fluorophore (TAMRA) which acts as a silencer of fluorescence, while, at the other one there is a "reporter" constituted by a fluorescent fluorophore (FAM or VIC). The action of silencing by the quencher occurs by transfer of energy from one fluorochrome to the other one when they are near to each other. In the reaction two different allele-specific probes, labeled with different fluorophores (fluorochrome FAM or VIC), are placed: one contains a perfect match to the wild type (allele 1) and the other one presents a perfect match to the mutation (allele 2). The allelic discrimination assay classifies unknown samples as homozygous for the wild-type, heterozygous, or homozygous for the variant allele.

TaqMan probe-based chemistry uses a fluorogenic probe to detect specific PCR product as it accumulates during PCR cycles. During the denaturation step, the reporter (R) and the quencher (Q) are attached to the 5' and 3' ends of a TaqMan probe. When both dyes are attached to the probe, reporter dye emission is quenched. During each extension cycle, the hot-start DNA polymerase system cleaves the reporter dye from the probe. After being separated from the quencher, the reporter dye emits its characteristic fluorescence which is recorded by a detector (Figure 15).

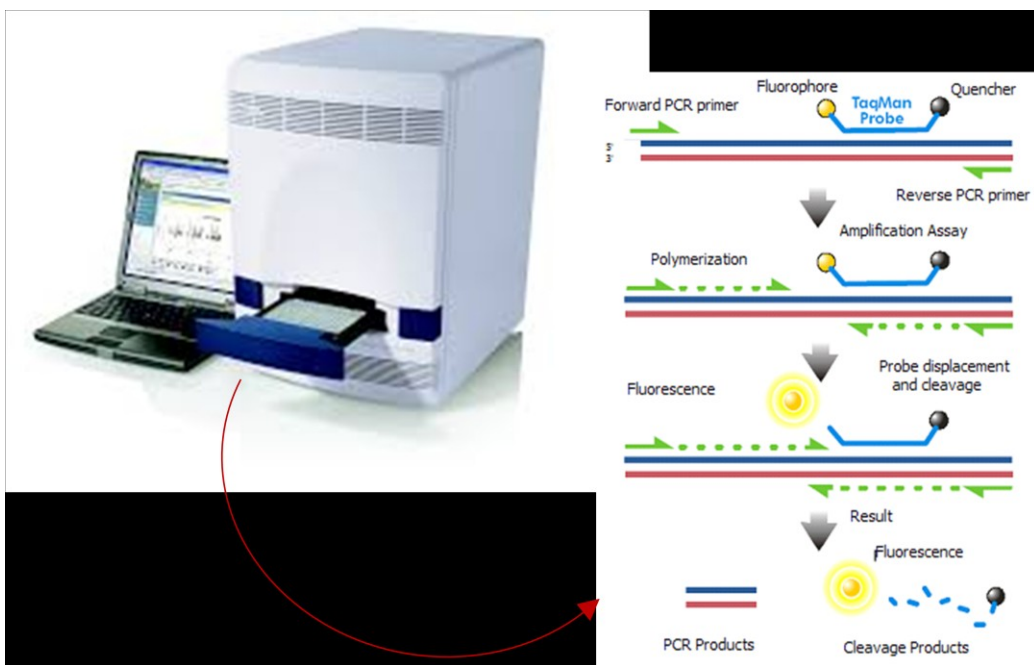


**Figure 15** Schematic representation of TaqMan® technology.

The probes are chosen according to certain characteristics:

- ✓ the Tm must be at least 5°C higher than the Tm of the two PCR primers because they must bind to the nucleotide sequence when executing the synthesis of the complementary strand;
- ✓ the oligonucleotide must have a length of about 20-30 bp and 50% of G and C;
- ✓ the extension phase must be performed at a temperature lower than the 72°C used in the PCR, in order not to cause the detachment of the probe from the template (for this reason we use high concentrations of MgCl<sub>2</sub>);
- ✓ the probe must not form dimers or even pair with itself.

Samples are analyzed using the Applied Biosystems 7500 Real-Time PCR System instrument. The allelic discrimination was performed with the SDS software 2.3 (Applied Biosystems).

For SNP assay a preformed “TaqMan® SNP Genotyping Assay” is employed: it is available on-line in the catalogue of Applied Biosystems ([http://www3.appliedbiosystems.com/AB\\_Home/index.htm](http://www3.appliedbiosystems.com/AB_Home/index.htm)). As an alternative, you can use the service offered by the same company that, on sending the gene sequence containing the nucleotide variation, develops and tests specifically an assay called "Custom SNP Genotyping assay TaqMan®".

The practical procedure of the TaqMan® technology is very simple and allows to analyze quickly the genotype using a universal mix (master mix) and a solution containing PCR primers and the

two allele-specific probes. The step of sample preparation involves the use of 96-well plates with specific optical properties. The reaction mixture is prepared by combining the specific mix for the SNP under investigation (SNP Assay 20X or 40X), containing primers (sense and antisense) and the two probes labeled with FAM or VIC, to the Master Mix (TaqMan Genotyping Master Mix 2X). The latter one is universal for all genotyping analyses and contains dNTPs, Taq Polymerase, MgCl<sub>2</sub> and salts in a suitable concentration creating an adequately buffered environment. The solution is dispensed into wells and, finally, genomic DNA is added (approximately 20 ng of DNA for each sample).

Once set up, the plate is covered with an adhesive film and centrifuged for a few minutes to eliminate the presence of any air bubbles at the bottom of the wells. Then the plate is loaded into the ABI PRISM 7900HT machine, where the RT-PCR conditions (temperature, duration and cycles) and the test volumes (20 µl) are determined, and the markers (FAM and VIC) are assigned to polymorphism's alleles. The amplification is carried out with a thermal cycler integrated into the instrument using the following thermal profile:

50° C for 2 min;

95° C for 10 min;

40 cycles for (92° C for 15 seconds; 60° C for 1 minute)

At the end of the PCR reaction an end point scanning of the 96-well plate containing the samples is carried out, in order to detect the fluorescence signal produced in each well by the two fluorophores (FAM and VIC) associated to the allele-specific probes. Finally, thanks to the processing of obtained data by software SDS 2.3, the assignment of the genotype corresponding to each sample occurs.

In this thesis, *DPYD-rs67376798*, *DPYD-rs17376848*, and *DPYD-rs1801160* were analyzed by pre-designed TaqMan SNP genotyping assays with the Applera TaqMan Universal Master Mix used on ABI 7900HT (AB Applied Biosystems, Foster City, CA) according to the manufacturer's instructions.

## Direct Sequencing

In 1974, an American team and an English team independently developed two methods to sequence DNA. The Americans, led by Maxam and Gilbert, used a "chemical cleavage protocol", while the English group, led by Sanger, designed a procedure similar to the natural process of DNA

replication (Sanger 1977). Even though both teams shared the 1980 Nobel Prize, Sanger's method became the standard because of its practicality.

Actually, it takes advantage of the peculiar characteristics of the DNA polymerases. These enzymes copy single-stranded DNA templates adding nucleotides to a growing chain. Chain elongation occurs at the 3' end of a primer, an oligonucleotide that anneals to the template. The extension product grows by the formation of a phosphodiester bridge between the 3'-hydroxyl group at the growing end of the primer and the 5'-phosphate group of the incoming deoxynucleotide (Watson et al., 1987).

DNA polymerases can also incorporate analogues of nucleotide bases. The "dideoxy method of DNA sequencing" developed by Sanger takes advantage of this by using 2',3'-dideoxynucleotides (ddNTPs) as substrates. When one of this unnatural ddNTP terminators is incorporated at the 3' end of the growing chain, chain elongation is terminated selectively at A, C, G, or T because the chain lacks a 3'-hydroxyl group (Speed, 1992).

The DNA polymerase used for this method is called AmpliTaq® DNA Polymerase, and it is a mutant form of Taq DNA polymerase containing a point mutation in the active site, replacing phenylalanine with tyrosine at residue 667 (F667Y). This mutation results in less discrimination against dideoxynucleotides, and leads even to a much more peak intensity pattern (Tabor and Richardson, 1995). Moreover, this enzyme contains a point mutation in the amino terminal domain, replacing glycine with aspartate at residue 46 (G46D), which removes almost all of the 5'-3' nuclease activity. This eliminates artifacts that arise from the exonuclease activity.

Furthermore, the enzyme has been formulated with a thermally stable inorganic pyrophosphatase that cleaves the inorganic pyrophosphate (PPi) byproduct of the extension reaction and prevents its accumulation in the sequencing reaction. In the presence of high concentrations of PPi the polymerization reaction can be reversed (Kornberg and Baker, 1992), a reaction called pyrophosphorolysis: in this reaction, a nucleoside monophosphate is removed from the extension product with the addition of PPi to form the nucleoside triphosphate.

In a sequencing reaction, if a dideoxynucleotide is frequently removed at a particular position and replaced by a deoxynucleotide, eventually there is little or no chain termination at that location. This results in a weak or missing peak in the sequence data (Tabor and Richardson, 1990).

The dideoxynucleotides are labeled at 3' with different dyes that are used to identify the A, C, G, and T extension reactions. Each dye emits light at different wavelengths when excited by an argon

ion laser. All four colors and therefore all four bases can be detected and distinguished in a single gel lane or capillary injection (Figure 16).

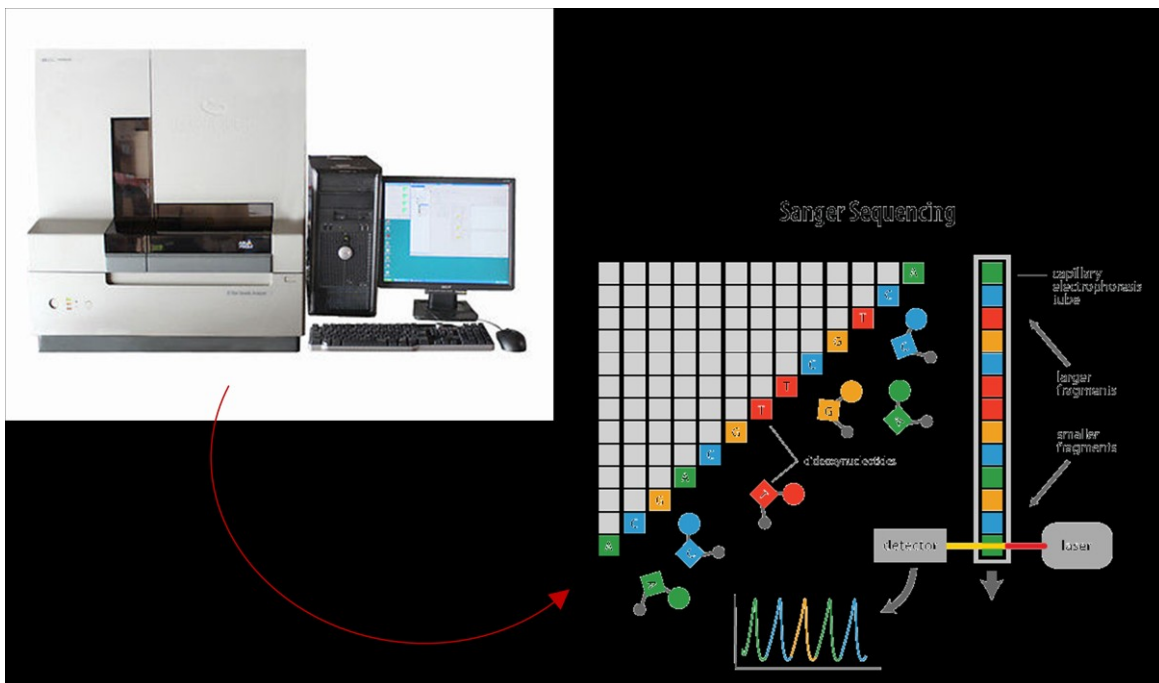


**Figure 16** Schematic representation of automated Sanger sequencing technology.

After PCR amplification, the resulting product is in solution along with PCR primers, dNTPs, enzyme, and buffer components, that could affect the performance of the sequencing reaction and lead to generation of noisy and non-specific data. For this reason, it is necessary to remove them.

There are several methods for purifying PCR products:

- ✓ Column purification
- ✓ Enzyme purification (e.g. EXOsap)
- ✓ Tips purification

In this thesis, we used the Rapid Diffinity Tip2® marketed by Sigma. Diffinity RapidTip2 effectively removes dNTPs, primers, primer dimers and DNA polymerase while providing greater than 90% recovery of pure DNA fragments from 100 bp to 10 kb. The tip is filled with a proprietary adsorption technology that has a differential affinity for PCR components. The impurities are removed from the solution as it enters the pipette tip and, after mixing for just one minute, dispensing the solution yields purified, high quality DNA ready to use for downstream applications is obtained.

After the purification, the amplification step requires the use of a proper mix containing dNTPs and labeled ddNTPs.

For each sample, a 10 µL mix was set-up as listed above:

- 1.2 µL buffer
- 1 µL BigDye (dNTPs, ddNTPs, DNA polymerase)
- 1 µL sequence primer (0.33 µM)
- 4.8 µL milliQ water
- 2 µL purified amplicon

The amplification of the samples takes place following this thermal cycler program:

-96°C 1 min  
-50°C 30 seconds 30 cycles  
-60°C 2 min

All the reactions start from the same nucleotide and end with a specific base, when the dideoxynucleotides are added. Thus, in solution DNA chains with different lengths covering all the nucleotides' positions are obtained <sup>96</sup>. After the amplification, unincorporated dye terminators have to be removed. Excess dye terminators in sequencing reactions indeed can interfere with basecalling. Several protocols are currently used to purify these products. In this thesis, a simple and cheap precipitation method was applied based on the use of a resin-based protocol in 96-well plate format. This resin – generally hydrated superfine Sephadex-G50 – retains salts, reactants, primers and unincorporated dyes while allowing the purified DNA to pass through this matrix during centrifugation. The purified samples are collected in a clean plate.

Once these reactions are completed, the DNA is chemically denatured with formamide and also thermally denatured with a rapid cycle of heating and freezing.

The samples, then, are ready to be loaded in the Genetic Analyzer ABI Prism 3130 (Applied Biosystems, Foster City, CA), where a capillary electrophoresis associated with fluorescence detection happens.

Since the four dyes emit fluorescence signals at different wavelengths, a laser reads the gel to determine the identity of each band. The results are then depicted in the form of a chromatogram, which is a diagram of colored peaks that correspond to the nucleotide in that location in the sequence.

The obtained data are then analyzed using the free download software Chromas lite ([www.technelysium.com.au/chromas.html](http://www.technelysium.com.au/chromas.html)).

In this thesis, four SNPs (*DPYD*-rs55886062, *DPYD*-rs1801158, *DPYD*-rs1801159, *DPYD*-rs2297595) were genotyped by Sanger sequencing. Three of them (*DPYD*-rs55886062, *DPYD*-rs1801158, *DPYD*-rs1801159) were genotyped simultaneously.

The region of interest was amplified using primers forward 5'- CGGATGCTGTGTTGAAGTGATT-3' and reverse 5'- GTGTAATGATAAGTCTTGTCAAATAGT-3', designed using the web-based tool primer3plus (<http://www.bioinformatics.nl/cgi-bin/primer3plus/primer3plus.cgi>). PCR products were amplified using AmpliTaq Gold® DNA Polymerase.

The PCR thermal profile is the following: 10 min denaturation at 95°C then 37 cycles of 30 s denaturation at 95°C, 30 s annealing 63°C and 30 s extension at 72°C and a last cycle consisting of 7 min extension at 72°C.

The region containing the other SNP analyzed with Sanger sequencing (*DPYD* rs2297595) was amplified using these primers: forward 5'-TGTTGAGGATGTAAGCTAGTTCA-3' and reverse 5'-AAACTGAAACATTGGAAAAAGAACCA-3'. PCR products were amplified using AmpliTaq Gold® DNA Polymerase .

PCR conditions were: 10 min denaturation at 95°C then 37 cycles of 30 s denaturation at 95°C, 30 s annealing 61°C and 30 s extension at 72°C and a last cycle consisting of 7 min extension at 72°C.

#### **4.1.4. CLINICAL DATA COLLECTION AND ELABORATION**

Patients' clinical data have been collected by oncologists using the suitable created Case Report Form (CRF) (see results).

All personal and clinical data were catalogued in appropriate databases, prepared in accordance with the Privacy Policy, in order to be associated with genetic data.

#### **4.1.5. STATISTICAL ANALYSIS**

Clinical data are presented as means and standard deviation or as absolute frequencies and percentages as appropriate.

Differences in mean were analyzed with Mann–Whitney test, whereas differences in absolute frequencies were analyzed with Fisher exact test. The frequency of each variant was compared with the published frequencies in dbSNP and tested for deviation from Hardy–Weinberg equilibrium.

Multivariate logistic regression analysis was used to access variables independently associated with toxicity, and the following variables were considered for inclusion: sex, age, association therapy, FL administration, administration setting and *DPYD* polymorphisms. In case of complete or quasicomplete separation (as in the case of rare allelic variants) a penalized model was used (Firth model). Model evaluation was performed using a bootstrap approach. The bootstrap resampling technique was used to confirm the reliability of the final parameter estimates and their 95% confidence intervals (CI). The median and bootstrapped 95% CI of the ORs were obtained from 2000 bootstrap replicates.

An explorative analysis was carried out for *DPYD*-rs2297595, *DPYD*-rs1801160, *DPYD*-rs1801158, *DPYD*-rs1801159, and *DPYD*-rs17376848 to investigate a possible clinical effect of these SNPs. We performed this exploratory analysis in a selected subgroup of cases. Specifically, we compared the group of all the patients with at least one event Grade 3 or more during the first three cycles of FL-therapy (95 cases) with a control group randomly extracted from the set of patients without severe toxicity (Grade 0–2 only) and homogeneous for the most relevant clinical demographic characteristics (i.e., age, association therapy, FL administration, and setting). In order to have at least three controls for each toxicity case, 315 subjects were selected. The frequencies *DPYD* variants in this subgroup population should reflect the incidences in the overall population of controls used for comparison with the cases.

In order to define the clinical validity of a pre-treatment *DPYD* test, the diagnostic power of the were calculated.

The following terms are fundamental to understanding the validity of clinical tests:

1. True positive: the patient has the disease and the test is positive.
2. False positive: the patient does not have the disease but the test is positive.

3. True negative: the patient does not have the disease and the test is negative
4. False negative: the patient has the disease but the test is negative (Figure 17).

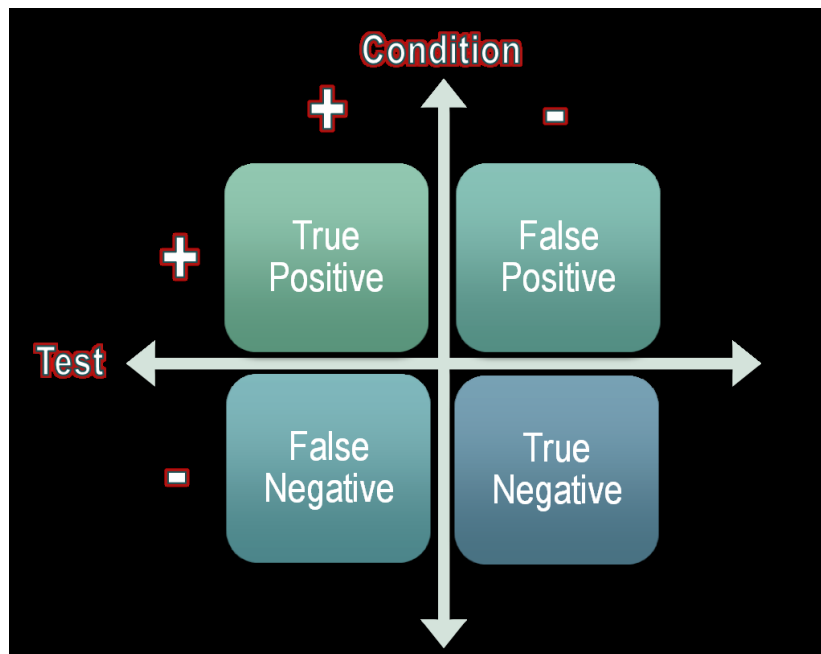


**Figure 17** Schematic representation of the fundamental parameters to define the validity of a clinical test. The condition represents the presence (+) or absence (-) of severe toxicity, while the test represents the presence (+) or absence (-) of the variant allele.

When evaluating a clinical test, the terms sensitivity and specificity are used. They are independent of the population of interest subjected to the test.

The sensitivity of a clinical test refers to the ability of the test to correctly identify those patients with the disease.

$$\text{Sensitivity} = \frac{\text{True positives}}{\text{True positive} + \text{False negatives}}$$

The specificity of a clinical test refers to the ability of the test to correctly identify those patients without the disease.

$$\text{Specificity} = \frac{\text{True negatives}}{\text{True negatives} + \text{False positives}}$$

The terms positive predictive value (PPV) and negative predictive value (NPV) are used when considering the value of a test to a clinician and are dependent on the prevalence of the disease in the population of interest.

The PPV of a test is a proportion that is useful to clinicians since it answers the question: 'How likely is it that this patient has the disease given that the test result is positive?'

$$\text{Positive predictive value} = \frac{\text{True positives}}{\text{True positives} + \text{False positives}}$$

The NPV of a test answers the question: 'How likely is it that this patient does not have the disease given that the test result is negative?'

$$\text{Negative predictive value} = \frac{\text{True negatives}}{\text{True negatives} + \text{False negatives}}$$

P Values less than 0.05 were considered as statistically significant. A Bonferroni correction for multiple testing of three SNPs (*DYPD*-rs3918290, *DYPD*-rs55886062, and *DYPD*-rs67376798) was applied for p obtained from bootstrap approach.

All the analyses were carried out with Stata 11.2 (Stata-Corp, TX).

## 4.2. SUNITINIB PROJECT

### 4.2.1. HIGH PERFORMANCE LIQUID CHROMATOGRAPHY COUPLED WITH MASS SPECTROMETRY METHOD

Mass spectrometry is a powerful analytical tool for both drug quantitative and qualitative analysis. In particular, Accurate and sensible quantification is obtained by operating in tandem mass (MS/MS) mode. MS/MS is necessary because many compounds have the same intact mass, while the fragmentation pattern is compound specific. The combination of parent mass and its fragment ions is used to monitor selectively the compound that has to be quantified. MS/MS fragmentation is also fundamental for qualitative information, because the mass spectrum of every compound is unique and it can be used like a chemical fingerprint to characterize the sample, even in case where only picogram amounts of analyte are available.

Moreover, coupling the mass spectrometer with LC provided significant improvements in assay sensitivity, specificity and capability to analyze samples with very different concentration ranges. Indeed, LC-MS has become the method of choice for quantitative drug analysis to support PK and

drug metabolism studies<sup>97</sup>. The increase in sensitivity and specificity caused three important effects:

- ✓ the possibility to detect drugs and metabolites at very low concentration;
- ✓ the possibility to use very small amount of sample (that is particularly important in preclinical studies conducted in small animals or in pediatric studies);
- ✓ a selective analytes detection in presence of complex matrices such as tissues or whole blood.

In LC-MS experiment the sample is introduced into the mass spectrometer after its separation in a LC column. Charged ions of the analytes are then produced into the ion source of the mass spectrometer. These ions are separated by the MS analyzer on the basis of their mass to charge ( $m/z$ ) ratio. There are different types of MS ion sources, but the most commonly used in pharmacokinetic studies is Electrospray Ionization (ESI), an atmospheric pressure ionization.

ESI is a soft ionization technique and does not cause decomposition of labile compounds. It is characterized by an efficient ion production, mainly by protonation or cationization reactions, and it can operate in either positive or negative ion mode.

Electrospray spectra are produced by passing a liquid stream through a metal capillary maintained at high voltage (2000-5000 V). This forces the spraying of charged droplets from the needle with a surface charge of the same polarity of the charge on the needle.

In a typical ESI source (Figure 18), the solution is injected in a stainless steel capillary. Between this capillary and their counter electrode, a voltage in the order of 3–5 kV is applied. Under these conditions, the formation of a solution cone just outside the capillary occurs. The cone formation is due to the presence of charged species inside the solution, which experiment the electrostatic field existing between the capillary and the counter electrode<sup>98</sup>. After the cone production, the droplets formation from the cone apex is observed, charged droplets further migrate through the atmosphere to the counter electrode<sup>98</sup>. Droplets formation is strongly influenced by solvent chemical–physical characteristics, ionic analytes concentration, inorganic salts concentration, and the applied voltage. The so generated charged droplets decrease their radius after solvent evaporation still conserving their total charge amount. The energy required for the solvent evaporation is due to the environment thermal energy, further enhanced through by the use of a heated capillary or by collisions with heated gas flow. As the droplet radius decreases, the surface charge density increases; when the radius reaches the Rayleigh stability limit, the electrostatic repulsion equals the surface tension. For lower radii, the charged droplets are unstable and

decompose through a process defined “Columbic Fission” <sup>99</sup>. This produces smaller droplets that ultimately liberate unsolvated charged analyte molecules.

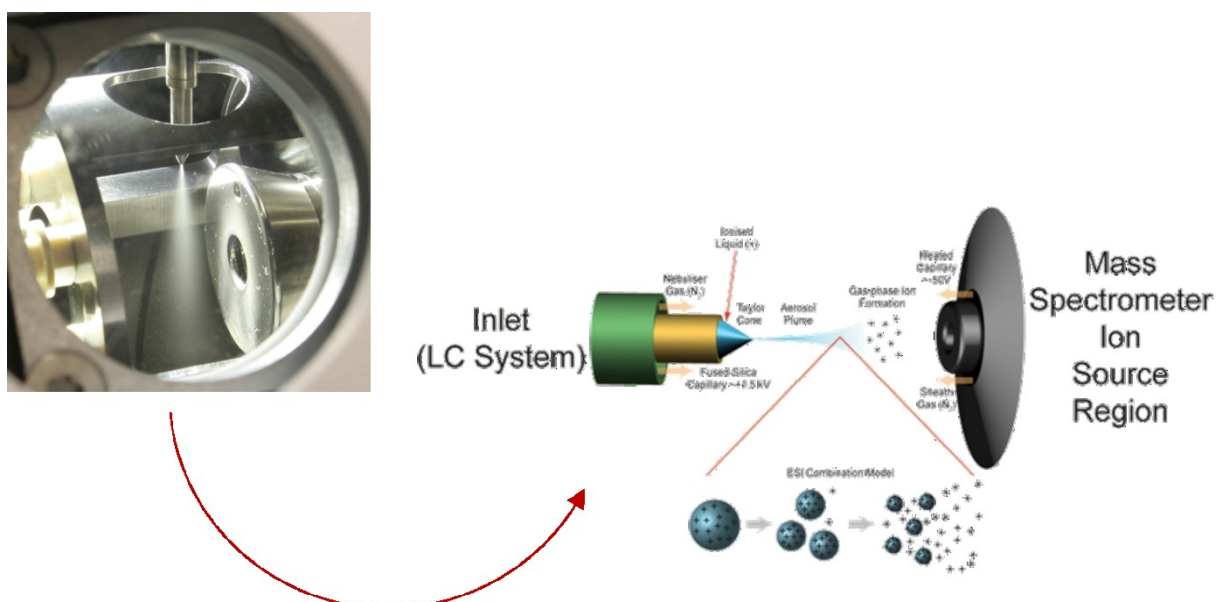


**Figure 18** Schematic representation of the ions formation process in positive ESI source. Under these conditions the capillary is placed at a positive voltage, while the counter electrode is placed to a negative voltage.

From the ion source, ions are transferred to the mass spectrometer, where they are analyzed.

A triple quadrupole mass spectrometer is characterized by three consecutive quadrupole analyzers: the first and the third ones work as mass filters, while the second as a collision cell. A quadrupole consists of four parallel rods arranged symmetrically around a central axis.

Opposite rod pairs are connected electrically and a voltage, consisting of both radiofrequency (RF) and direct-current (DC) components, is applied with the RF components on the different pairs being 180° out of phase. The RF value is a constant of a specific quadrupole type, while the DC voltage is varied in order to allow only ions of a particular  $m/z$  to follow a stable trajectory through the rods and reach the detector, while all other ions hit the quadrupoles because of their unstable path.

According to the aims of the analysis, the first and the third quadrupole can be used in different scan modes to acquire and visualize data. Each quadrupole can be set to filter only one  $m/z$  ratio or to scan over a wide  $m/z$  range. The most common scan mode for a quantitative analysis is defined as Selected Reaction Monitoring (SRM), characterized by the use of two quadrupoles as mass filters: the first quadrupole selects the precursor ion of the analyte and the second, after fragmentation in the collision cell, selects the specific product ion.

Several steps are needed to optimize every phase of a bioanalytical method. In particular, the set-up considered:

- ✓ the definition of the processing method for the analytical samples,
- ✓ the optimization of the chromatographic conditions,
- ✓ the optimization of the MS/MS conditions.

#### **4.2.2. DEVELOPMENT OF A BIOANALYTICAL METHOD**

##### **Standards and chemicals**

Analytical reference standard of sunitinib was purchased from Sigma-Aldrich Co. (Milan, Italy) while N-desethyl sunitinib and the deuterated internal standard sunitinib D10 were purchased from Toronto Research Chemicals, Inc. (North York, Ontario, Canada). LC-MS grade methanol and formic acid were supplied by Sigma-Aldrich Co. (Milan, Italy) and Baker (JT Baker, Deventer, NL), respectively. Filtered, deionized water was obtained from a Milli-Q Plus system (Millipore, Billerica, MA, USA). The transfusion unit of the National Cancer Institute (Aviano, Italy) provided control human plasma/K<sub>2</sub>EDTA, used to prepare daily standard calibration curves and quality control (QC) samples from healthy volunteers.

##### **Standards and quality control solutions**

Stock solutions for sunitinib, N-desethyl and IS were prepared in dimethyl sulfoxide (DMSO) at a concentration of 1.00 mg/mL. Dilution in acetonitrile from the solutions of sunitinib and N-desethyl sunitinib (for standards and QC) were prepared at concentration of 100 µg/mL, 10 µg/mL and 1 µg/mL. A series of working solutions (G to A) to prepare the plasma standard points of the calibration curve and the plasma QC samples (L, M and H) were obtained by mixing and diluting the stock. The IS working solution was prepared at 0.1 µg/mL by diluting the stock solution with acetonitrile. All the solutions were kept in polypropylene tubes and stored at -80°C.

##### **Preparation of standards and quality control samples**

A seven-point plasma calibration curve was prepared freshly every day during the validation study. Each calibration sample was prepared by adding 1.5 µL of the respective standard solution from G to A (ULOQ) to 28.5 µL of pooled blank human plasma to obtain the final concentrations reported in Table 4. Each calibration curve included a blank sample and a zero blank sample (plasma

processed with the IS). At least three concentrations of quality control (QC) need to be prepared: one within three times the LLOQ (low QC), one in the midrange (middle QC), and one approaching the high end (high QC) of the range of the expected study concentrations.

To prepare QC samples, 1.14 mL aliquots of control human plasma were mixed with 60 µL of each working QC solutions (L, M and H) obtaining the QC plasma concentration reported in Table 4. Several 30 µL-aliquots of the three QCs were stored at -80°C to check the analytes stabilities and as controls for future assays.

	SUNITINIB (ng/mL)	N-DESETHYL SUNITINIB (ng/mL)
G	0.1	0.1
F	0.5	0.5
E	10	2.5
D	50	10
C	100	50
B	250	100
A	500	250
QC L	0.25	0.1
QC M	25	25
QC H	400	250

**Table 4** Final concentrations of calibration curve points and QC.

## Processing samples

After have thawed plasma samples, they were vortexed for 10 s and centrifuged at 3000 g for 10 min. Then 30 µL of the actual sample, standard or QC sample were transferred to a 1.5 mL Eppendorf polypropylene tube, and 1.5 µL of the IS working solution (0.1 µg/mL) were added and the mixture was vortexed.

Plasma is rich in proteins, lipids and other contents that may interfere with the investigational drug. The complexity of the biological matrix presents challenges for efficient sample preparation and adequate sensitivity for mass spectrometry analysis of drugs. For this reason, a protein precipitation is made adding 150 µL of CH<sub>3</sub>OH. Each tube was thoroughly vortexed for 10 s and centrifuged at 13000 g for 10 min. Then 100 µL of the obtained supernatant were transferred to an autosampler glass vial pending analysis.

Since all the sample handling steps described above occur without any light-protection, we have introduced an additional step in order to revert the isomerization and thus to obtain only the

active Z-isomer that we want to measure. For this reason, the samples were heated at 90°C for 5 min in a thermostatic bath and, then, transferred into the autosampler. This last step is the only one in the entire processing procedure that needs to be done in the dark (Figure 19).

Different amounts (2–5 µL), inversely related to the concentrations, were injected into the HPLC system to minimize the carry-over effect. Moreover, after the injection of the ULOQ, three samples of mobile phase and one blank sample were injected to demonstrate the absence of carry-over effect. This procedure guaranteed that no peak higher than 10% of LLOQ was detected.

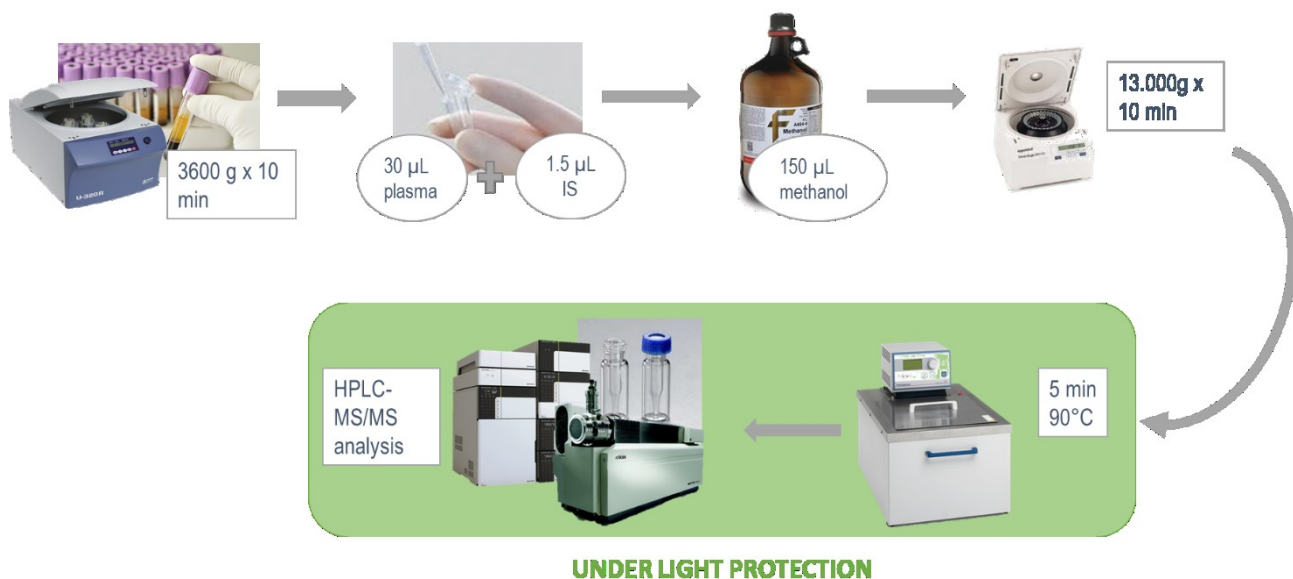


**Figure 19** Schematic representation of the processing sample procedure.

## Chromatographic conditions

The HPLC system consisted of a SIL-20AC XR auto-sampler and LC-20AD UFCL XR pumps (Shimadzu, Tokyo, Japan). Samples were separated on a Synergy Fusion RP C18, 4 µM, 80 Å, 2 x 50 mm (pre-column: Gemini-NX C18 4.0 x 2.0 mm) and thermostatically controlled at 50°C. The mobile phases were 0.1% CHOOH/bidistilled water (MP A) and 0.1% CHOOH/acetonitrile (MP B).

The HPLC system was set up with a flow rate of 0.3 mL/min and the following linear gradient:

step 1: the initial condition of 90% MP A held for 0.5 min;

step 2: from 90% MP A to 30% over 1 min;

step 3: constant for 1.2 min;

step 4: from 30% MP A to 60% over 0.3 min;

step 5: : from 60% MP A to the initial condition over 0.5 min and reconditioning for 4 min.

The total run time was 7.5 min.

## **Mass spectrometry conditions**

The HPLC system was coupled with an API 4000 triple quadrupole mass spectrometer AB SCIEX (Massachusetts, USA). Standard solutions prepared in 0.1% CH<sub>3</sub>COOH acetonitrile/ water 1:1 (50 ng/mL) of sunitinib, n-desethyl sunitinib, and IS were infused at a flow rate of 10 µL/min in order to optimize all the MS parameters. Positive ion mode was used to obtain the mass spectra (MS1) and the product ion spectra (MS2). The instrument was equipped with a Turbo Ion Spray source operated at 625°C and with ion spray voltage of 5000 V. The biological samples were analyzed with electrospray ionization (ESI), using zero air as nebulizer gas (30 psi) and as heater gas (70 psi). Nitrogen was employed as curtain gas (20 psi) and as collision gas at medium intensity (CAD). After fragmentation, the characteristic product ions of the compounds were monitored in the third quadrupole at *m/z* 326, *m/z* 283 and *m/z* 238.

Quantification was done in SRM mode using the following transitions: *m/z* 399 > 326 for sunitinib, *m/z* 371 > 283 for N-desethyl sunitinib, and *m/z* 409 > 328 for IS. To quantify the chromatographic peaks, data were processed with Analyst 1.5.2 (quantification with MultiQuant 2.1) software package (AB SCIEX).

### **4.2.3. VALIDATION OF A BIOANALYTICAL METHOD**

Selective, sensitive, and validated analytical methods for the quantitative evaluation of drugs and their metabolites are critical for the successful conduct of nonclinical and clinical pharmacology studies. Indeed, the quantitative measurements of drugs, metabolites, and biomarkers in nonclinical and clinical studies provide essential information in the assessment of safety and efficacy of drugs. Drug or biomarker concentrations frequently serve as the primary or secondary endpoints of many clinical studies in drug development. Consequently, the reliability or quality of that data underpins the study outcome<sup>74,100</sup>. For this reason, validating bioanalytical methods includes performing all of the procedures that demonstrate that a particular method used for quantitative measurement of analytes in a given biological matrix (e.g. blood, plasma, serum, or urine) is reliable and reproducible for the intended use<sup>74</sup>.

The measurements should be based on established principles and scientists should utilize a common, vetted paradigm of practices, independent of the analytical platform to demonstrate that the assays provide reliable data. The necessity to establish the main guiding principles for the validation of the analytical method and to disseminate them to the pharmaceutical community

was received, in 1990, by the first American Association of Pharmaceutical Scientist (AAPS)/ FDA Bioanalytical Workshop <sup>101</sup>. Scientists in the bioanalytical field worked with the regulatory community to establish a common language and expectations in generating pharmacokinetic data for drugs and metabolites. These validation principals were introduced into regulations by Health Canada in 1992 <sup>102</sup> and then by the FDA which published the first edition of its Guidance on Bioanalytical Method Validation in 2001 <sup>103</sup>.

This guidance explains the course of action for the validation of analytical procedures such as gas chromatography; high-pressure liquid chromatography; GC-MS; LC-MS; ligand binding assays, immunological assays and microbiological procedures. In doing so the specific features of these methods in the quantitative determination of drugs and metabolites in biological matrices, such as blood, serum, plasma, urine and different tissues are taken into account. Validation involves documenting, through the use of specific laboratory investigations, that the performance characteristics of the method are suitable and reliable for the intended analytical applications. The acceptability of analytical data corresponds directly to the criteria used to validate the method. Fundamental parameters for this validation include the following: accuracy, precision, selectivity, sensitivity, reproducibility, stability. The FDA guidance described in detail all this parameters and the correct way to validate them.

Since the publishing of this guidance in 2001, the dialogue has broadened significantly through scientific conferences not only within the USA, but globally. In 2011 the Guidance on Bioanalytical Method validation was introduced in EU <sup>75</sup>. Successively, in September 2013 the FDA released a draft revision of the Guidance for Industry Bioanalytical Method Validation that included a number of changes to the expectations for bioanalysis<sup>74</sup>.

In particular, taking into account the AAPS/FDA Workshop on Incurred Sample Reanalysis <sup>104</sup>, this revised version has introduced an additional measure of assay reproducibility: the Incurred Sample Reanalysis (ISR). This analysis is now well established as an important element of bioanalysis and is intended to verify the reliability of the reported subject sample analyte concentrations. ISR is conducted by repeating the analysis of a subset of subjects' samples from a given study in a separate run to critically support the performance of assays.

## **Recovery**

The percentage extraction recovery was determined for each analyte (sunitinib, N-desethyl sunitinib, IS) at three plasma concentrations (QCL, QCM and QCH) prepared in quintuplicate. The peak area of each analyte extracted from plasma QC samples were compared to those from standards prepared in methanol.

The recovery of IS is evaluated in the same way at a plasma concentration of 0.1 µg/mL. The recovery experiments were performed at three different concentrations (QCL, QCM and QCH). Moreover, for every analyte and IS, the percentage recovery was even determined by comparing the peak area of the analyte extracted from plasma QC samples, prepared at the three concentrations, with the peak area of the extracted matrix prepared in five replicates and added with the same amount of the analytes.

Recovery of the analyte and the IS need not to be 100%, but it is important that the extent of recovery is consistent, precise and reproducible.

## **Linearity**

The linearity of the calibration curves was validated over five different working days. Each day, a calibration curve was prepared by spiking the biological matrix with known concentrations of the analyte (as reported in Preparation of Standard and Quality Control samples section) to define the relationship between concentration and instrument response. It consisted of seven standard points in a range chosen on the base of expected concentrations in the samples and was obtained using the same biological matrix of samples to measure. For each standard point, the ratio of the HPLC–MS/MS peak area for sunitinib and N-desethyl sunitinib to the IS was calculated and plotted against the nominal concentration of each analyte in the sample.

The linearity for each calibration curve was assessed by weighted least squares method, using  $1/x^2$  as weighting factor.

The y axis intercept ( $q$ ) and the slope ( $m$ ) of the equation  $y = mx + q$  were calculated elaborating the  $y_j$  and  $x_i$  values obtained from the calibration points, where:

$$y_j = \frac{A_j}{A_{is}} \quad A_j = \text{peak area of the } j\text{-eme analyte}$$

$A_{is}$  = peak are of the Internal Standard

$x_i$  = actual concentration of the analyte in the curve point sample.

The goodness of the fitting was evaluated by the Pearson's determination coefficient  $R^2$ .

The reproducibility of each calibration curve was assessed by the mean, standard deviation (SD) and coefficient of variation (CV%) of the estimated m and  $R^2$ . The back-calculated values of individual calibrants had to be within  $\leq 15\%$  of their theoretical concentration ( $\leq 20\%$  at the limit of quantitation).

### **Intra-day and inter-day precision and accuracy and reproducibility**

Precision and accuracy of the method were evaluated on five different days by determining the analyte in three replicates at different nominal concentrations corresponding to the three quality control (QC) samples. Five different standard calibration curves were prepared and processed each day to analyze the QCs.

The precision of an analytical method describes the closeness of individual measures of an analyte when the procedure is applied repeatedly to multiple aliquots of a single homogeneous volume of biological matrix. This parameter, at each QC concentration, was reported as the CV%, expressing the standard deviation as a percentage of the mean calculated concentration and it must not exceed 15% of CV.

The accuracy of an analytical method describes the closeness of mean test results obtained by the method to the actual value (concentration) of the analyte. This parameter was determined by expressing the mean calculated QC concentration as percentage of the nominal concentration. In each run, the measured concentration for at least six out of nine QC samples had to be within 15% of the nominal value. Only one QC sample could be excluded at each concentration level.

ISR is intended to verify the reliability of the reported subject sample analyte concentrations. ISR is conducted by repeating the analysis, with the same bioanalytical method procedures, of a subset of subject samples from a given study in separate runs on different days to critically support the precision and accuracy measurements established with spiked QCs. The selection of samples for reanalysis should be done guaranteeing adequate coverage of the PK profile in its entirety including a sample around the maximum concentration ( $C_{max}$ ) and in the elimination phase. The analyses can be considered equivalent if two-thirds (67%) of the percentage difference [ $(repeat-original)*100/mean]$  of the results is within 20%.

## **Limit of detection, limit of quantification and selectivity**

The limit of detection (LOD) was defined as the concentration at which the signal-to noise ratio was 3. The limit of quantitation (LOQ) was defined as the smallest amount of the analyte that could be measured in a sample with sufficient precision and accuracy (within 20% for both parameters) and as the concentration at which the signal-to-noise (S/N) ratio was at least 5. The LOQ was chosen as the lowest concentration on the calibration curve (LLOQ).

The LLOQ of the present method was assessed by adding G working solution to six samples of blank human plasma. Selectivity was proved using six independent sources of blank human plasma, which were individually analyzed and evaluated for interference: a single 28.5 µL-aliquot from each of the six matrices was spiked with the analytes at the LLOQ concentration. Both LLOQ and selectivity had to have acceptable accuracy (20%) and precision (between 80% and 120%).

## **Matrix effect**

Matrix effects arise due to effects of endogenous components of the plasma matrix on the ionization of the analytes of interest and IS. In the ESI source a process of charging and desolvation transforms the analytes in the liquid phase into gas ions that are introduced in MS analyzer. It seems clear that the coeluting compounds interfering with either the desolvation or the charging step alter the ionization of the analyte<sup>105</sup>. Although they are generally the principal cause, not only endogenous components in the biological matrix (e.g. salts, amines, triglycerides) cause matrix effect, also some exogenous compounds (plasticizers from sample containers or anticoagulants in case of plasma) are susceptible to alter the ionization process<sup>106</sup>. Furthermore, other substances can be present in the mobile phase and can alter the signal of the analyte by causing ion suppression or enhancement. Nevertheless this is not considered a ME source since it is not sample specific<sup>105</sup>.

Current FDA requirements underline the importance to assess this phenomenon in mass spectrometry, because it may compromise the precision, the accuracy, the sensitivity and the selectivity of the developed method and, consequently, the reliability of analytical data produced. The same definition reported in the FDA guidance for matrix effect is given by EMA in the *Guideline on bioanalytical method validation of 2011*<sup>75</sup>. Both guides agree that the variability in the matrix effect, which would cause lack of reproducibility in the method, should be studied using six lots of blank matrix from individual donors. Indeed, a quantitative evaluation of matrix effect should be achieved by comparing the response of the analyte in solvent to the response obtained

by spiking the analyte into six extracted independent sources of black human plasma. The matrix effect is calculated as the ratio of the peak area in the presence of matrix to the peak area in absence of matrix at the three different QC concentrations (L, M and H) of each analyte. The CV should be within 15%.

In addition, a common method to evaluate qualitatively the matrix effect is the post-column infusion, described by Bonfiglio and colleagues <sup>107</sup>, which permits to identify the chromatographic region where the matrix effect manifests itself <sup>105</sup>. A constant concentration of the analyte is introduced in the ion source of the mass spectrometer by using an infusion pump connected with a zero-dead-volume “T” junction after the HPLC column, while a blank extracted sample is injected onto the chromatographic system. The signal of the infused drug, followed in a SRM scan mode, is steady, unless endogenous components eluting from the column cause a reduction or a gain of the response. To assure the reliability of the results, it is important that these ion suppression or enhancement effects do not happen near the analyte’s retention time. To perform the post-column infusion experiments standard solutions, prepared in 0.1% CH<sub>3</sub>COOH acetonitrile/water 1:1 (50 ng/mL) for each analyte and IS, were infused by a syringe pump.

## **Stability**

Studying the stability of the analyte in stock solutions and matrix is vital to ensure the reliability of the results provided by the analytical method. These include assessments that cover all the situations that can be encountered during the whole analytical procedure such as freeze-thaw stability, short and long term stability, stock stability and post preparative stability.

The stability of the analyte of interest was evaluated by analyzing the QC matrix samples in triplicate at each QC concentration level. Bench-top stability was determined after 4 h at room temperature and the stability of the processed samples in the autosampler was assessed by repeatedly analyzing the processed QC samples 24, 48 and 72 h after the first injection. To check freeze/thaw stability, a freshly prepared aliquot of each QC sample concentration was processed and analyzed, and then again after one and two freeze/thaw cycles. Long-term stability need to be assessed in plasma and in working solutions stored at approximately -80°C. Each analyte was considered stable at each concentration when the differences between the freshly prepared samples and the stability of testing samples did not deviate more than 15% from the nominal concentrations.

## **4.3. IRINOTECAN PROJECT**

The title of the genotype-guided phase 1b study in which I am involved is “*A genotype-guided phase 1 study of irinotecan administered in combination with 5-fluorouracil/leucovorin (FOLFIRI) and cetuximab as first-line therapy in metastatic colorectal cancer patients*”. The protocol of this trial has been revised and approved by the CRO ethical committee, the AIFA (Agenzia Italiana del Farmaco) and the ISS (Istituto Superiore di Sanità) and the main characteristics of this study are briefly described above.

### **4.3.1. PATIENTS CHARACTERISTICS**

The eligibility criteria for this study are:

- ✓ histologically or cytologically confirmed diagnosis of mCRC expressing EGFR;
- ✓ RAS wild-type status;
- ✓ no prior chemotherapy for metastatic disease;
- ✓ age  $\geq 18$ ;
- ✓ Eastern Cooperative Oncology Group (ECOG) performance status (PS) of 0 or 1;
- ✓ life expectancy  $> 3$  months;
- ✓ measurable or evaluable disease (defined as  $> 1$  cm on spiral computed tomography scan);
- ✓ adequate organ function, including bone marrow (absolute neutrophil count (ANC)  $\geq 1500/\mu\text{L}$ , haemoglobin  $\geq 9\text{g/dL}$ , platelets  $\geq 100000/\mu\text{L}$ ); hepatic (total bilirubin  $< 1.6 \text{ mg/dL}$ , international normalized ratio or  $\leq 2x$  for Gilbert's Syndrome, aspartate aminotransferasealanine aminotransferase  $< 2.5 \times$  upper limit of normal for patients without liver metastases,  $< 5 \times$  upper limit of normal for patients with liver metastases); and kidneys (serum creatinine  $\leq 1.5 \times$  upper limit of normal) function;
- ✓ patients who are eligible to be registered in the study, based upon the above criteria, will be genotyped for *UGT1A1\*28* polymorphism and stratified into two groups based on the presence of *\*1/\*1* or *\*1/\*28* genotype. Patients with both variant alleles *\*28/\*28* will be excluded;
- ✓ for patients valuable for response (secondary end point), at least one measurable cancer lesion as defined by RECIST, i.e. lesions that can be accurately measured in at least one

- dimension with the longest diameter  $\geq 20$  mm using conventional techniques or  $\geq 10$  mm using spiral computerized tomography scan;
- ✓ signed informed consent and local ethical committee approval are requested.

The exclusion criteria are:

- ✓ cardiac pathology (cardiac decompensation, infarction during the period of 6 months preceding the study, atrioventricular block, serious arrhythmia);
- ✓ patients with specific contraindications for the use of EGFR inhibitors (pulmonary fibrosis, interstitial pneumonia history);
- ✓ unresolved diarrhea and bowel obstruction;
- ✓ hemorrhagic syndrome;
- ✓ documented cerebral metastasis;
- ✓ serious active infectious disease;
- ✓ serious functional alteration of visceral and metabolic disease;
- ✓ pregnancy status;
- ✓ radiotherapy or major surgery within 4 weeks;
- ✓ all patients in fertile age must have been under contraceptive treatment;
- ✓ presence of previous or concomitant neoplasm with exclusion of in situ cervical cancer;
- ✓ non collaborative and/or unreliable patients;
- ✓ patients with a chronic toxicity  $\geq$  grade 2;
- ✓ refusal of informed consent;
- ✓ patients who could not attend periodic clinical check-ups.

#### **4.3.2. DRUG ADMINISTRATION, DOSE ESCALATION AND DLT/MTD DEFINITIONS**

Patients will be treated with FOLFIRI regimen plus cetuximab, where CPT-11 will be administered at doses higher than the standard dose in patients with *UGT1A1 \*1/\*1* and *\*1/\*28* genotypes.

The starting dose of CPT-11 for the two groups of patients (*UGT1A1 \*1/\*1* and *\*1/\*28* groups) will be  $260 \text{ mg/m}^2$  administered as a 120 min intravenous infusion every 2 weeks.

The dosage of CPT-11 was escalated applying a “3 + 3” cohort expansion design to reach the maximally tolerated dose (MTD)<sup>108</sup>.

The rationale for the 3 + 3 cohort expansion design is pragmatic with regard to determining toxicity-based dose escalation. Three patients are required for the initial cohort size in order to determine whether a 33% toxicity rate has been reached and, in this case, dose-escalation has to be stopped. Treatment may be escalated to the next higher dose level if no DLT occurs; however, if one drug-related DLT occurs in these three patients, the cohort is expanded to six patients to verify that the toxicity rate has reached 33% (i.e., two of six or fewer patients). When the toxicity rate reaches 33% in a cohort, the next lower dose level will be called the MTD and the cohort will be expanded typically to 10 patients total to establish the preliminary safety profile of the study agent<sup>109</sup> (Figure 20)

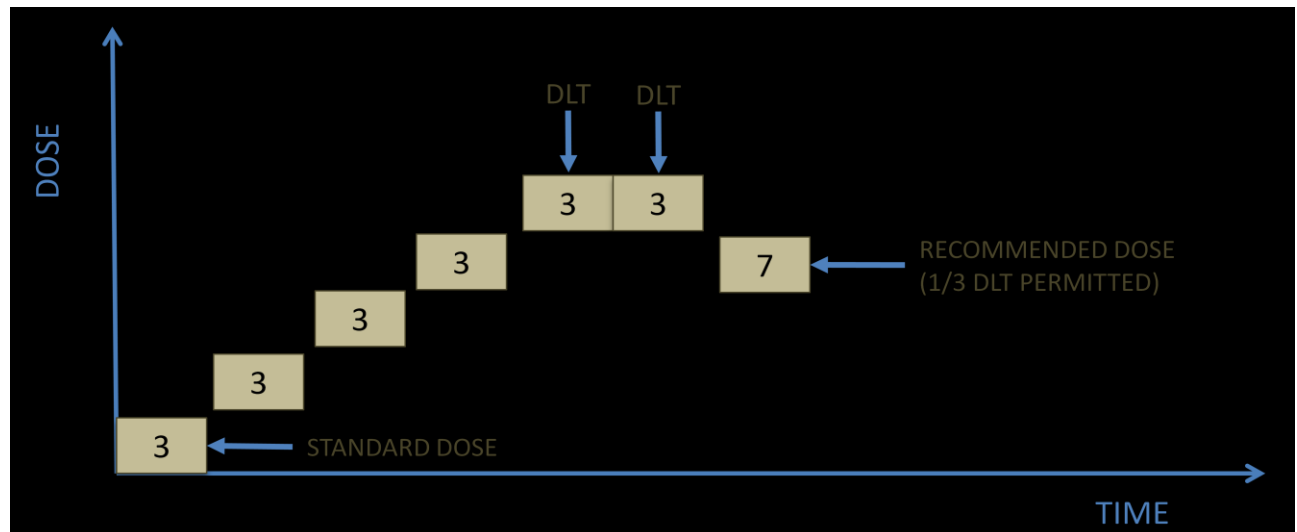


**Figure 20** Schematic description of the 3+3 cohort expansion design.

Applying this design, the dosage of CPT-11 will be increased to 310, 370, and 420 mg/m<sup>2</sup>, and further CPT-11 doses will be increased of 14%; 5-FU will be administered as 400 mg/m<sup>2</sup> bolus right after the end of the CPT-11 infusion, followed by 2400 mg/m<sup>2</sup> over a 46-h continuous infusion plus LV 200 mg/m<sup>2</sup> every two weeks. Cetuximab will be administered every two weeks as an intravenous infusion at a dose of 500 mg/m<sup>2</sup> with prophylactic intravenous steroids and anti-histaminic agents. No dose modification will be performed for 5-FU, LV and cetuximab. One cycle is 28 days (two CPT-11 administrations). Before starting CPT-11, patients will be pre-treated with atropine 0.5 mg, dexamethasone 8 mg, granisetron 3 mg or ondansetron 8 mg. Diarrhoea will be promptly treated with loperamide 4 mg at the onset, and then with 2 mg every 2 h, until the patient will be diarrhoea-free for at least a minimum of 12 h. Growth factors (i.e., G-CSF) will be allowed only in patients who will have Grade ≥ 3 neutropenia at previous cycles.

DLT is defined as haematological Grade 4 toxicity or non-haematological grade 3-4 toxicity and developed or persisted despite supportive measures (i.e. anti-diarrhoeas or anti-emetics). DLT will be evaluated during the first cycle of chemotherapy. Toxicity is classified and graded according to the United States NCI's common toxicity criteria (version 4.03).

The cumulative haematological and non-hematological toxicities as well as the number of dose reductions and a delay in starting the next cycle of treatment will be used as secondary indicators to differentiate the two genotype cohorts of patients.

Patients can continue receiving the same dose of CPT-11 in absence of major toxicity according to the following criteria: before re-treatment, full recovery from any non-hematological toxicity, absolute neutrophil count  $\geq 1500/\mu\text{L}$  and platelet count  $\geq 100000/\mu\text{L}$ , are required. Chemotherapy is discontinued on evidence of disease progression, or the appearance of new lesions on serial magnetic resonance or CT scans.

#### **4.3.3. PHARMACOKINETICS STUDIES**

To improve the current knowledge about the potential pharmacokinetic and pharmacodynamic interactions between cetuximab and CPT-11, this open label drug-drug interaction study evaluates the pharmacokinetic profile of CPT-11 in absence and presence of cetuximab in the same patient within the first chemotherapy cycle.

In all patients enrolled in the study and at each dose level, the pharmacokinetic profile of CPT-11 alone will be evaluated at the first chemotherapy treatment (on days 1-3) during which cetuximab will be administered on day 3 (48 h from the end of CPT-11 administration). Instead, the pharmacokinetics of CPT-11 in combination with cetuximab will be performed on days 15-17 of the second treatment of the first cycle of therapy where a second dose of cetuximab will be administered concomitantly to CPT-11.

Serial blood samples are collected into tubes containing K-EDTA (4.9 mL). The sampling times is: before drug administration and at 1.0, 2.0, 2.25, 2.50, 3.0, 4.0, 6.0, 8.0, 10.0, 26.0 and 50.0 h following the start of the CPT-11 infusion during both the treatments of the first cycle of therapy, as schematized in Figure 21.

Plasma is obtained immediately by centrifugation of blood samples (3000 g for 10 min at 4°C), then splitted into 2 aliquotes and stored at -80°C in 2 different freezers.

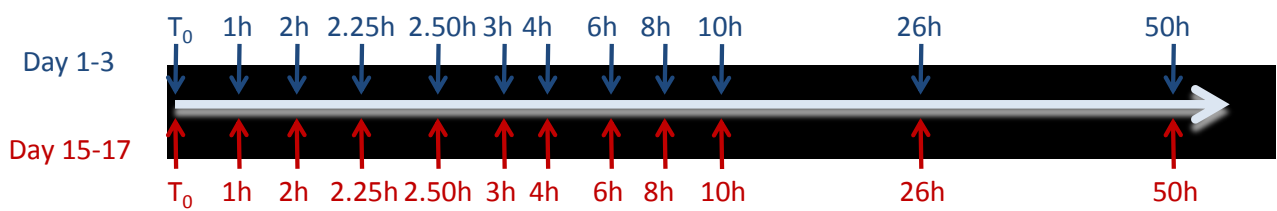


**Figure 21** Schematic representation of the sampling times scheduled for the pharmacokinetic study during the first and second administration of the first chemotherapy cycle.

The quantification of the total plasma concentration of CPT-11 (lactone plus carboxylate) and its main metabolites (SN-38, SN-38G and APC) in plasma samples is performed by using a new LC-MS/MS method previously developed and validated according to FDA guidelines by Experimental and Clinical Pharmacology Unit of CRO-Aviano. As regard this analytical method, which I have applied for the analysis of patient's plasma samples enrolled in the phase Ib clinical trial reported above, all the development and validation parameters can be found in the already published paper<sup>110</sup>.

#### 4.3.4. PHARMACOKINETICS PARAMETERS

Pharmacokinetics (PK) describes the temporal patterns of response to drug administration following acute or chronic dosing. In order to understand and control the therapeutic action of drugs in the human body, it is necessary to know how much drug will reach the site(s) of drug action and when this will occur. In fact, understanding and employing pharmacokinetic principles can increase the probability of therapeutic success and reduce the occurrence of adverse drug effects in the body<sup>5</sup>.

PK studies are essential to determine how the body handles drug, that is, how drug is absorbed, distributed, metabolized and eliminated. All these processes are influenced by patient's characteristics (i.e., genetics, body size, age, and co-morbidity) and by dosage, drug formulation, route of administration and by the possible co-administration of other drugs. Bioavailability is a term used to indicate the fractional extent to which a dose of drug reaches its site of action or a biological fluid from which the drug has access to its site of action. By definition, when a drug is administered intravenously, its bioavailability is 100% and, on the contrary, when a drug is administered via other routes, its bioavailability decreases because of several losses during the absorption phase.

Drug circulating in the bloodstream is responsible of pharmacological activity and its level is regulated by several processes: the organs uptake; the drug binding with plasma proteins (albumin is a major carrier for acidic drugs;  $\alpha$ 1-acid glycoprotein binds basic drugs. The binding is usually reversible), red cells or platelets; the permeability of tissue membranes and the drug metabolism and elimination.

Drugs are eliminated from the body either unchanged by the process of excretion or converted to metabolites. In fact, drug elimination occurs by two processes, excretion and metabolism; excretion is the irreversible loss of chemically unchanged drug in urine and in faeces (renal excretion of unchanged drug is a major route of elimination for 25–30% of drugs), and metabolism is the conversion of one chemical species to another. Excretory organs, the lung excluded, eliminate polar compounds more efficiently than substances with high lipid solubility. Lipid-soluble drugs thus are not readily eliminated until they are metabolized to more polar compounds. Drug metabolism is obtained by two types of enzymatic reactions: phase I (biotransformation) characterized by reactions of oxidation, hydroxylation, reduction and hydrolysis and phase II (conjugation) characterized by reactions of addition of a new functional group such as glucuronide, sulphate, methyl and acetyl groups, glutathione and amino acids. Even if drug metabolism is the physiological way to detoxification, some metabolites can retain (or increase) the pharmacological activity.

Measuring drug plasma concentration in samples collected at specific time points, it is possible to obtain the plasma concentration-time profile and the shape and the mathematical elaboration of this profile provide the main pharmacokinetic parameters reported in Table 5.

<b>Parameter</b>	<b>Name</b>	<b>Significance</b>	<b>Key features</b>
$C_{max}$	Maximum plasma concentration	The highest drug concentration observed in plasma following administration	$C_{max}$ and $T_{max}$ are correlated and both depend on how quickly the drug enters into and is eliminated from the body
$T_{max}$	Time until $C_{max}$ is reached	The time at which the highest drug concentration occurs	
$AUC$	Area under the concentration-time curve	The measure of the total systemic exposure to the drug	It represents the amount of unchanged drug that has reached the general circulation and it is useful to define the bioavailability of a drug
$V_d$	Volume of distribution	The apparent volume into which the drug is dissolved	It depends on binding to plasma proteins and tissues and it is useful to correlate the drug concentration in plasma with its amount in the body
$t_{1/2}$	Half-life in the terminal phase	The time taken for the plasma concentration to fall by one half once distribution equilibrium has been achieved	It is independent of the amount of drug in the body and it is useful for the determination of the frequency of drug administration
$Cl$	Clearance	The rate of drug elimination by all routes normalized to the concentration of the drug	It is the sum of all organs clearance, especially hepatic and renal clearance

**Table 5** Main pharmacokinetic parameters and their clinical significance.

## **5. RESULTS**

### **5.1. FLUOROPYRIMIDINE PROJECT**

#### **5.1.1. PATIENTS CHARACTERISTICS**

For this multicenter study, a set of 603 patients was retrospectively selected from a collection of 5126 cases enrolled in a multi-institution biobank stored at the Experimental and Clinical Pharmacology Unit of CRO-Aviano.

The aim of the study was to define the role of *DPYD* SNPs in a “real-world” group of patients therefore the subjects selected for this study suffered for different solid tumors and were treated with different FL-based treatments.

More in detail, 432/603 (71.6%) patients had a diagnosis of CRC, 143/603 (23.7%) of breast cancer and 28/603 patients (4.7%) suffered for other solid tumors. Accordingly with the clinical use of FL, the major part of the patients (528/603, 87.6%) were treated with an association therapy (Table 6) and only 75/603 (12.4%) were treated with a monotherapy of 5-FU or CAPE.

The complete baseline patients characteristics are listed in Table 6.

Characteristics	N	%
<b>Sex</b>		
Male	310	51.4
Female	293	48.6
<b>Age, years</b>		
Median (range)	62 (17-99)	
<b>FL-based association therapy</b>		
Yes	528	87.6
<sup>1</sup> FOLFIRI	210	39.8
CMF	143	27.1
<sup>2</sup> FOLFOX	132	25.0
CAPOX	29	5.5
FOLFOXIRI	7	1.3
TPF	5	0.9
<sup>3</sup> Other	2	0.4
No	75	12.4
5-FU/FA	49	65.3
CAPE	26	34.7
<b>Administration Setting</b>		
Neo-adjuvant/Adjuvant	336	55.7
First-line metastatic	236	39.2
N.A.	31	5.1
<b>Any kind of toxicity<sup>4</sup></b>		
<sup>5</sup> G0	65	10.8
<sup>5</sup> G1-G2	443	73.5
<sup>5</sup> G3-G5	95	15.7

**Table 6** Baseline characteristics of the 603 enrolled patients

<sup>1</sup>2/210 were treated with FOLFIRI regimen associated with bevacizumab

<sup>2</sup>2/132 were treated with FOLFOX regimen associated with bevacizumab

<sup>3</sup>1 patient was treated with CAPOXIRI regimen and 1 patient was treated with DOC regimen

<sup>4</sup>Maximum grade of toxicity developed within the first 3 drug administrations.

<sup>5</sup>According to NCI-CTC version 3

**Abbreviations:** G, grade; 5-FU, 5-fluorouracil; CAPE, capecitabine ; FOLFIRI, 5-fluorouracil+leucovorin+irinotecan; CMF, cyclophosphamide+methotrexate+5-fluorouracil; FOLFOX, 5-fluorouracil+leucovorin+oxaliplatin; CAPOX, capecitabine+oxaliplatin+irinotecan; FOLFOXIRI, 5-fluorouracil+leucovorin+oxaliplatin+irinotecan; TPF, Docetaxel+cisplatin+5-fluorouracil; CAPOXIRI, capecitabine+oxaliplatin+irinotecan; DOC, docetaxel+oxaliplatin+capecitabine; 5-FU/FA, 5-fluorouracil+folinic acid.

Dosage, schedule, and duration of treatment were based on FL current clinical setting and the starting standard dose of FL for the principal regimens is reported in Table 7.

<b>REGIMEN</b>	<b>FL</b>	<b>ADMINISTRATION</b>	<b>DOSAGE</b>	<b>DURATION</b>
<b>FOLFIRI</b>	5-FU	Continuous infusion	400 mg/m <sup>2</sup> bolus +2400 mg/m <sup>2</sup>	on day 1 every 2 weeks
<b>CMF</b>	5-FU	Continuous infusion	600 mg/m <sup>2</sup>	on day 1 and day 8
<b>FOLFOX</b>	5-FU	Continuous infusion	400 mg/m <sup>2</sup> bolus +600 mg/m <sup>2</sup>	on day 1 and day 2
<b>FOLFOXIRI</b>	5-FU	Continuous infusion	3200 mg/m <sup>2</sup>	from day 1 to day 2
<b>TPF</b>	5-FU	Continuous infusion	1000 mg/m <sup>2</sup>	from day 1 to day 4
<b>5-FU/FA</b>	5-FU	Continuous infusion	370-400 mg/m <sup>2</sup>	daily from day 1 to day 14, treatment repeated every 28 days
<b>CAPE</b>	CAPE	Oral administration	1250 mg/m <sup>2</sup>	twice daily from day 1 to day 14, treatment repeated every 21 days
<b>CAPOX</b>	CAPE	Oral administration	1000-850 mg/m <sup>2</sup>	twice daily from day 1 to day 14

**Table 7** Dosage, administration mode and duration of FL in the principal regimens used in the clinical practice.

According to our study criteria. 65 out of 603 patients (10.8%) did not develop any toxicity, 443/603 patients (73.5%) developed Grade 1–2 toxicities, while 95/603 (15.7%) subjects developed severe toxicity (Grade ≥3), , during the first three treatment cycles. These data are consistent with previously published studies. In fact, the percentage reported in our study (15.7%) is comparable with the one reported by Froehlich et al. <sup>43</sup> (14%) who analyzed the toxicities with Grade 3 or higher developed after the first two cycles of treatment. Loganayagam et al. <sup>46</sup> reported 24% of Grade 3 or higher toxicity rate in the first four cycles of treatment.

Within the group of patients with Grade ≥3 toxicity, 44/95 (46.3%) developed non-hematological toxicities, 28/95 (29.5%) hematological toxicities and 23/95 (24.2%) both.

Among the 95 patients with severe toxicities, the most common Grade ≥3 toxicities developed during the first three cycles were neutropenia and diarrhea, followed by leukopenia, stomatitis,

and nausea/vomiting. More details about the severe toxicities developed by the patients during the first three treatment cycles are reported in Table 8.

Adverse event	Total of patients (n=603)	
	N	%
<b>Hematologic toxic effects</b>		
Neutropenia	44	33.1
Leukopenia	9	6.8
Other hematological toxicities <sup>1</sup>	6	4.5
<b>Non-hematologic toxic effects</b>		
Diarrhea	4	30.0
Nausea/vomiting	9	6.8
Stomatitis	9	6.8
Epatic toxicity	9	6.8
Other non-hematological toxicities <sup>2</sup>	7	5.2

**Table 8** Most common adverse events (Grade  $\geq 3$ ) developed during the first three cycles of treatment.

<sup>1</sup>Piastirinopenia, trombocitopenia, non neutropenic infection.

<sup>2</sup>Enteritis, asthenia, alopecia, neurotoxicity.

### 5.1.2. CLINICAL DATA MANAGEMENT

Clinical data collection was a key process in the management of the study due to its importance in ensuring high-quality and reliable results.

The medical records of the enrolled patients were analyzed retrospectively and a specific case report form (CRF) was filled out in order to collect all the necessary information, according to the aims of the study. For the patients enrolled in other centers, the CRF formats were delivered to the responsible clinicians.

The CRFs were composed by different forms (Appendix 1):

1. Patient registration form (Form 1): used for the collection of patient personal data.
2. Primitive tumor form (Form 2): used to delineate the tumor characteristics (diagnosed disease stage, primitive tumor surgery) and the therapeutic course that the patient underwent before FL treatment.

3. Chemotherapy form (Form 3): used to describe clinical information (weight, height, BSA, PS) and the chemotherapy regimen (date of start, schedule and dose).
4. Chemotherapy toxic event form (Form 4): used to collect the information of the cycle therapy in which a severe toxicity occurred. The reason for a possible interruption of the treatment, the consequence of the toxic event and the history of prior FL-based treatment were also requested.
5. Toxic event form (Form 5): used to collect the toxicities developed during the cycle in which the severe toxic event occurred.

### 5.1.3. GENOTYPING RESULTS

All the enrolled 603 patients were genotyped for three *DPYD* variants (*DPYD-rs3918290*, *DPYD-rs67376798*, and *DPYD-rs55886062*). The successful genotyping ranged from 97% (588 cases, *DPYD-rs55886062*) to 100% (603 cases, *DPYD-rs3918290*) due to the low quality of some DNA samples. All the *DPYD* variant alleles were detected only in heterozygosity and the genotypes distributions of these SNPs are consistent with data from NCBI (<http://www.ncbi.nlm.nih.gov/SNP>) (Table 9).

<b>Polymorphism</b>	<b>Total</b>	<b>N°</b>	<b>%</b>	<b>Observed allelic frequency</b>	<b>NCBI allelic frequency</b>
<i>DPYD-rs3918290</i>	603				
GG		591	98.1	G=99.05	G=99.1
AG		12	1.9	A=0.95	A=0.9
<i>DPYD-rs67376798</i>	588				
AA		583	99.1	A=99.55	A=99.6
AT		5	0.9	T=0.45	T=0.4
<i>DPYD-rs55886062</i>	595				
TT		593	99.7	T=99.85	T=99.9
AA		2	0.3	A=0.15	A=0.1

**Table 9** *DPYD-rs3918290*, *DPYD-rs67376798*, and *DPYD-rs55886062* genotyping data and the comparison between the frequencies observed in the study population and the NCBI ones.

For the secondary aim of this study, additional five *DYPD* SNPs (*DYPD-rs1801158*, *DYPD-rs1801159*, *DYPD-rs2297595*, *DYPD-s17376848*, and *DYPD-rs1801160*) were investigated in a subgroup constituted by 95 cases, who were all the patients in our study with Grade 3–5 toxicities during the first three cycles of chemotherapy. Additionally, these analyses were conducted also in 315 randomly selected control patients who experienced Grade 0–2 toxicity. No significant difference in terms of sex, age, association therapy, FL administration and setting was found between the 315 patients' subgroup and the overall population of controls. The minor allele frequencies (MAF) of *DYPD-rs1801158*, *DYPD-rs1801159*, *DYPD-rs2297595*, *DYPD-rs17376848*, and *DYPD-rs1801160* were 4.3%, 17.1%, 10.5%, 1.9% and 6.5%, respectively, consistently with previously reported data (<http://www.ncbi.nlm.nih.gov/SNP>).

#### **5.1.4. CLINICAL VALIDITY OF *DYPD* SNPs FOR THE PREDICTION OF SEVERE TOXICITY**

Eighteen patients (3.0%) carried at least one variant allele for any of the three SNPs that represented the first aim of our study.

In particular, 11 for *DYPD-rs3918290*, 5 for *DYPD-rs67376798*, 1 for *DYPD-rs55886062*, 1 both for *DYPD-rs3918290* and *DYPD-rs55886062*). Interestingly, 11 out of 18 patients (61.1%) developed Grade ≥3 toxicity.

Among the 603 patients, the incidence of Grade ≥3 toxicity in *DYPD-rs3918290*, *DYPD-rs67376798* or *DYPD-rs55886062* heterozygous genotype carriers were 8/12 (66.7%), 3/5 (60.0%) and 1/2 (50.0%) respectively.

To limit the possibility of false positive findings due to multiple testing and to provide an internal validation, we performed a bootstrap test on our results and applied the conservative Bonferroni correction.

We found a significant association between the occurrence of Grade ≥3 toxicity after a FL-based treatment and the presence of the variant allele of *DYPD-rs3918290* or *DYPD-rs67376798*.

These results remain significant also after bootstrap analysis and after correction for multiple testing (Table 10).

	Total	<sup>4</sup> Toxicity G≥3				
Genotype	n	n	(%)	OR	<sup>2</sup> 95%CI	<sup>3</sup> p
<i>DYPD</i> -rs3918290						
GG	591	87	(14.7)	<sup>1</sup> 1		
AG	12	8	(66.7)	12.6	2.9 - 51.0	0.003
<i>DYPD</i> -rs67376798						
AA	583	92	(15.8)	<sup>1</sup> 1		
AT	5	3	(60.0)	7.8	1.5 - 41.8	0.048

**Table 10** Association of *DYPD*-rs3918290 and *DYPD*-rs67376798 with Grade 3-5 toxicity after bootstrap.

<sup>1</sup>Reference Category.

<sup>2</sup>Adjusted for sex, age, and association therapy.

<sup>3</sup>With Bonferroni correction.

<sup>4</sup>According to NCI-CTC version 3.

#### ✓ ***DYPD*-rs3918290**

*DYPD*-rs3918290 was significantly associated with Grade ≥3 toxicity of any type (Bonferroni adjusted p=0.003, OR: 12.6, 95% CI from 2.9 to 51.0). The association remained significant also when considering hematological or non-hematological severe toxicity separately (Bonferroni adjusted p=0.003, OR: 12.2, 95% CI from 2.8 to 53.3; and p=0.003, OR: 10.8, 95% CI from 2.7 to 42.9, respectively).

One *DYPD*-rs3918290 variant allele was carried by 12 patients, and eight of them (66.7%) developed severe toxicity according to the study criteria. All of them experienced Grade 4 toxicity; in particular four patients experienced hematological toxicity, three non-hematological toxicity, and one both.

Six of these 12 patients (50.0%) interrupted the treatment due to toxicity and the other four (33.3%) required a therapy delay, or a FL dosage reduction, according to the normal clinical practice. Only one patient was heterozygous for both *DYPD*-rs3918290 and *DYPD*-rs55886062, and this subject died for toxicity (Grade 4 diarrhea and stomatitis) after the first cycle of adjuvant treatment with 5-FU mono-therapy in combination with leucovorin (LV) for stomach cancer. Four subjects (33.3%) carried the *DYPD*-rs3918290 SNP in heterozygosity without Grade ≥3 toxicity. Nevertheless, one of those patients experienced Grade 2 diarrhea and Grade 2 anemia during the first three cycles and another one suffered Grade 2 rectal hemorrhage. In these two patients, the treatment needed to be delayed of 10 and 28 days, respectively (Table 11).

<i>ID</i>	Primary tumor site	Therapy	Treatment	Toxicity	Toxicity Cycle	Treatment Interruption (Cause)	Treatment Delay (Cause)	Dose Reduction (Cause)
<b>1</b>	Rectum	FOLFIRI	Metastatic	Diarrhea G2 Anemia G2	3	No	Yes (Toxicity)	No
<b>2</b>	Colon	FOLFIRI	Metastatic	Rectal hemorrhage G2	3	Yes (Toxicity)	Yes (Toxicity)	No
<b>3</b>	Colon	FOLFIRI	Metastatic	No	/	No	No	No
<b>4</b>	Colon	FOLFIRI	Metastatic	No	/	No	No	No
<b>5</b>	Colon	CAPE	Adjuvant	Leukopenia G4 Neutropenia G4 Diarrhea G4	1	Yes (Toxicity)	No	No
<b>6</b>	Nasopharynx	TPF	Neo-adjuvant	Diarrhea G4	2	Yes (Toxicity)	No	No
<b>7</b>	Stomach	5-FU/FA	Adjuvant	Stomatitis G4 Diarrhea G5	1	Yes (Toxic death)	No	No
<b>8</b>	Colon	CAPE	Adjuvant	Neutropenia G4 Thrombocytopenia G4	1	Yes (Toxicity)	No	No
<b>9</b>	Stomach	DOC	Metastatic	Neutropenia G4	1	Yes (Toxicity)	No	No
<b>10</b>	Colon	CAPOX	Adjuvant	Vomiting G4 Diarrhea G4	1	Yes (Toxicity)	No	No
<b>11</b>	Rectum	FOLFOX	Adjuvant	Neutropenia G4	3	No	Yes (Toxicity)	Yes (Toxicity)
<b>12</b>	Colon	FOLFOX	Adjuvant	Neutropenia G4	1	No	Yes (Toxicity)	No

**Table 11** Clinical information of heterozygous patients for *DYPD*-rs3918290.

✓ **DPYD-rs67376798**

*DPYD-rs67376798* was significantly associated with the occurrence of any kind of Grade ≥3 toxicity and this result was still significant after bootstrap analysis and Bonferroni correction (Bonferroni adjusted p=0.048, OR: 7.8, 95% CI from 1.5 to 41.8). The association with *DPYD-rs67376798* was still significant when considering only non-hematological Grade≥3 toxicity (p=0.022, OR: 7.1, 95% CI from 1.3 to 37.8). However, this association was lost after the application of the Bonferroni correction (p=0.066). No association was found between *DPYD-rs67376798* and severe hematological toxicity (Bonferroni adjusted p=0.366, OR: 2.6, 95% CI from 0.2 to 24.4).

In total, five patients were heterozygous for *DPYD-rs67376798* and three of them (60.0%) developed Grade ≥3 toxicities. These three patients suffered Grade 3 non-hematological toxicity (hepatic toxicity, asthenia, diarrhea, and alopecia), one of these experienced also concomitant Grade 3 neutropenia. Two of these subjects required treatment delay or a drug dosage reduction and one needed to interrupt the therapy. Two patients (40.0%) heterozygous for *DPYD-rs67376798* did not develop any severe toxicity according to the study criteria. One of them experienced Grade 2 diarrhea and Grade 2 stomatitis after the first cycle of therapy leading to a delay of 6 days in the second drug administration. The other one developed neutropenia Grade 1 during the first cycle (Table 12).

ID	Primary site of tumor	Therapy	Treatment	Toxicity	Toxicity Cycle	Treatment Interruption (Cause)	Treatment Delay (Cause)	Dose Reduction (Cause)
1	Rectum	5-FU/FA	Adjuvant	Neutropenia G1	1	No	No	No
2	Colon	FOLFIRI	Metastatic	Diarrhea G2 Stomatitis G2	1	Yes (Disease progression)	Yes (Toxicity)	No
3	Breast	CMF	Adjuvant	Alopecia G3 Hepatic Toxicity G3	3	Yes (Toxicity)	No	No
4	Colon	FOLFOX	Adjuvant	Diarrhea G3	1	No	Yes (Toxicity)	No
5	Rectum	FOLFIRI	Metastatic	Neutropenia G3 Asthenia G3 Diarrhea G3	1	No	Yes (Toxicity)	Yes (Toxicity)

**Table 12** Clinical information of heterozygous patients *DPYD-rs67376798*

✓ ***DPYD-rs55886062***

In our population sample, only two patients were heterozygous for *DPYD-rs55886062*. One patient (who carried in heterozygosity also *DPYD-rs3918290* and was already mentioned above) died from toxicity and the other one suffered from G2 leukopenia, G1 stomatitis and G1 cystitis that led to a dose reduction (Table 13).

Nevertheless, probably due to the low frequency of this SNP, no significant association with severe toxicity was observed (Bonferroni adjusted p=0.131, OR: 6.0, 95% CI from 0.6 to 61).

<b>ID</b>	<b>Primary site of tumor</b>	<b>Therapy</b>	<b>Treatment</b>	<b>Toxicity</b>	<b>Toxicity Cycle</b>	<b>Treatment Interruption (Cause)</b>	<b>Treatment Delay (Cause)</b>	<b>Dose Reduction (Cause)</b>
<b>1</b>	Stomach	5-FU/FA	Adjuvant	Stomatitis G4 Diarrhea G5	1	Yes (Toxic death)	No	No
<b>2</b>	Breast	CMF	Adjuvant	Leukopenia G2 Cystitis G1 Mucositis G1	3	No	Yes (Other)	Yes (Toxicity)

**Table 13** Clinical information of heterozygous patients for *DPYD-rs55886062*.

Genotyping and statistical analyses were performed also on the five additional *DPYD* variants (*DPYD-rs1801158*, *DPYD-rs1801159*, *DPYD-rs2297595*, *DPYD-s17376848*, and *DPYD-rs1801160*) that are considered for the secondary aim of the study. No significant association between these SNPs and Grade ≥3 toxicity of any kind was found in this explorative analysis.

### 5.1.5.PREDICTIVE POWER OF THE PHARMACOGENETIC TESTS

To verify the real clinical impact of the SNPs cited by CPIC guidelines, the sensitivity, specificity, PPV and NPV for these *DPYD* variants have been computed in our group of patients (Table14).

These values were calculated both for each individual SNP and for every possible combination of them. Both the single and the combination analyses showed a low sensitivity (between 1% and 12%) and a high specificity (between 99% and 100%). The highest sensitivity was reached taking into account the simultaneous analysis of *DPYD-rs3918290*, *DPYD-rs67376798*, and *DPYD-*

*rs55886062* (12%), the lowest one was obtained considering only *DPYD-rs55886062* analysis (1%). The specificity reached 100% taking into consideration the single analysis of *DPYD-rs67376798* and of *DPYD-rs55886062*, and was 99% for all the other possible SNPs combinations.

The PPV spanned from 50% to 67% and the highest one was reached taking into account only *DPYD-rs3918290* (Table14).

The NPV presented small oscillation between 84% and 86% and the highest values were achieved evaluating either the combination of *DPYD-rs3918290* and *DPYD-rs67376798* or the combination of all the considered three SNPs (Table14).

The PPV and the NPV for the three-markers test were 61% and 86%, respectively.

<b><i>DPYD variant</i></b>	<b>Sensitivity (%)</b>	<b>Specificity (%)</b>	<b>PPV (%)</b>	<b>NPV (%)</b>
rs3918290	8	99	67	85
rs67376798	3	100	60	85
rs55886062	1	100	50	84
rs3918290 + rs67376798	12	99	65	86
rs3918290 + rs55886062	9	99	62	85
rs3918290 + rs67376798 + rs55886062	12	99	61	86

**Table 14** Sensitivity, specificity, PPV, and NPV of the three *DPYD* variants in single analysis and in different variants combination.

The sensitivity of the pharmacogenetic test considering both *DPYD-rs3918290*, *DPYD-rs67376798*, *DPYD-rs55886062*, and the additional five *DPYD* SNPs was higher (64%) than the test combining only the three CPIC markers (12%). This most comprehensive test presented a fairly low specificity reaching a value of 63%. The PPV and the NPV for the eight-markers test were 26% and 91%, respectively.

## **5.2. SUNITINIB PROJECT**

### **5.2.1. STUDY ON THE E/Z ISOMERIZATION**

The major part of the published analytical methods developed for the quantification of sunitinib and its main metabolite described the sample handling under strict light protection. Sample preparation in light-protected conditions is time-consuming and requires a dark room.

In order to obtain a fast, specific, and easy to use method, we setup a processing procedure able to avoid the light protection relying on the peculiar characteristics of sunitinib isomerization.

Sistla et al.<sup>93</sup>, indeed, showed that the E isomer reverted to the Z isomer following storage in the dark with an increase in the reconversion rate at higher temperatures ( $\ln K$  vs.  $1/T$ :  $r^2=0.96$ ). This observation indicates that the reversion of E to Z isomer is a thermal reversion.

Based on these data we have studied the reversion kinetics of sunitinib in the dark at different temperatures.

More in detail, at first, an extracted sample, after light exposure, (for the extraction method, see “material and methods”) was split in different glass vials and put in a heated bath, at 60°C for 5 (T1), 10 (T2), 15 (T3) and 20 (T4) min. The peak area of the two isomers were compared to the one obtained from the same extracted light-exposed sample directly injected without heating process (T0).

Figure 22 shows the differences in terms of peak area in the different conditions. Already after 5 min at 60°C the peak area of E-isomer was more than 5-fold lower than T0 sample while the peak area of the Z-isomer resulted proportionally increased. Table 15 shows the area of E and Z isomers at different time-points and the sum of the two isomers areas. The reproducibility of the total area guaranteed that the decrease of the E-isomer area was due to its conversion in the active isomer and excluded the possibility of analyte degradation.

After 10 min at 60°C, the equilibrium between E- and Z-isomers was reached and no variations in their areas were obtained prolonging the time of incubation.

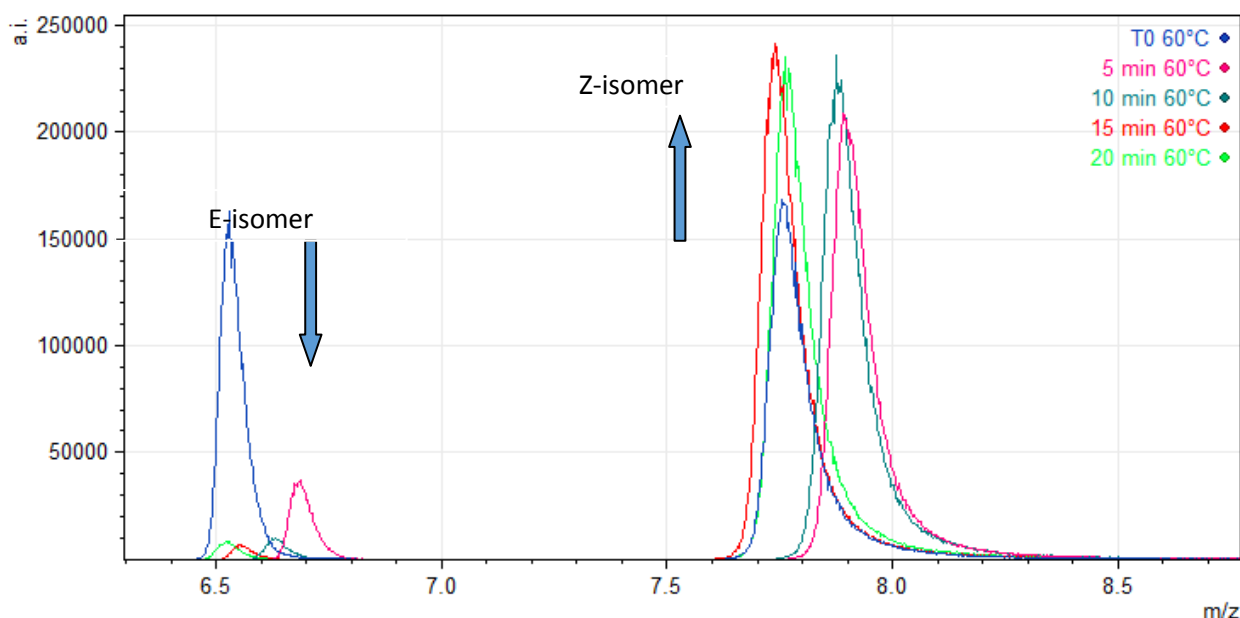


**Figure 22** Interconversion from E- to Z- isomer in different temperature conditions. The samples were analyzed at T0, without any heating process (blue line), and respectively after 5 (pink line), 10 (dark green line), 15 (red line), and 20 min (light green line) at 60°C.

Time	E-isomer Area (%)		Z-isomer Area (%)		Total Area (%)	
T0	6.94 e+5	(44.12)	8.79 e+5	(55.87)	15.73 e+5	(100)
T1 (5 min)	1.34 e+5	(8.69)	14.14 e+5	(91.30)	15.48 e+5	(100)
T2 (10 min)	0.36 e+5	(2.27)	15.72 e+5	(97.72)	16.08 e+5	(100)
T3 (15 min)	0.23 e+5	(1.44)	16.00 e+5	(98.55)	16.23 e+5	(100)
T4 (20 min)	0.30 e+5	(1.95)	15.53 e+5	(98.04)	15.83 e+5	(100)

**Table 15** Areas of E-isomer, Z-isomer, and the sum of the two isomers areas measured at T0 (without any heating process), T1, T2, T3, and T4 at 60°C.

In order to further decrease the E-isomer signal and to reduce the time required for the treatment, additional experiments have been made increasing the heat bath temperature up to 90°C.

Therefore, extracted samples were heated at 90°C for 5 min and then placed in the autosampler (heated at 40°C) to be analyzed by means of LC-MS/MS. Moreover, with the aim to determine the PK profile of the two analytes, the following experiments were performed at two different concentrations: 50 and 500 ng/mL. Finally, in order to understand if prolonging the time in the autosampler could further increase the Z- to E-isomers ratio, the same sample was re-analyzed 20 times to investigate the kinetics of the isomer reconversion in dark conditions in the autosampler for about 3 hours.

In the following Figure 23, the peaks of Z-and E-isomers of samples prepared at the concentration of 50 ng/mL are reported.

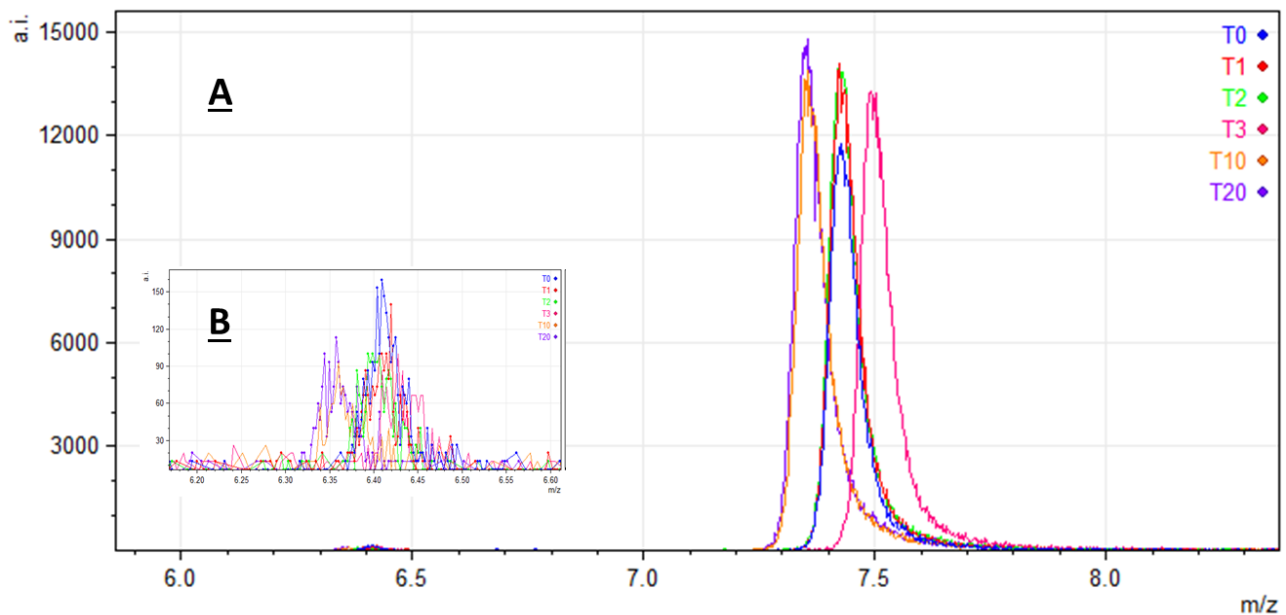


**Figure 23 Panel A:** Z- and E-isomer peaks of the sample at a concentration of 50 ng/mL after different intervals in dark condition. The sample was analyzed at T0, immediately after the step at 90°C for 5 min (blue line), and then re-analyzed after 10 (T1), 20 (T2), 30 (T3), 100 min (T10), and 200 (T20) min in the autosampler at 40°C. **Panel B:** Enlargement of the E isomer peaks.

As clear by the previous Figure 23, at 50 ng/mL, the signal of the E-isomer was barely noticeable from the noise signal, anyway, an attempt of quantification was done and the results are reported in the following table (Table 16):

Sunitinib 50 ng/mL				
Time	E-isomer Area (%)	Z-isomer Area (%)	Total area (%)	
T0	0.004 e+5 <b>(0,666)</b>	0,582 e+5 <b>(99,334)</b>	0,586 e+5	<b>(100)</b>
T1 (10 min)	0.003 e+5 <b>(0,410)</b>	0,681 e+5 <b>(99,590)</b>	0,684 e+5	<b>(100)</b>
T2 (20 min)	0.003 e+5 <b>(0,413)</b>	0,697 e+5 <b>(99,587)</b>	0,700 e+5	<b>(100)</b>
T3 (30 min)	0.003 e+5 <b>(0,377)</b>	0,692 e+5 <b>(99,623)</b>	0,695 e+5	<b>(100)</b>
T10 (100 min)	0.002 e+5 <b>(0,319)</b>	0,706 e+5 <b>(99,681)</b>	0,708 e+5	<b>(100)</b>
T20 (200 min)	0.003 e+5 <b>(0,347)</b>	0,766 e+5 <b>(99,653)</b>	0,769 e+5	<b>(100)</b>

**Table 16:** Areas of E-isomer, Z-isomer, and the sum of the two isomers areas of samples prepared at a concentration of 50 ng/mL. The samples were measured at T0 (analyzed immediately after the step at 90°C for 5 min), and after 10 (T1), 20 (T2), 30 (T3), 100 (T10), and 200 (T20) min in the autosampler at 40°C.

The results obtained using the concentration of 500 ng/mL are reported in the following Figure 24 and Table 17.

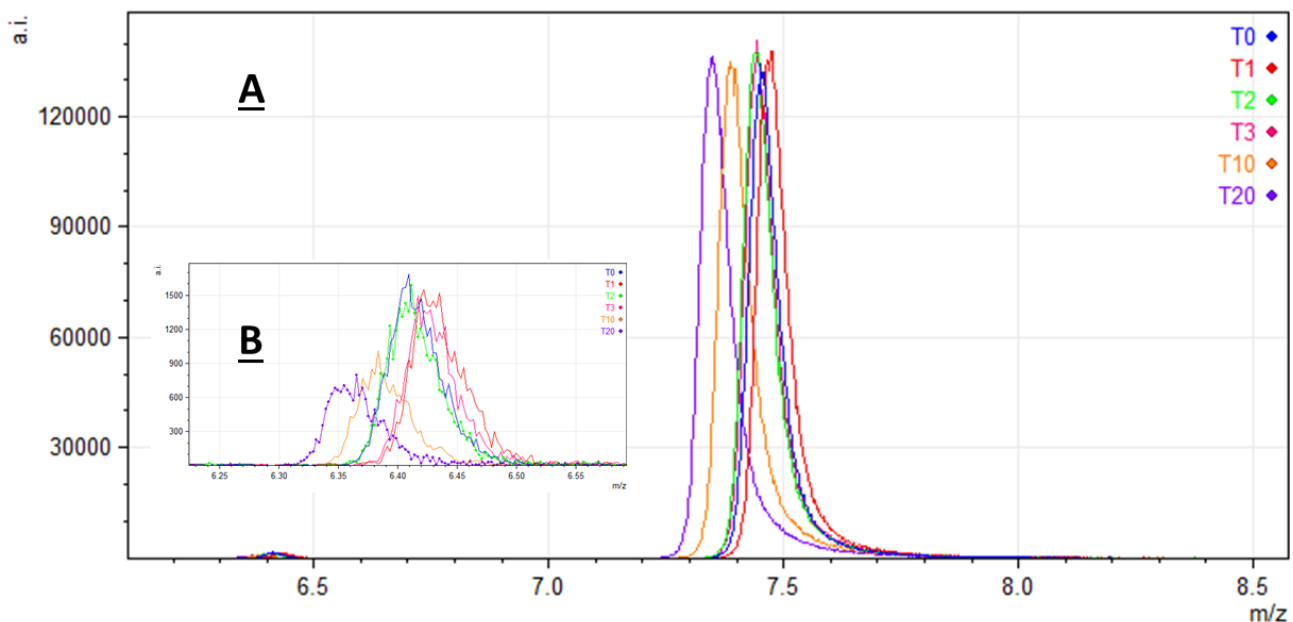


**Figure 24** **Panel A:** Z- and E-isomer peaks of the sample at a concentration of 500 ng/mL after different intervals in dark condition. The sample was analyzed at T0, immediately after the step at 90°C for 5 min (blue line), and then re-analyzed after 10 (T1), 20 (T2), 30 (T3), 100 (T10), and 200 (T20) min in the autosampler at 40°C. **Panel B:** Enlargement of the E isomer peaks.

Sunitinib 500 ng/mL					
Time	E-isomer Area (%)		Z-isomer Area (%)		Total area (%)
T0	0.049 e+5	(0.735)	6.669 e+5	(99.265)	6.718 e+5 (100)
T1 (10 min)	0.048 e+5	(0.670)	7.084 e+5	(99.330)	7.132 e+5 (100)
T2 (20 min)	0.046 e+5	(0.645)	7.106 e+5	(99.355)	7.152 e+5 (100)
T3 (30 min)	0.042 e+5	(0.592)	7.083 e+5	(99.408)	7.125 e+5 (100)
T10 (100 min)	0.027 e+5	(0.374)	7.240 e+5	(99.626)	7.267 e+5 (100)
T20 (200 min)	0.023 e+5	(0.321)	7.247 e+5	(99.679)	7.270 e+5 (100)

**Table 17** Areas of E-isomer, Z-isomer, and the sum of the two isomers areas of the sample prepared at a concentration of 500 ng/mL. The sample was measured at T0 (analyzed immediately after the step at 90°C for 5 min), and after 10 (T1), 20 (T2), 30 (T3), 100 (T10), and 200 (T20) min in the autosampler at 40°C.

The increasing of the temperature promoted the E- to Z-isomer conversion, thus increasing the Z-isomer signal and decreasing the E-isomer signal at both the investigated concentrations (50 and 500 ng/mL). In fact, the percentage of the E-isomer even after 20 min at 60°C was equal to 1.951% (T4, Figure 22), while after only 5 min at 90°C it resulted reduced to 0.666 and 0.735% at 50 (T0, Figure 23) and 500 ng/mL (T0, Figure 24), respectively.

The maintenance of the samples into the autosampler, thus in dark condition and at 40°C, resulted to be not worth of consideration for the set up of the method due to the very slightly difference between different re-injected samples. In fact, the E-isomer percentage decreased from 0.666% to 0.347% and from 0.735 to 0.321% in about 3 hours at 50 and 500 ng/mL, respectively. Moreover, in each analytical run a series of samples, collectively called system suitability test, are requested to be analyzed before samples injection to verify instrument conditions. The system suitability test requires about 1 hour and, from these results, it is possible to assume that this period is enough for stabilize the Z- to E-isomer ratio.

Since the N-desethyl sunitinib structure is similar to the sunitinib one, the isomerization process involved also this metabolite.

For this reason, the same experiments were performed in sample at low and high concentration of N-desethyl sunitinib heated at 90°C for 5 min.

The results obtained are comparable with the sunitinib ones, the E-isomer signal was barely observable from the noise signal, and it resulted even lower than the sunitinib one (Figure 25,26 and Table 18,19).

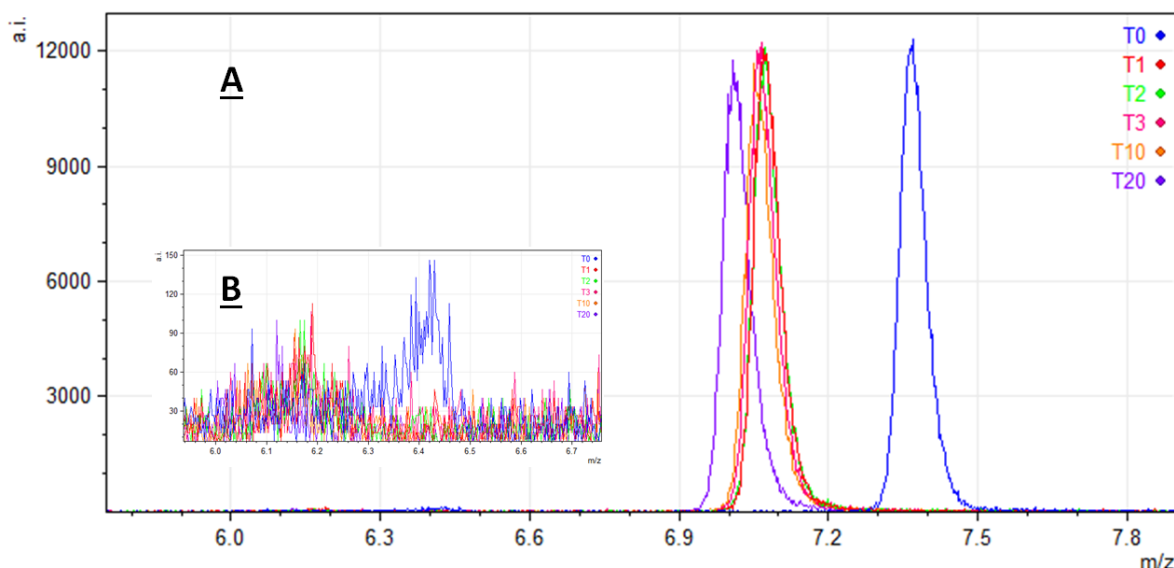


**Figure 25 Panel A:** Z- and E-isomer peaks of N-desethyl sunitinib of the sample at a concentration of 50 ng/mL after different intervals in dark condition. The sample was analyzed at T0, immediately after the step at 90°C for 5 min (blue line), and then re-analyzed after 10 (T1), 20 (T2), 30 (T3), 100 min (T10), and 200 (T20) min in the autosampler at 40°C.  
**Panel B:** Enlargement of the E isomer peaks.

<b><i>N</i>-desethyl sunitinib 50 ng/mL</b>					
<b>Time</b>	<b>E-isomer Area (%)</b>		<b>Z-isomer Area (%)</b>		<b>Total area (%)</b>
T0	0.004 e+5	(0.893)	0.480 e+5	(98.615)	0.484 e+5 (100)
T1 (10 min)	0.004 e+5	(0.755)	0.478 e+5	(99.245)	0.482 e+5 (100)
T2 (20 min)	0.002 e+5	(0.533)	0.476 e+5	(99.467)	0.478 e+5 (100)
T3 (30 min)	0.002 e+5	(0.362)	0.481 e+5	(99.638)	0.483 e+5 (100)
T10 (100 min)	0.001 e+5	(0.298)	0.468 e+5	(99.702)	0.469 e+5 (100)
T20 (200 min)	0.001 e+5	(0.226)	0.472 e+5	(99.774)	0.473 e+5 (100)

**Table 18** Areas of N-desethyl sunitinib E-isomer, Z-isomer, and the sum of the two isomers areas of samples prepared at a concentration of 50 ng/mL. The samples were measured at T0 (analyzed immediately after the step at 90°C for 5 min), and after 10 (T1), 20 (T2), 30 (T3), 100 (T10), and 200 (T20) min in the autosampler at 40°C.

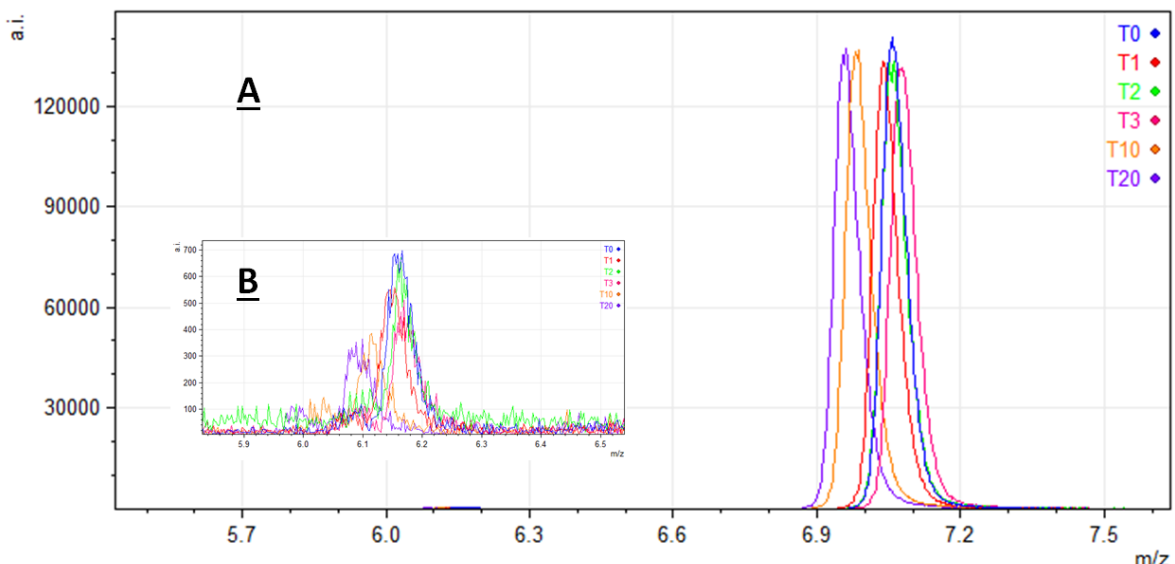


**Figure 26 Panel A:** Z- and E-isomer peaks of N-desethyl sunitinib of the sample at a concentration of 500 ng/mL after different intervals in dark condition. The sample was analyzed at T0, immediately after the step at 90°C for 5 min (blue line), and then re-analyzed after 10 (T1), 20 (T2), 30 (T3), 100 min (T10), and 200 (T20) min in the autosampler at 40°C. **Panel B:** Enlargement of the E isomer peaks.

<b>N-desethyl sunitinib 500 ng/mL</b>					
<b>Time</b>	<b>E-isomer Area (%)</b>		<b>Z-isomer Area (%)</b>		<b>Total area (%)</b>
T0	0.022 e+5	(0.404)	5.473 e+5	(99.596)	5.495 e+5 (100)
T1 (10 min)	0.019 e+5	(0.366)	5.257 e+5	(99.634)	5.276 e+5 (100)
T2 (20 min)	0.015 e+5	(0.290)	5.324 e+5	(99.710)	5.339 e+5 (100)
T3 (30 min)	0.014 e+5	(0.262)	5.398 e+5	(99.738)	5.412 e+5 (100)
T10 (100 min)	0.010 e+5	(0.190)	5.472 e+5	(99.810)	5.482 e+5 (100)
T20 (200 min)	0.010 e+5	(0.192)	5.456 e+5	(99.808)	5.466 e+5 (100)

**Table 19** Areas of N-desethyl sunitinib E-isomer, Z-isomer, and the sum of the two isomers areas of samples prepared at a concentration of 500 ng/mL. The samples were measured at T0 (analyzed immediately after the step at 90°C for 5 min), and after 10 (T1), 20 (T2), 30 (T3), 100 (T10), and 200 (T20) min in the autosampler at 40°C.

To conclude, the conditions chosen for E-isomer reconversion to Z-isomer consisted of a heating process at 90°C for 5 mi.

### 5.2.2.HPLC-MS/MS CONDITIONS

To optimize the mass spectrometer conditions, an infusion of each standard solution and IS at 50 ng/mL in mobile phases (50:50) was used. The response of sunitinib and its main metabolite was assessed in positive and negative ion mode but the better one was obtained in positive mode. Using an ESI source in positive ion mode, sunitinib and its main metabolite formed mainly a protonated molecule [M+H]<sup>+</sup>.

The precursor ion of sunitinib, N-desethyl sunitinib, and sunitinib D-10 as IS (*m/z* 399.2, *m/z* 371.2, and *m/z* 409.3 respectively) passed through the first quadrupole into the collision cell and the collision energy (CE) and the Collision Cell Exit Potential (CXP) were optimized to obtain their product ions with a high signal.

The fragmentation patterns are represented in Figure 27.

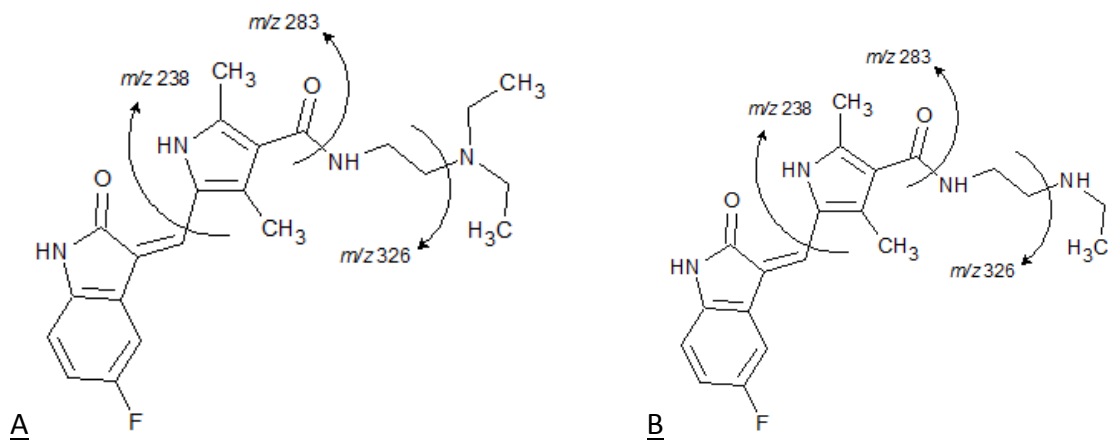


**Figure 27** Chemical structures of sunitinib (A) and N-desethyl sunitinib (B) and identification of the main fragment ions.

For each compound, the daughter ion with the highest signal was used as quantifier, as follows: 399.2>326.2 for sunitinib, 371.2>283.2 for N-desethyl sunitinib, 409.3>326.2 for IS, all expressed in *m/z*. Two additional daughter ions, for each analyte and IS, were chosen as qualifiers and the details of the transitions and the correspondent CE and CXP were reported in Table 20.

Compound	Q1 ( <i>m/z</i> )	DP (V)	EP (V)	Q3 ( <i>m/z</i> )	CE (V)	CXP (V)
sunitinib	399	72	11	<b>326.2</b>	<b>28</b>	<b>21</b>
				283.1	36	18
				238.1	60	14
<i>N</i> -desethyl-sunitinib	371	57	10	<b>283.2</b>	<b>27</b>	<b>14</b>
				326.2	22	18
				238.2	54	21
<i>sunitinib-D10</i> (IS)	409	67	11	<b>326.2</b>	<b>30</b>	<b>21</b>
				283.2	39	18
				238.2	63	14

**Table 20** Source- and compound-dependent parameters and ion transitions of each analyte and IS used for the mass spectrometer method.

Figure 28 presents typical SRM chromatograms, using the quantifier transitions noted above. Panel A shows an extracted blank plasma sample; Panel B displays an extracted blank plasma sample with IS added; Panel C shows an extracted plasma sample at the LLOQ with IS added, and Panel D displays a point of the calibration curve at a concentration equal to 250 ng/mL for sunitinib and 100 ng/mL for N-desethyl sunitinib.

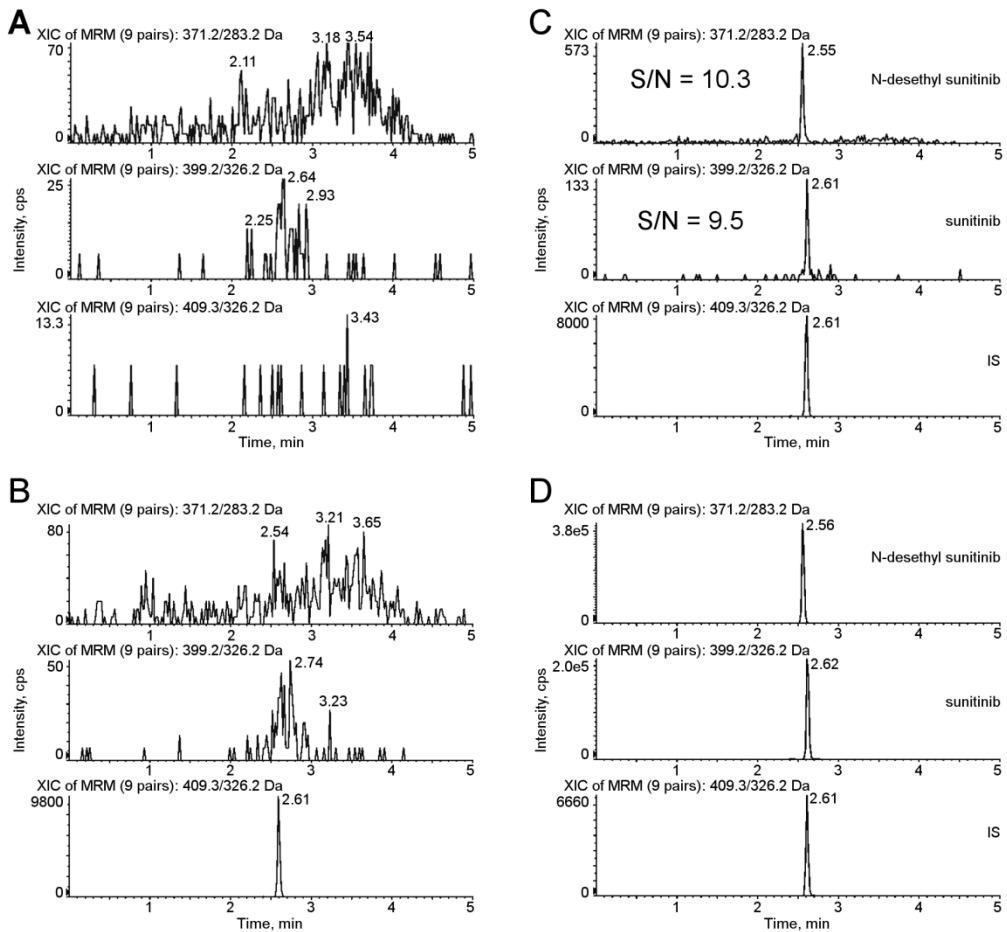


**Figure 28** Representative SRM chromatograms. Panel A: SRM chromatograms of a human blank plasma sample; Panel B: SRM chromatograms of a human blank plasma sample with IS added; Panel C: S/N of sunitinib and N-desethyl sunitinib at the LLOQ (0.1 ng/mL for both the analytes); Panel D: SRM chromatograms of an extracted plasma sample of a calibration curve point. The concentrations measured were 250 ng/mL for sunitinib and 100 ng/mL for N-desethyl sunitinib.

The elution of the analytes was rapid and selective with adequate separation of all the peaks within 2.5 min: sunitinib, N-desethyl sunitinib and IS were eluted at approximately 2.61, 2.55, and 2.61 min, respectively. No interfering peaks were observed at these retention times, and the peaks were completely resolved from plasma matrix, with a good shape.

### **5.2.3.METHOD VALIDATION**

The main parameters considered for the validation of the methods, accordingly with the FDA guidelines, were recovery, linearity of the calibration curve, precision and accuracy, limit of detection, limit of quantitation and stability.

However, for a completely validation it is necessary to test our method in patients samples and to conduct the ISR to verify the reliability of the reported subject sample analyte concentrations.

For this reason, we already prepared a request for the institutional review board (IRB) of the CRO institute in order to obtain plasma samples of patients and complete the validation process.

### **Recovery**

The extraction method is based on simple deproteinization with five volumes of CH<sub>3</sub>OH relative to plasma sample. The recovery, evaluated in five replicates at three QC concentrations, was in the range 93.9-111.1% (CV ≤ 9.2%) for sunitinib and 95.7-108.1% (CV≤ 12.3%) for N-desethyl sunitinib, as shown in Table 21. The recovery of IS was evaluated in five replicates at a concentration of 100 ng/ml and it was 104.9 % (CV 5.2 %).

<b>Analyte</b>	<b>Nominal concentration (ng/mL)</b>	<b>Recovery (%) ± SD</b>	<b>CV %</b>
<i>sunitinib</i>	0.25	100.5±9.3	9.2
	25	93.9±5.4	5.8
	400	111.1±1.0	0.9
<i>N-desethyl sunitinib</i>	0.25	104.6±12.9	12.3
	25	95.7±5.9	6.1
	200	108.1±2.9	2.7
<i>sunitinib-D10 (IS)</i>	100	104.9±5.4	5.2

**Table 21** Recovery of the analytes and the IS from human plasma.

### **Calibration curves**

Table 22 reports the results for the calibration curves of sunitinib and its main metabolite freshly prepared every day during the validation study, and the accuracy and precision for each standard. The peak-area ratios of the analyte/IS compared to the nominal concentrations were plotted and a least-squares linear regression, weighted by the reciprocal of the concentrations, were plotted and a weighted quadratic regression function ( $1/x^2$ ) was applied to generate calibration curves (Figure

29). The calibration curves prepared on five different days showed good linearity and acceptable results of the back-calculated concentrations over the validated range of 0.1–500 ng/mL for sunitinib and 0.1–250 ng/mL for N-desethyl sunitinib.

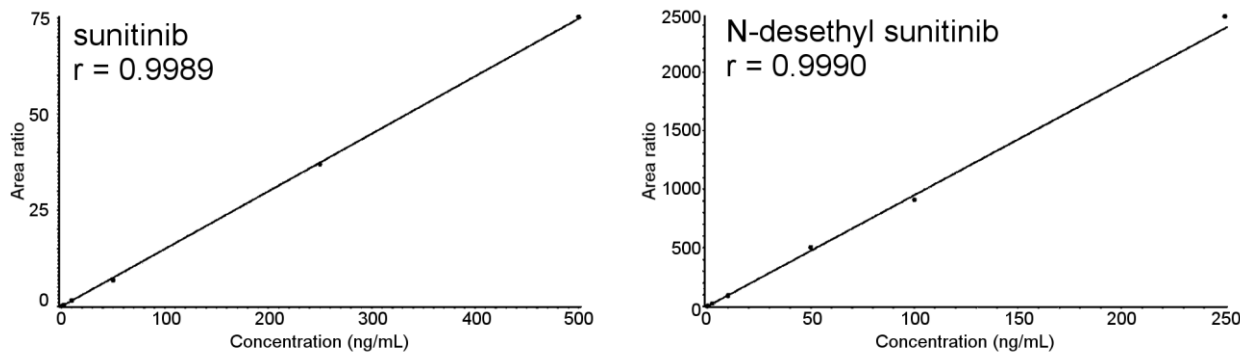


**Figure 29** Calibration curves of sunitinib and N-desethyl sunitinib in human plasma

Pearson's coefficient of determination  $R^2$  was  $\geq 99.3$  for each run, the mean accuracy was always close to 100% (range from 95.8% to 102.9% for sunitinib and from 92.3 to 106.2% for N-desethyl sunitinib) and the precision, expressed as CV%, ranged from 1.6 to 7.7 % for sunitinib, from 0.8 to 10.8% for N-desethyl sunitinib. The carry-over effect was minimized injecting three samples of mobile phase between successive test samples and after the injection of the ULOQ. This action guaranteed peak response no higher than 10% of LLOQ.

<b>Analytes</b>	<b>Nominal conc. (ng/mL)</b>	<b>Mean <math>\pm</math> SD</b>	<b>Precision %</b>	<b>Accuracy %</b>
<i>sunitinib</i>	0.1	0.10 $\pm$ 0.00	1.6	101.0
	0.5	0.48 $\pm$ 0.04	7.7	95.8
	2.5	2.41 $\pm$ 0.14	5.6	96.5
	10	10.25 $\pm$ 0.47	4.6	102.5
	50	49.38 $\pm$ 2.04	4.1	98.8
	250	256.67 $\pm$ 12.29	4.8	102.7
	500	514.50 $\pm$ 16.16	3.1	102.9
<i>N-desethyl sunitinib</i>	0.1	0.10 $\pm$ 0.00	0.8	101.2
	0.5	0.47 $\pm$ 0.02	3.9	94.2
	2.5	2.31 $\pm$ 0.11	4.8	92.3
	10	9.72 $\pm$ 1.05	10.8	97.2
	50	51.48 $\pm$ 2.96	5.7	103.0
	100	104.93 $\pm$ 9.07	8.6	104.9
	250	265.41 $\pm$ 19.16	7.2	106.2

**Table 22** Linearity, accuracy, and precision data for calibration curves of sunitinib and N-desethyl sunitinib

## Intra-day and inter-day precision and accuracy

The precision and accuracy of the method were evaluated by analyzing three replicates of QC samples (QCL, QCM and QCH) within a single-run analysis for intra-day assessment and over five consecutive runs for inter-day assessment. The accuracy and precision (CV%) obtained are shown in Table 23.

Analytes	Nominal concentration (ng/mL)	Mean ± SD	Precision %	Accuracy %
<i>Intra-day (N=5)</i>	sunitinib	0.25	0.25±0.03	11.0
		25	25.93±0.69	2.7
		400	447.86±5.10	1.1
	N-desethyl sunitinib	0.25	0.26±0.03	11.7
		25	26.71±2.57	9.6
		200	223.30±6.28	2.8
<i>Inter-day (N=15)</i>	sunitinib	0.25	0.26±0.02	6.1
		25	25.40±1.27	5.0
		400	423.48±29.23	6.9
	N-desethyl sunitinib	0.25	0.25±0.02	9.1
		25	24.18±1.76	7.3
		200	214.45±14.17	6.6

**Table 23** Intra and inter-day precision and accuracy of the method for the analysis of sunitinib and its main metabolite in human plasma samples.

The method was very precise, with intra- and inter-day CV ≤ 11.0 % and ≤ 6.9% for sunitinib, ≤ 11.7% and ≤ 9.1% for N-desethyl sunitinib. Moreover, the method showed intra- and inter-day accuracy within the range from 98.5 ad 112.0% and from 101.6 and 105.9% for sunitinib, from 103.7 to 111.7% and from 96.7 and 107.2% for N-desethyl sunitinib.

## Limit of detection, limit of quantification, selectivity and matrix effect

The LOD was defined as the concentration at which the S/N was at least 3. The LOD was 32 pg/ml for sunitinib and 29 pg/ml for N-desethyl sunitinib. The LLOQ was defined as the lowest concentration that could be measured with a precision within 20% and accuracy between 80% and 120%. Furthermore, the LLOQ values were chosen on the basis of the concentration range expected in plasma samples of patients.

Therefore, the LLOQ was fixed at 0.1 ng/mL for both sunitinib and N-desethyl sunitinib and was validated through analysis of six replicates. The accuracy and precision at the LLOQ were determined by analyzing six replicates of the sample at the LLOQ concentration. The accuracy and CV% were, respectively, 87.4% and 14.7% for sunitinib, 107.8% and 8% for N-desethyl sunitinib. The method was not affected by endogenous components in the matrix or other components in the sample. In fact, spiking six different sources of human plasma with sunitinib and its main metabolite at a concentration corresponding to the LLOQ, the precision was 8.4% for sunitinib and 5.9% for N-desethyl sunitinib, respectively, and the accuracy was 89.5% for sunitinib and 114.9% for N-desethyl sunitinib, respectively. There were no significant variations (<15%) in the peak area of each analyte in the six lots of matrix, therefore it was possible to exclude the presence of any matrix effect of ion suppression or enhancement.

## Stability

The stability of sunitinib and its main metabolite, under different conditions, was assessed by analyzing QC samples, prepared in triplicate. All these analytes in human plasma were stable for 4 h at room temperature (Table 24).

For the peculiarity of this method, it is particularly important to assess the stability in autosampler after the extraction. In fact, the temperature set for the autosampler in order to enhance and stabilize the conversion to the active Z-isomer is at 40°C, while standard methods usually consider an autosampler temperature of 4°C.

Therefore, we demonstrated the stability of the extracted samples for 48 h in the autosampler at 40°C. (Table 25).

Analytes	T = 4h (RT)			
	Nominal conc. (ng/mL)	Mean ± SD	Prec. %	Acc. %
<i>sunitinib</i>	0.25	0.23±0.01	5.9	90.6
	25	23.37±0.86	3.7	93.5
	400	440.84±22.23	5.0	110.2
<i>N-desethyl sunitinib</i>	0.25	0.25±0.03	12.6	101.0
	25	22.81±1.12	4.9	91.2
	200	227.44±4.10	1.8	113.7

**Table 24** Short term stability of sunitinib and its main metabolite in human plasma samples at room temperature (RT)

T = 48h in autosampler (40°C)				
Analytes	Nominal conc. (ng/mL)	Mean ± SD	Prec. %	Acc. %
<i>sunitinib</i>	0.25	0.23±0.02	8.4	90.6
	25	23.94±1.95	8.1	95.8
	400	418.56±24.90	5.9	104.6
<i>N-desethyl sunitinib</i>	0.25	0.25±0.02	7.2	101.3
	25	25.20±0.45	1.8	100.8
	200	209.57±7.56	3.6	104.8

**Table 25** Stability of sunitinib and its main metabolite in human plasma samples in autosampler for 48h

Sunitinib and N-desethyl sunitinib were stable in human plasma over two freeze/thaw cycles: precision as CV% and accuracy for freeze/thaw samples were ≤8.6% and within 99.9–108.2% for sunitinib, ≤12.4% and within 101.9–106.1% for N-desethyl sunitinib, (Table 26).

After 2 freeze-thaw cycles				
Analytes	Nominal conc. (ng/mL)	Mean ± SD	Prec. %	Acc. %
<i>sunitinib</i>	0.25	0.26±0.02	6.5	105.9
	25	24.97±0.74	3.0	99.9
	400	432.80±37.20	8.6	108.2
<i>N-desethyl sunitinib</i>	0.25	0.26±0.02	9.2	104.8
	25	26.52±0.26	1.0	106.1
	200	203.82±25.24	12.4	101.9

**Table 26** Stability of sunitinib and its main metabolite, in human plasma samples, after 2 freeze-thaw cycles and after 4 months of storage at -80°C.

Several aliquots of QC samples has been stored at -80°C in order to complete the assessment of the long-term stability. This part of the validation will be conducted in the next months in order to define the stability on the analytes in plasma at 1, 3 and 6 months.

## 5.3. IRINOTECAN PROJECT

### 5.3.1. PATIENTS CHARACTERISTICS

In the two centers involved in this ongoing study, four patients were screened for the *UGT1A1\*28* SNP and for the panel of mutations within the *RAS* gene family necessary to be eligible for this study. More in detail, the mutational analysis for *K-RAS/N-RAS/B-RAF* is necessary to assess that the patient is wild-type for all the mutations present in the exons 2, 3 and 4 of *K-RAS* and *N-RAS* in correspondence of the amino acid residues 12, 13, 59, 61, 117, and 146<sup>111</sup>. Moreover, the wild-type status needs to be assessed for the *B-RAF* mutation within the exon 15 at the residue 600.

Due to the relative high frequencies of these mutations in CRC patients and to the additional step of the *UGT1A1\*28* screening, the enrollment is quite low and, at the moment, only one patient resulted eligible for this study.

The details of the enrollment status of this study are summarized in Table 27.

Patient	Enrollment status	<i>UGT1A1</i>	EXON 2		EXON 3		EXON 4		EXON 15	
		<i>UGT1A1*28</i>	<i>K-RAS</i>	<i>N-RAS</i>	<i>K-RAS</i>	<i>N-RAS</i>	<i>K-RAS</i>	<i>N-RAS</i>	<i>B-RAF</i>	
1	Eligible	*1/*1	wt							
2	Not eligible	*28/*28	wt							
3	Not eligible	*28/*28	wt							
4	Not eligible	*1/*1	wt	mut	wt	wt	wt	wt	wt	

**Table 27** Genotype information about the four screened patients.

### 5.3.2. COLLECTION AND STORAGE OF THE SAMPLES

The patient was hospitalized for 3 days during the two treatments of the first therapy cycle and the sampling was strictly monitored by the dedicated staff (MD clinical staff and research nurses dedicated to clinical studies). The blood samples were collected, immediately centrifuged and split into two plasma aliquots that were stored at -80°C.

The samplings were recorded, in details, in forms suitable to indicate the correct timing and any possible variation from it. Some basic information of the patient, such as the PS, the BSA, the scheduled treatment, the CPT-11 dose, and the date of start of the therapy were also reported (Appendix 2).

### 5.3.3.PHARMACOKINETICS ANALYSIS

The PK of the enrolled patient was followed during the days 1-3 and the days 15-17, accordingly to the protocol design. Even if, during the validation process, the stability of CPT-11 and its main metabolites was assessed at 4 months in plasma, patients' samples are analyzed as soon as possible after the collection. For this reason, the data regarding the first patient enrolled in this study are already available. In Figure 30 the plasma concentration-versus-time curves of CPT-11, SN-38, SN-38G, and APC are shown. They were determined, during the first cycle of therapy, using the validated LC-MS/MS method <sup>110</sup>, in the patient receiving 260 mg/m<sup>2</sup> of CPT-11 as a 2-h continuous intravenous infusion.

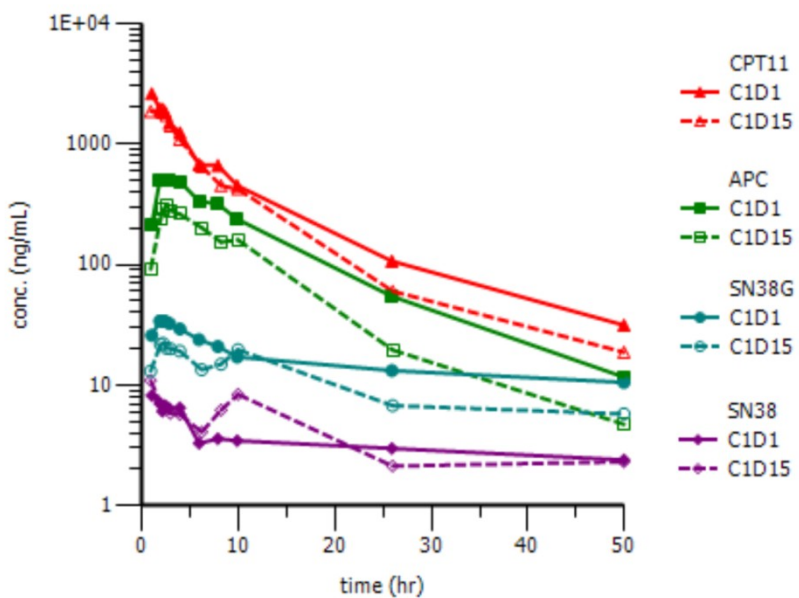


**Figure 30** Plasma concentration-versus-time profiles of CPT-11 and its main metabolites (SN-38, SN-38G, and APC) in one patient receiving 260 mg/m<sup>2</sup> of irinotecan during the I (C1D1) and the II (C1D15) administration of the first therapy cycle.

CPT-11 plasma concentrations appeared to decline in a bi-exponential manner, with a rapid initial phase and an extended terminal phase. Looking at the PK profiles, it is possible to observe that

APC presents a curve very similar to CPT-11 while the two regarding SN-38 and SN-38G show the same multi-exponential manner to decline with a very prolonged terminal phase.

In order to define the pharmacokinetic interactions between CPT-11 and cetuximab, the pharmacokinetic profile of CPT-11 was evaluated in absence and presence of the monoclonal antibody in the same patient. The pharmacokinetic profile of CPT-11 alone was assessed at the first chemotherapy treatment in which cetuximab was administered on day 3 (50 h after the start of CPT-11 infusion). Whereas, CPT-11 pharmacokinetics in combination with cetuximab was performed during the second treatment of the first cycle, when the antibody was administered before CPT-11 dosage.

In order to calculate very accurately the PK parameters, the exact timing of the sampling is needed and in the left column of Table 28 and 29 is reported the actual sampling time used to define the PK profile obtained during the first and the second treatments of the patient so far enrolled.

#### **Days 1-3**

	<b>Time</b>	<b>Scheduled time</b>	<b>Actual time</b>
1	<b>0'</b>	09.30	09.30
2	<b>1.0 h</b>	11.35	11.40
3	<b>2.0 h</b>	12.35	12.40
4	<b>2.25 h</b>	12.45	12.47
5	<b>2.50 h</b>	13.00	13.03
6	<b>3.0 h</b>	13.30	13.30
7	<b>4.0 h</b>	14.30	14.35
8	<b>6.0 h</b>	16.30	16.33
9	<b>8.0 h</b>	18.30	18.30
10	<b>10.0 h</b>	20.30	20.30
11	<b>26.0 h</b>	12.30	12.30
12	<b>50.0 h</b>	12.30	12.30

**Table 28** Sampling at day 1-3 occurred at the following time-points: before drug administration, and at 1.0, 2.0, 2.25, 2.50, 3.0, 4.0, 6.0, 8.0, 10.0, 26.0, 50.0 h following the start of irinotecan infusion. The scheduled time and the actual time for each sampling are also reported.

***Days 15-17***

	<b>Time</b>	<b>Scheduled time</b>	<b>Actual time</b>
<b>1</b>	<b>0'</b>	11.30	11.30
<b>2</b>	<b>1.0 h</b>	15.00	14.58
<b>3</b>	<b>2.0 h</b>	16.00	15.59
<b>4</b>	<b>2.25 h</b>	16.15	16.15
<b>5</b>	<b>2.50 h</b>	16.30	16.35
<b>6</b>	<b>3.0 h</b>	17.00	17.00
<b>7</b>	<b>4.0 h</b>	18.00	17.59
<b>8</b>	<b>6.0 h</b>	20.00	20.15
<b>9</b>	<b>8.0 h</b>	22.00	22.15
<b>10</b>	<b>10.0 h</b>	24.00	24.00
<b>11</b>	<b>26.0 h</b>	16.00	16.00
<b>12</b>	<b>50.0 h</b>	16.00	16.00

**Table 29** Sampling at day 15-17 occurred at the following time-points: before drug administration, and at 1.0, 2.0, 2.25, 2.50, 3.0, 4.0, 6.0, 8.0, 10.0, 26.0, 50.0 h following the start of irinotecan infusion. The scheduled time and the actual time for each sampling are also reported.

In the following tables (Table 30 and 31) the main PK parameters of CPT-11 and its metabolites, obtained during the first and the second treatment respectively, are reported. They were determined applying a non-compartmental analysis.

***Days 1-3***

<i>Compound</i>	C <sub>max</sub> (ng/mL)	t <sub>max</sub> (h)	AUC <sub>last</sub> (hr*ng/mL)	AUC <sub>inf</sub> (hr*ng/mL)	t <sub>1/2</sub> (h)	V <sub>z</sub> (mL/m <sup>2</sup> )	Cl (mL/hr/m <sup>2</sup> )
<i>CPT-11</i>	2599.96	1.08	16968.01	17448.08	10.60	227849.34	14901.35
<i>SN-38</i>	8.20	1.08	164.16	426.44	75.66	-	-
<i>SN-38G</i>	33.97	1.92	767.06	1652.60	58.24	-	-
<i>APC</i>	507.14	2.47	6576.38	6732.95	9.31	-	-

**Table 30** PK parameters obtained in one patient receiving 260 mg/m<sup>2</sup> of irinotecan as a 2-h continuous intravenous infusion during the first administration (Day 1-3) of the first chemotherapy cycle.

**Days 15-17**

<i>Compound</i>	C <sub>max</sub> (ng/mL)	t <sub>max</sub> (h)	AUC <sub>last</sub> (hr*ng/mL)	AUC <sub>inf</sub> (hr*ng/mL)	t <sub>1/2</sub> (h)	V <sub>z</sub> (mL/m <sup>2</sup> )	Cl (mL/hr/m <sup>2</sup> )
<i>CPT-11</i>	1933.13	2.25	14420.32	14667.84	9.15	234100.75	17725.86
<i>SN-38</i>	10.93	0.97	198.31	277.22	23.57	-	-
<i>SN-38G</i>	22.18	2.25	521.74	722.15	24.05	-	-
<i>APC</i>	304.92	2.58	3644.86	3700.01	8.07	-	-

**Table 31** PK parameters obtained in one patient receiving 260 mg/m<sup>2</sup> of irinotecan as a 2-h continuous intravenous infusion during the second administration (Day 15-17) of the first chemotherapy cycle.

## 6. DISCUSSION

The different approaches described in this PhD thesis shared the same final aim: to translate the research results in the clinical practice and, consequently, to ameliorate the cancer patients' life through the implementation of the clinical routine.

In fact, after years of research in the field of the personalized therapy, the time is ripe to leave the traditional "one-dose-fit-all" method, and to apply a real tailored therapy for each patient.

In order to reach this ambitious goal, in this PhD thesis, different innovative strategies were chosen and in one case, our results led to the introduction, in the hospital routine, of new tests that improves the chemotherapy dosing.

More in detail, regarding the FLs, the retrospective study on a group of 603 cancer patients clearly assessed the clinical validity of three *DYPD* genotypes and, together with the international guidelines and the more recent literature, enhanced the set-up of a PGx diagnostic service at CRO institute.

The search for the optimized CPT-11 dose in one of the most effective regimen such as FOLFIRI plus cetuximab is ongoing in the genotype-guided phase Ib study entitled: "*A genotype-guided phase I study of irinotecan administered in combination with 5-fluorouracil/leucovorin (FOLFIRI) and cetuximab as first-line therapy in metastatic colorectal cancer patients*".

Unfortunately, until now, only one patient turned out to be eligible for this protocol. However, previous studies on different CPT-11-based regimens assessed the importance of this kind of studies to personalize the therapy according to the *UGT1A1\*28* genotype<sup>64,65</sup>.

Regarding sunitinib, no significant PGx data were available, therefore the strategy adopted to ameliorate the drug dosage was the TDM. The greater effort in this case, regarded the set-up of a method that could really be used in the clinical routine. Since this method was developed in a diagnostic perspective, it has been already validated accordingly to the FDA and EMA guidelines and the request to the IRB in order to obtain patients' samples was submitted to test the method robustness in quantifying real samples.

The results of each strategy and their consequent possible implementation in the clinical practice, are discussed, in detail, below.

## 6.1. FLUOROPYRIMIDINES PROJECT

In recent years, a great emphasis has been given to the genetic basis of FL-related side effects, especially with regard to severe toxicity. A set of studies <sup>47,112,113</sup> highlighted the pivotal role of *DPYD* gene polymorphisms in the insurgence of severe toxicity and led to the definition of pharmacogenetic guidelines for the diagnostic use of some *DPYD* SNPs testing (i.e. *DPYD-rs3918290*, *DPYD-rs67376798*, and *DPYD-rs55886062*) <sup>54</sup>.

These results were further validated in successive studies which assessed the role of these SNPs in three recent meta-analysis <sup>36,51,114</sup>.

Terrazzino et al. evaluated 4094 patients (15 studies) for *DPYD-rs3918290* and 2308 patients for *DPYD-rs67376798*. They confirmed the clinical validity of these SNPs as risk factors for the development of FL-associated severe toxicities. The second meta-analysis, performed by Rosmarin et al., included data of 4855 patients (17 studies). They described eight *DPYD* variants, among which *DPYD-rs3918290* and *DPYD-rs67376798* also showed convincing evidence of an association with toxicity. The third meta-analysis of Meulendijks et al., included data of 7365 patients (eight studies) and confirmed the association between severe toxicity and the variants *DPYD-rs3918290* and *DPYD-rs67376798*, but also for *DPYD-rs55886062* and another SNP not considered in our study, *DPYD-rs56038477*.

Despite the efforts of the scientific community to thrust the introduction of the *DPYD* PGx tests in the everyday clinical practice for FL treatment personalization, clinicians only occasionally decide to rely on these clinical tools. A traditional non-genetic strategy (i.e. based on the body surface area, organ function, etc.) is currently adopted to prevent FL-related toxicity <sup>115</sup>.

One of the principal hurdle that potentially hampered the clinical implementation of prospective *DPYD* testing could be the perceived lack of scientific evidences. In fact, many clinicians strongly demanded a randomized clinical trial (RCT) to prove definitely the effectiveness of these tests. However, the only prospective RCT for upfront DPD deficiency screening was terminated prematurely for ethical reason. More in detail, one patient in the control arm B (patients retrospectively tested for a DPD deficiency) died due to a 5-FU early-onset toxicity and it was confirmed that this patient was DPD deficient <sup>116</sup>.

Therefore, this kind of trials have to be deemed unethical and unnecessary if we considered that some other predictive biomarkers, such as *K-RAS* <sup>117</sup>, were previously implemented without evidence from an RCT.

Moreover, adequate evidences can also be provided by prospective clinical trials<sup>36,42,45</sup>, and retrospective patients collections like ours.

Therefore, in our study, we found a significant association between the occurrence of grade  $\geq 3$  toxicity after a FL based treatment and *DPYD-rs3918290* or *DPYD-rs67376798*, consistently with previously reported data<sup>42,45,46,118</sup>. We internally validated these associations applying the bootstrap methodology, and the results were still significant after correction for multiple testing.

This association is consistent with the reported phenotypic effect of *DPYD-rs3918290* and *DPYD-rs67376798* variants, which have a deleterious impact on the mature protein leading to the occurrence of severe toxicity ascribable to an impaired FL detoxification process (conversion of 5-FU to dihydrofluorouracil)<sup>41</sup>.

Quite notably, when considering only severe life-threatening toxicity, the *DPYD-rs3918290* polymorphism appeared particularly impacting on patients' safety, since all the eight heterozygous subjects in the severe toxicity group developed grade  $\geq 4$  toxicity.

*DPYD-rs55886062* is also considered by the international pharmacogenetic guidelines as a predictive biomarker for toxicity<sup>54</sup>. According to the extremely low minor allele frequency in our study population (0.3%), *DPYD-rs55886062* heterozygosity was observed only in two patients. One of these exhibited a compound heterozygosity with *DPYD-rs3918290* and died of toxicity. The other patient developed a grade 2 toxicity that required a delay in the treatment administration and a FL dosage reduction.

Therefore, although in our study the association between the *DPYD-rs55886062* variant allele and grade  $\geq 3$  toxicity was not statistically significant, probably because of the low prevalence of the polymorphism, we think that its involvement in FL related severe toxicity must be considered.

Toxic death after FL administration is extremely uncommon (about 0.5%)<sup>119</sup>. It has been hypothesized that the simultaneous presence of more than one defective *DPYD* variant could exacerbate the toxicity. We found that the only patient who carried two defective *DPYD* variants (*DPYD-rs55886062* and *DPYD-rs3918290*) died from toxicity after the first cycle of adjuvant treatment with 5-fluorouracil/LV. This is consistent with the results of Lee and colleagues<sup>45</sup>, reporting a toxic death after the treatment of a patient carrying two *DPYD* variants (*DPYD-rs67376798* and *DPYD-rs3918290*). It must be considered that both patients experiencing a toxic death (in our and Lee's study) exhibited the *DPYD-rs3918290*, although the associated *DPYD* variant was different (either *DPYD-rs55886062* or *DPYD-rs67376798*).

The assessment of the predictive power of the upfront pharmacogenetic genotyping for the *DYPD* polymorphisms requires definition of the test specificity, PPV, NPV, and sensitivity. Based on the PPV values, *DYPD-rs3918290* appears the most informative SNP (67%) even if comparing the combined analysis including all the three SNPs (61%). However, the sensibility of the tests remained low with all the possible combination (at least 12%) while the specificity was assessed at values  $\geq 99\%$ . Finally, the NPV values were relatively high and ranger from 84% to 86%.

Important to note is that values for diagnostic test criteria of a PGx test based on SNPs in *DYPD* can never reach 100%, because not all DPD deficiencies and toxicity can be explained by variants in *DYPD*<sup>120</sup>. It must also be said that the high specificity ( $\geq 99\%$ ) and high NPV (84% - 86%) in this setting are most crucial, when the goal is to treat all patients with a variant (including false-positives). The consequence of a false positive result is a relatively low-risk dose reduction for the first of many cycles, which can be adjusted in safe conditions in the second cycle and onwards if no toxicity occurs. The consequence of a false negative result may be much larger since it could result in a too high systemic drug exposure that subsequently leads to severe, potentially lethal toxicity, which is associated with long-lasting hospital and/or intensive care unit admissions.

It should also be stressed out that a treatment adjustment based on combined three *DYPD* test could avoid not only grade  $\geq 3$  toxicities but also moderate chronic toxicities (grade  $\leq 2$ ) that could, anyway, put at risk the success of the treatment and the compliance. In fact, in our study seven out of eighteen patients (38.9%) carrying a variant allele for at least one of the three SNPs did not develop grade  $\geq 3$  toxicity. However, four out of the seven heterozygous patients (57%) had to delay the treatment or reduce the FL dose for toxicity-related reasons (i.e. chronic grade 2 diarrhea, leucopenia, stomatitis, or rectal bleeding).

Despite the high specificity of the *DYPD* markers test, the sensitivity of the test was relatively low even when considering the combined analysis of the three *DYPD* markers (12%). In an attempt to increase this value, we tested also some additional promising *DYPD* SNPs (*DYPD-rs1801158*, *DYPD-rs1801159*, *DYPD-rs2297595*, *DYPD-rs17376848*, and *DYPD-rs1801160*). In our study, none of these *DYPD* variants resulted significantly related to the patients' toxicity outcome. As expected, the sensitivity of the test including also these five SNPs notably increased (from 12% to 64%) but the strong decrement of both specificity (from 100% to 63%) and PPV (from 61% to 26%), and the lack of association with any kind of severe toxicity, do not support the introduction of any of these five polymorphisms in a pre-treatment PGx test. Consistently with these findings, during the execution

of the present work, the CPIC consortium downgraded three of these SNPs (*DPYD*-rs1801158, *DPYD*-rs1801159, *DPYD*-rs1801160) to “still functional” and related to a normal activity of DPD enzyme (<http://www.pharmgkb.org/guideline/PA166122686>).

Our study provides a further advancement in the *DPYD* testing validation. Previously published studies on the clinical effect of *DPYD* polymorphisms are based on highly selected patient groups, mostly derived by clinical studies, with strict inclusion criteria, and this could represent a limit for a generalized application of the test in the current practice to unselected patients, as highlighted by Lee and colleagues<sup>45</sup>. We have been able to confirm the *DPYD* SNPs and toxicity association in the largest independent study with heterogeneous treatments, FL dosages, combination therapy, and primary tumor site. Another criticism of some of the previous reports on the association between *DPYD* variants and FL-related toxicity occurrence could be that they did not consider previous FL treatments, making it difficult to interpret the validity of an upfront *DPYD* analysis. The patients experiencing severe toxicity in our study had never been exposed to FL before, and only toxicities developed during the first three cycles of therapy have been considered. This allowed to avoid the bias related to previous treatment and cumulative toxicities.

We believe that our data, supported by the previously published papers, clearly demonstrate the clinical validity of testing *DPYD*-rs3918290, *DPYD*-rs67376798, and *DPYD*-rs55886062 to predict FL related severe toxicity.

Moreover, as a natural continuation of this study, the Experimental and Clinical Pharmacology Unit of CRO (Aviano) has set up a clinical PGx service accessible to Medical and Radiotherapy Oncology Units to assess also the clinical utility of the *DPYD* PGx tests.

Up to date, 239 cancer patients candidate to a therapy with FL were referred to this service prior to treatment. Accordingly to genotype data for *DPYD*-rs3918290, *DPYD*-rs55886062, *DPYD*-rs67376798 a starting dose adjustment was suggested for 5 patients.

This kind of studies moved in the right direction in order to finally come to an end on the *DPYD* testing clinical utility.

In addition, in January 2016, the results of a prospective multicenter study conducted in Netherlands was published in which 2038 patients were screened for *DPYD*-rs3918290 prior to start with FL treatment<sup>121</sup>.

That study aimed to determine the feasibility, safety and costs of *DPYD*-rs3918290 genotype-guided dosing. For this reason, variant allele carriers received an initial dose reduction of ≥ 50% followed by dose titration based on tolerance. The data obtained about toxicities and costs were

compared with historical controls (i.e. *DPYD*-rs3918290 variant alleles carriers receiving standard dose described in literature).

Toxicity results showed that the risk of Grade  $\geq 3$  toxicity was significantly reduced to 28% compared to 73% in historical controls ( $p < 0.001$ ) and the FL-induced death was reduced from 10% to 0%.

Beyond these convincing results about the safety of the pre-treatment genotyping test, this study also shown the feasibility of this approach in the clinical practice. Indeed, establishing the genotyping costs at €75 per test, the average total treatment cost per patient was slightly lower for screening (€2772) than for non-screening (€2817), outweighing screening costs.

Probably, the results of these study could be ameliorated if they will consider also other critical *DPYD* SNPs such as *DPYD*-rs67376798, and *DPYD*-rs55886062 and if we bear in mind that genotyping technology is developing fast and prices continue to decline.

In conclusion, our results highlighted the high clinical validity and specificity of genotyping the three polymorphisms *DPYD*-rs3918290, *DPYD*-rs67376798 and *DPYD*-rs55886062 in predicting the occurrence of severe toxicity to FL in the everyday clinical practice.

Therefore, in our institute the *DPYD* screening has already became a routinely test for all the cancer patients candidate to a FL-based therapy.

Considering that, worldwide, hundreds of thousands of patients receive FL-based chemotherapy each year, genotype based dose adaptation could seriously prevent thousands of patients from developing FL-induced severe and potentially lethal toxicity.

## 6.2. SUNITINIB PROJECT

Currently, there are 45 FDA-approved targeted cancer therapies, 26 of which are kinase inhibitors and 19 monoclonal antibodies.

The huge interest of pharmaceutical and biotechnology companies for these drugs was highlighted also by the data about the US sales of chemotherapies and target therapies. In 2009, US sales of targeted anticancer therapies reached \$10.4 billion and the small molecules drugs, such as the tyrosine kinase inhibitors, constituted the 23% of the total US sales of targeted therapies<sup>122</sup>.

Although this new class of drugs dramatically changed the chemotherapy strategies and, in some cases, strongly improved the outcome of the patients, it has become apparent that the targeted cancer therapy action is not without adverse effects or complications. There is a misconception that target therapies create fewer classic toxicities, such as diarrhoea, nausea, vomiting, alopecia

or neutropenia, and that the toxicities experienced with target therapies are less severe than conventional chemotherapy agents. Instead, patients could developed off-target toxicities related to cross-reactivity between the target in cancer and in healthy cells<sup>26</sup>.

Some recent meta-analyses confirmed, indeed, that the addition of kinase inhibitors to chemotherapy significantly increases the risk of fatal adverse events, treatment discontinuations and non-hematological toxicities.<sup>123,124</sup>

It is increasingly appreciated that the variability observed in response to newer targeted drugs is influenced not only by the genetic heterogeneity of drug targets (determining tumor sensitivity), but also by the PGx background of the patient (e.g. cytochrome P450 and ABC drug transporter polymorphisms), the patient adherence to treatment, and environmental factors that influence the PK<sup>125</sup>.

Standard dosage regimens rarely result in comparable circulating concentrations of the active drug in all patients, possibly favoring the selection of resistant cellular clones (in case of sub-therapeutic drug exposure) or the development of undesirable toxicities (in case of overexposure)<sup>10</sup>. In this respect, the vast majority of targeted drugs are characterized by a wide spread of plasma concentrations observed following standard dosage regimens, with inter-individual variability at the end of the dosage interval (trough concentrations) of up to 23-fold<sup>126</sup>.

Sunitinib is an oral multi-targeted tyrosine kinase inhibitor with antiangiogenic and antitumor activities attributable to the inhibition of several related tyrosine kinase receptors, including vascular endothelial growth factor receptors (VEGFRs) types 1 and 2 (FLT1 and FLK1/KDR), platelet-derived growth factor receptors (PDGFR- $\alpha$  and PDGFR- $\beta$ ), stem cell factor receptor (c-KIT), and FMS-related tyrosine kinase 3 (FLT-3), which are implicated in tumor proliferation, angiogenesis, and metastasis<sup>7,127</sup>.

Sunitinib has a pKa-value of 8.95 and is metabolized by the P450 enzyme CYP3A4 to N-desethyl sunitinib, which is equipotent to the parent compound and has an exposure that is between 23% and 37% of the total one. Protein binding of sunitinib and N-desethyl sunitinib are 95% and 90%, respectively. AUC and  $C_{max}$  increase proportionally with the dose increment within a range of 25–100 mg and are not affected by food.

This positive dose-efficacy relationship for sunitinib treatment indicates that it should be the aim to treat patients with the higher possible dose. Target total plasma concentrations of sunitinib plus active metabolite (N-desethyl sunitinib) are in the range of 50-100 ng/mL, as deduced from PK/PD preclinical data<sup>128</sup>. Total trough concentrations below 50 ng/mL have been associated with

decreased therapeutic efficacy, whereas concentrations above 100 ng/mL have been associated with an increased risk for toxicity. Taking into account the low therapeutic index, the large interindividual variability in the systemic exposure, and the positive exposure-efficacy relationship of sunitinib, there is a strong rationale for TDM of this drug.

In the literature, previously published LC-MS/MS methods were developed for the detection of sunitinib alone or with its active metabolite. The main characteristics of these methods are reported in Table 32.

Year	Authors	Sunitinib and metabolites analyzed	Other analytes analyzed	Sample Volume (mL)	Extraction Method	LLOQ (ng/mL)	Linearity Range (ng/mL)	Runtime
2008	Minkin et al	Sunitinib		0.2	LLE	0.2	0.2-500	3 min
2009	Haouala et al	Sunitinib	Imatinib, nilotinib, dasatinib, sorafenib, lapatinib	0.1	PP	1	1-500	20 min
2010	De Bruijin et al	Sunitinib, N-desethyl sunitinib		0.1	LLE	0.2	0.2-50	4 min
2010	Zhou et al	Sunitinib		0.01	PP	1.37	1.37-1000	3.2 min
2010	Honeywell et al	Sunitinib	Erlotinib, sorafenib, gefitinib	0.02	PP	5	1-4000	<4 min
2011	Rodamer et al	Sunitinib, N-desethyl sunitinib		0.1	PP	0.06	0.06-100	4 min
2012	Lankheet et al	Sunitinib	Dasatinib, erlotinib gefitinib, imatinib, lapatinib, nilotinib, sorafenib	0.05	PP	5	5-2500	10 min
2012	Rais et al	Sunitinib, N-desethyl sunitinib		0.05	LLE	0.1 sunitinib, 0.2 N-desethyl sunitinib	0.1-100 sunitinib, 0.2-200 N-desethyl sunitinib	5 min
2012	Qiu et al	Sunitinib, N-desethyl sunitinib, N,N didesethyl		0.05	PP	0.1	0.1-100	4 min
2012	Gotze et al	Sunitinib	Erlotinib, imatinib, lapatinib, nilotinib, sorafenib	0.1	PP	10	10-1000	12 min
2013	Andriamanana et al	Sunitinib	Bortezomib dasatinib erlotinib imatinib lapatinib nilotinib sorafenib vandetanib	0.05	PP	2	2-250	10
2013	Lankheet et al	Sunitinib, N-desethyl sunitinib		0.5	PP	2.5	2.5-500	10 min
2014	Musijowski et al	Sunitinib , N-desethyl sunitinib		0.5	LLE	0.1	0.1-150	6 min

**Table 32** Principal characteristics of the published method for the quantification of sunitinib and its main metabolites.

Only six published methods considered the quantification of both sunitinib and N-desethyl sunitinib and, except for the method developed by Qiu et al<sup>129</sup>, they used a deuterated internal standard.

One of the pivotal characteristics of a good method to be applicable to the clinical routine is the use of limited quantity of biological samples. The published methods considered a quantity of plasma that ranges from 50 µL<sup>129,130</sup> to 500 µL<sup>131</sup>. Our method requires only 30 µL of plasma, strongly simplifying the collection of the samples and the compliance of the patients to the TDM procedure.

Another crucial point to consider in the set-up of a TDM method is surely the ease and the rapidity of the processing procedure. Three published methods use protein precipitation (PP), whereas the other three require a more complex liquid-liquid extraction (LLE). Our processing method consists of an easy protein precipitation (PP) with 150 µL of methanol.

The additional heating step of 5 min in the heated bath little extends the processing time, however strongly facilitates the handling of the samples avoiding the necessity of sodium or UV-light<sup>132</sup> and the setting of suitable dark rooms.

In fact, the major part of the methods aims to avoid the light exposure in any step, from the collection to the analysis of the sample. This is a clear limit in the perspective of the applicability of the method to the clinical practice.

Some authors<sup>133</sup> found a quite elegant way to bypass the light protection: as the two isomers showed equal mass spectrometry response, to process the data, the sum of single reaction monitoring responses of both separated isomers of each analyte was used. Consequently, protection from light during shipment, handling and processing of samples was not necessary.

However, in order to apply this method, quantifiable peak of both the isomers are necessary in any analytical run. This consideration could explain the quite LLOQ (2.5 ng/mL).

In our method, the LLOQ is 25 fold lower for both the analytes and the calibration range was 0.1-500 ng/mL for sunitinib and 0.1-250 ng/mL for N-desethyl sunitinib.

Considering that the trough plasma concentration during the sunitinib therapy is typically in a range from 10 to 200 ng/mL for sunitinib and from 5 to 100 ng/mL for N-desethyl sunitinib, our method generously covered the clinical range and could be feasible also for PK studies in which really low concentrations should be detected in order to very accurately determine parameters as half-life.

Finally, regarding the chromatographic conditions of our method, the retention time of the analytes results 2.61 and 2.55 min for sunitinib and N-desethyl sunitinib, respectively and the total analytical run, including the recondition time, lasts only 7 min.

In conclusion, our method described an innovative approach to overtake the troublesome step of the light protection and a rapid and easy preparation process consistent with our aim of introducing the TDM of sunitinib in the clinical laboratory routine.

### **6.3. IRINOTECAN PROJECT**

FOLFIRI is a frequently used chemotherapy regimen for the first-line treatment of mCRC. Results of the phase III CRYSTAL trial showed that the addition in this setting of the EGFR antibody cetuximab improves the clinical outcome in patients whose tumors did not have mutations at *K-RAS* codons 12 and 13. This clinical trial, that compared FOLFIRI alone with FOLFIRI plus cetuximab, showed, indeed, improved progression-free survival and, in patients without *K-RAS* mutations, a particularly significant increase in response- (59.3%) and metastasis resection (7.0% vs 3.7%) rate<sup>117</sup>. Some other striking results were observed by Heinemann and colleagues<sup>134</sup>, in an open-label, randomized phase III clinical trial with the first aim of comparing the efficacy of cetuximab or bevacizumab in FOLFIRI first-line treatment of mCRC. Although the interpretation of the results is quite controversial<sup>135</sup>, it seemed that a statistically significant overall survival advantage was reported in favor of cetuximab (median duration 28.7 months [95% CI 24.0–36.6] vs 25.0 months [22.7–27.6]; HR 0.77 [95% CI 0.62–0.96]; p=0.017) and this was further increased in the subgroup of patients with tumors that were wild-type at all *RAS loci* (exon 2–4 *K-RAS* and *N-RAS*; 33.1 months vs 25.6 months; HR 0.70 [95% CI 0.53–0.92]; p=0.011).

Currently, the dose of CPT-11 in FOLFIRI schedule is 180 mg/m<sup>2</sup>. However, our group demonstrated that a higher dose of CPT-11 is tolerated in *UGT1A1 \*1/\*1* and *UGT1A1 \*1/\*28* patients than *UGT1A1 \*28/\*28* also if the regimen is combined with bevacizumab (Eudract 2009-012227-28; Protocol code CRO-2009-25, NCT01183494).

However, at our knowledge, no data have been generated to demonstrate if these higher doses are tolerated when cetuximab is added.

Having regards to the intriguing results obtained from the previous genotype-guided phase Ib studies and the information in the literature that assessed the regimen FOLFIRI plus cetuximab as

a promising treatment, there was a strong rationale to begin the phase Ib study entitled: “*A genotype-guided phase I study of irinotecan administered in combination with 5-fluorouracil/leucovorin (FOLFIRI) and cetuximab as first-line therapy in metastatic colorectal cancer patients*” in order to assess whether the addition of cetuximab has an impact on CPT-11 PK and, in turn, in its dosage, as already demonstrated for bevacizumab.

At the moment, due to the relative high frequencies of RAS mutations in CRC patients and to the additional step of the *UGT1A1\*28* screening, just one patient resulted eligible and was enrolled in this new clinical study.

A proper statistical analysis of the PK data obtained during this clinical study will be done when the patient’s enrollment will be concluded and the total plasma concentrations of CPT-11 and its three metabolites will be obtained. In fact, only at the end of the clinical study, the evaluation of the effect of cetuximab on the CPT-11 PK could have a statistical significance.

Anyway, it can be interesting to compare the PK parameters obtained for the first patient enrolled with the mean values of those obtained from the patients treated at the same CPT-11 dosage (260 mg/m<sup>2</sup>) during the previous phase I clinical trial of CPT-11 in combination with bevacizumab. In order that the comparison is homogeneous, only patients with the same *UGT1A1\*28* genotype (*UGT1A1\*1/\*1*) will be considered in the calculation of the mean values. As this clinical study is a phase Ib, that is a dose escalation study, for this preliminary analysis only C<sub>max</sub> and AUC<sub>last</sub> have been taken in consideration. CPT-11 C<sub>max</sub> (2599.96 and 1933.13 ng/mL for the I and the II administration, respectively) and AUC<sub>last</sub> (16968.01 and 14420.32 hr\*ng/mL for the I and the II administration, respectively) obtained were in good agreement with the mean C<sub>max</sub> and AUC<sub>last</sub> obtained in the previous study during both the I and the II administrations (C<sub>max</sub>: 2354.46±958.98 and 1967.14±479.73 ng/mL for the I and the II administration, respectively; AUC<sub>last</sub>: 15587.97±6996.21 and 13706.79±3824.02 hr\*ng/mL for the I and the II administration, respectively). On the contrary, SN-38 C<sub>max</sub> (8.20 and 10.93 ng/mL for the I and the II administration, respectively) and AUC<sub>last</sub> (164.16 and 198.31 hr\*ng/mL for the I and the II administration, respectively) were overall lower than the mean values previously obtained during both the I and II administrations (C<sub>max</sub>: 22.51±14.15 and 15.90±4.92 ng/mL for the I and the II administration, respectively; AUC<sub>last</sub>: 252.01±63.67 and 221.06±60.40 hr\*ng/mL for the I and the II administration, respectively). The same observation could be done for SN-38G. In fact, SN-38G C<sub>max</sub> (33.97 and 22.18 ng/mL for the I and the II administration, respectively) and AUC<sub>last</sub> (767.06 and 521.74 hr\*ng/mL for the I and the II administration, respectively) resulted lower than the

mean values previously obtained during both the I and the II administrations ( $C_{max}$ :  $94.56 \pm 40.78$  and  $82.95 \pm 35.72$  ng/mL for the I and the II administration, respectively;  $AUC_{last}$ :  $1326.29 \pm 499.24$  and  $1182.49 \pm 423.10$  hr\*ng/mL for the I and the II administration, respectively). Finally, also APC showed different results respect to the previous data. In fact, APC  $C_{max}$  (507.14 and 304.92 ng/mL for the I and the II administration, respectively) and  $AUC_{last}$  (6576.38 and 3644.86 hr\*ng/mL for the I and the II administration, respectively) resulted higher than the mean values observed during the phase I of CPT-11 in combination with bevacizumab ( $C_{max}$ :  $244.44 \pm 191.57$  and  $143.34 \pm 49.78$  ng/mL for the I and the II administration, respectively;  $AUC_{last}$ :  $2981.55 \pm 1859.81$  and  $1993.59 \pm 954.82$  hr\*ng/mL for the I and the II administration, respectively).

The formation of the two metabolites (SN-38 and APC), follows two different pathways (Figure 8). Therefore, the decrease of SN-38 and SN-38G concentrations and the parallel increase of APC plasma level, in comparison with the data concerning the previous clinical study, could probably be explained by a different activity of the enzymes involved in the metabolism.

## 7. REFERENCES

1. DeVita, V. T. & Chu, E. A history of cancer chemotherapy. *Cancer Res.* **68**, 8643–8653 (2008).
2. Heidelberger, C. *et al.* Fluorinated pyrimidines, a new class of tumour-inhibitory compounds. *Nature* **179**, 663–666 (1957).
3. Miller, D. R. A tribute to Sidney Farber - the father of modern chemotherapy. *Br. J. Haematol.* **134**, 20–26 (2006).
4. Nussbaumer, S., Bonnabry, P., Veuthey, J.-L. & Fleury-Souverain, S. Analysis of anticancer drugs: A review. *Talanta* **85**, 2265–2289 (2011).
5. *Goodman & Gilman's the pharmacological basis of therapeutics: [DVD incl.]*. (McGraw-Hill Medical, 2011).
6. Neidle, S. & Thurston, D. E. Chemical approaches to the discovery and development of cancer therapies. *Nat. Rev. Cancer* **5**, 285–296 (2005).
7. Sawyers, C. Targeted cancer therapy. *Nature* **432**, 294–297 (2004).
8. Widmer, N. *et al.* Review of therapeutic drug monitoring of anticancer drugs part two – Targeted therapies. *Eur. J. Cancer* **50**, 2020–2036 (2014).
9. Cortes, J. E., Egorin, M. J., Guilhot, F., Molimard, M. & Mahon, F. X. Pharmacokinetic/pharmacodynamic correlation and blood-level testing in imatinib therapy for chronic myeloid leukemia. *Leukemia* **23**, 1537–1544 (2009).
10. von Mehren, M. & Widmer, N. Correlations between imatinib pharmacokinetics, pharmacodynamics, adherence, and clinical response in advanced metastatic gastrointestinal stromal tumor (GIST): An emerging role for drug blood level testing? *Cancer Treat. Rev.* **37**, 291–299 (2011).
11. Hughes, T. *et al.* Monitoring CML patients responding to treatment with tyrosine kinase inhibitors: review and recommendations for harmonizing current methodology for detecting BCR-ABL transcripts and kinase domain mutations and for expressing results. *Blood* **108**, 28–37 (2006).
12. Pinkel, D. The use of body surface area as a criterion of drug dosage in cancer chemotherapy. *Cancer Res.* **18**, 853–856 (1958).

13. Pinkel, D. Cancer chemotherapy and body surface area. *J. Clin. Oncol. Off. J. Am. Soc. Clin. Oncol.* **16**, 3714–3715 (1998).
14. Freireich, E. J., Gehan, E. A., Rall, D. P., Schmidt, L. H. & Skipper, H. E. Quantitative comparison of toxicity of anticancer agents in mouse, rat, hamster, dog, monkey, and man. *Cancer Chemother. Rep.* **50**, 219–244 (1966).
15. Du Bois, D. & Du Bois, E. F. A formula to estimate the approximate surface area if height and weight be known. 1916. *Nutr. Burbank Los Angel. Cty. Calif* **5**, 303–311; discussion 312–313 (1989).
16. Gurney, H. Dose calculation of anticancer drugs: a review of the current practice and introduction of an alternative. *J. Clin. Oncol.* **14**, 2590–2611 (1996).
17. Veal, G. J., Coulthard, S. A. & Boddy, A. V. Chemotherapy individualization. *Invest. New Drugs* **21**, 149–156 (2003).
18. Kaestner, S. A. & Sewell, G. J. Chemotherapy Dosing Part I: Scientific Basis for Current Practice and Use of Body Surface Area. *Clin. Oncol.* **19**, 23–37 (2007).
19. Gurney, H. How to calculate the dose of chemotherapy. *Br. J. Cancer* **86**, 1297–1302 (2002).
20. FDA. Paving the Way for Personalized Medicine. (2013).
21. Kalia, M. Biomarkers for personalized oncology: recent advances and future challenges. *Metabolism* **64**, S16–S21 (2015).
22. Kalia, M. Personalized oncology: Recent advances and future challenges. *Metabolism* **62**, S11–S14 (2013).
23. American Cancer Society. Cancer Facts & Figures 2016. (2016). at <http://www.cancer.org/research/cancerfactsstatistics/cancerfactsfigures2016/>
24. Spear, B. B., Heath-Chiozzi, M. & Huff, J. Clinical application of pharmacogenetics. *Trends Mol. Med.* **7**, 201–204 (2001).
25. Gravitz, L. Therapy: This time it's personal. *Nature* **509**, S52–S54 (2014).
26. Gharwan, H. & Groninger, H. Kinase inhibitors and monoclonal antibodies in oncology: clinical implications. *Nat. Rev. Clin. Oncol.* (2015). doi:10.1038/nrclinonc.2015.213
27. Chakravarti, A. To a future of genetic medicine. *Nature* **409**, 822–823 (2001).

28. Duffy, M. J., O'Donovan, N. & Crown, J. Use of molecular markers for predicting therapy response in cancer patients. *Cancer Treat. Rev.* **37**, 151–159 (2011).
29. Patel, J. N. Application of genotype-guided cancer therapy in solid tumors. *Pharmacogenomics* **15**, 79–93 (2014).
30. Shankaran, V., Wisinski, K. B., Mulcahy, M. F. & Benson III, A. B. The role of molecular markers in predicting response to therapy in patients with colorectal cancer. *Mol. Diagn. Ther.* **12**, 87–98 (2008).
31. Huang, R. S. & Ratain, M. J. Pharmacogenetics and pharmacogenomics of anticancer agents. *CA. Cancer J. Clin.* **59**, 42–55 (2009).
32. Sawyers, C. L. The cancer biomarker problem. *Nature* **452**, 548–552 (2008).
33. Longley, D. B., Harkin, D. P. & Johnston, P. G. 5-Fluorouracil: mechanisms of action and clinical strategies. *Nat. Rev. Cancer* **3**, 330–338 (2003).
34. Wohlhueter, R. M., McIvor, R. S. & Plagemann, P. G. Facilitated transport of uracil and 5-fluorouracil, and permeation of orotic acid into cultured mammalian cells. *J. Cell. Physiol.* **104**, 309–319 (1980).
35. Diasio, R. B. & Harris, B. E. Clinical pharmacology of 5-fluorouracil. *Clin. Pharmacokinet.* **16**, 215–237 (1989).
36. Rosmarin, D. *et al.* A candidate gene study of capecitabine-related toxicity in colorectal cancer identifies new toxicity variants at *DYPD* and a putative role for *ENOSF1* rather than *TYMS*. *Gut* **64**, 111–120 (2015).
37. Amstutz, U., Froehlich, T. K. & Largiadèr, C. R. Dihydropyrimidine dehydrogenase gene as a major predictor of severe 5-fluorouracil toxicity. *Pharmacogenomics* **12**, 1321–1336 (2011).
38. Vreken, P. *et al.* A point mutation in an invariant splice donor site leads to exon skipping in two unrelated Dutch patients with dihydropyrimidine dehydrogenase deficiency. *J. Inherit. Metab. Dis.* **19**, 645–654 (1996).
39. McLeod, H. L. *et al.* Nomenclature for human *DYPD* alleles. *Pharmacogenetics* **8**, 455–459 (1998).
40. Henricks, L. M. *et al.* Translating *DYPD* genotype into DPD phenotype: using the *DYPD* gene activity score. *Pharmacogenomics* **16**, 1275–1284 (2015).

41. Offer, S. M. *et al.* Comparative Functional Analysis of DPYD Variants of Potential Clinical Relevance to Dihydropyrimidine Dehydrogenase Activity. *Cancer Res.* **74**, 2545–2554 (2014).
42. Deenen, M. J. *et al.* Relationship between Single Nucleotide Polymorphisms and Haplotypes in DPYD and Toxicity and Efficacy of Capecitabine in Advanced Colorectal Cancer. *Clin. Cancer Res.* **17**, 3455–3468 (2011).
43. Froehlich, T. K., Amstutz, U., Aebi, S., Joerger, M. & Largiadèr, C. R. Clinical importance of risk variants in the dihydropyrimidine dehydrogenase gene for the prediction of early-onset fluoropyrimidine toxicity: DPYD and fluoropyrimidine toxicity. *Int. J. Cancer* n/a–n/a (2014). doi:10.1002/ijc.29025
44. Johnson, M. R., Wang, K. & Diasio, R. B. Profound dihydropyrimidine dehydrogenase deficiency resulting from a novel compound heterozygote genotype. *Clin. Cancer Res. Off. J. Am. Assoc. Cancer Res.* **8**, 768–774 (2002).
45. Lee, A. M. *et al.* DPYD Variants as Predictors of 5-fluorouracil Toxicity in Adjuvant Colon Cancer Treatment (NCCTG N0147). *JNCI J. Natl. Cancer Inst.* **106**, dju298–dju298 (2014).
46. Loganayagam, A. *et al.* Pharmacogenetic variants in the DPYD, TYMS, CDA and MTHFR genes are clinically significant predictors of fluoropyrimidine toxicity. *Br. J. Cancer* **108**, 2505–2515 (2013).
47. van Kuilenburg, A. B. *et al.* Clinical implications of dihydropyrimidine dehydrogenase (DPD) deficiency in patients with severe 5-fluorouracil-associated toxicity: identification of new mutations in the DPD gene. *Clin. Cancer Res.* **6**, 4705–4712 (2000).
48. van Kuilenburg, A. B. P. *et al.* Novel disease-causing mutations in the dihydropyrimidine dehydrogenase gene interpreted by analysis of the three-dimensional protein structure. *Biochem. J.* **364**, 157–163 (2002).
49. Offer, S. M., Wegner, N. J., Fossum, C., Wang, K. & Diasio, R. B. Phenotypic profiling of DPYD variations relevant to 5-fluorouracil sensitivity using real-time cellular analysis and in vitro measurement of enzyme activity. *Cancer Res.* **73**, 1958–1968 (2013).
50. Morel, A. *et al.* Clinical relevance of different dihydropyrimidine dehydrogenase gene single nucleotide polymorphisms on 5-fluorouracil tolerance. *Mol. Cancer Ther.* **5**, 2895–2904 (2006).

51. Terrazzino, S. *et al.* DPYD IVS14+1G>A and 2846A>T genotyping for the prediction of severe fluoropyrimidine-related toxicity: a meta-analysis. *Pharmacogenomics* **14**, 1255–1272 (2013).
52. Collie-Duguid, E. S., Etienne, M. C., Milano, G. & McLeod, H. L. Known variant DPYD alleles do not explain DPD deficiency in cancer patients. *Pharmacogenetics* **10**, 217–223 (2000).
53. Ezzeldin, H. H., Lee, A. M., Mattison, L. K. & Diasio, R. B. Methylation of the DPYD promoter: an alternative mechanism for dihydropyrimidine dehydrogenase deficiency in cancer patients. *Clin. Cancer Res. Off. J. Am. Assoc. Cancer Res.* **11**, 8699–8705 (2005).
54. Caudle, K. E. *et al.* Clinical Pharmacogenetics Implementation Consortium Guidelines for Dihydropyrimidine Dehydrogenase Genotype and Fluoropyrimidine Dosing. *Clin. Pharmacol. Ther.* **94**, 640–645 (2013).
55. Swen, J. J. *et al.* Pharmacogenetics: From Bench to Byte— An Update of Guidelines. *Clin. Pharmacol. Ther.* **89**, 662–673 (2011).
56. Meulendijks, D. *et al.* Clinical relevance of DPYD variants c. 1679T>G, c. 1236G>A/HapB3, and c. 1601G>A as predictors of severe fluoropyrimidine-associated toxicity: a systematic review and meta-analysis of individual patient data. *Lancet Oncol.* **16**, 1639–1650 (2015).
57. Conti, J. A. *et al.* Irinotecan is an active agent in untreated patients with metastatic colorectal cancer. *J. Clin. Oncol.* **14**, 709–715 (1996).
58. Saltz, L. B. *et al.* Irinotecan plus fluorouracil/leucovorin for metastatic colorectal cancer: a new survival standard. *The Oncologist* **6**, 81–91 (2001).
59. Newton, K. F., Newman, W. & Hill, J. Review of biomarkers in colorectal cancer. *Colorectal Dis. Off. J. Assoc. Coloproctology G. B. Irel.* **14**, 3–17 (2012).
60. Tukey, R. H., Strassburg, C. P. & Mackenzie, P. I. Pharmacogenomics of human UDP-glucuronosyltransferases and irinotecan toxicity. *Mol. Pharmacol.* **62**, 446–450 (2002).
61. Bosma, P. J. *et al.* The genetic basis of the reduced expression of bilirubin UDP-glucuronosyltransferase 1 in Gilbert's syndrome. *N. Engl. J. Med.* **333**, 1171–1175 (1995).

62. Hall, D., Ybazeta, G., Destro-Bisol, G., Petzl-Erler, M. L. & Di Rienzo, A. Variability at the uridine diphosphate glucuronosyltransferase 1A1 promoter in human populations and primates. *Pharmacogenetics* **9**, 591–599 (1999).
63. Etienne-Grimaldi, M.-C. *et al.* UGT1A1 genotype and irinotecan therapy: general review and implementation in routine practice. *Fundam. Clin. Pharmacol.* **29**, 219–237 (2015).
64. Toffoli, G. *et al.* Genotype-Driven Phase I Study of Irinotecan Administered in Combination With Fluorouracil/Leucovorin in Patients With Metastatic Colorectal Cancer. *J. Clin. Oncol.* **28**, 866–871 (2010).
65. Manish, S. A UGT1A1 genotype-guided dosing study of irinotecan in metastatic colorectal cancer (mCRC) patients (pts) treated with FOLFIRI plus bevacizumab (BEV). (2014). at <http://meetinglibrary.asco.org/print/1417186>
66. Alnaim, L. Therapeutic drug monitoring of cancer chemotherapy. *J. Oncol. Pharm. Pract.* **13**, 207–221 (2007).
67. Sanavio, B. & Krol, S. On the Slow Diffusion of Point-of-Care Systems in Therapeutic Drug Monitoring. *Front. Bioeng. Biotechnol.* **3**, (2015).
68. Bardin, C. *et al.* Therapeutic drug monitoring in cancer--are we missing a trick? *Eur. J. Cancer Oxf. Engl. 1990* **50**, 2005–2009 (2014).
69. Paci, A. *et al.* Review of therapeutic drug monitoring of anticancer drugs part 1 – Cytotoxics. *Eur. J. Cancer* **50**, 2010–2019 (2014).
70. Hon, Y. Y. & Evans, W. E. Making TDM work to optimize cancer chemotherapy: a multidisciplinary team approach. *Clin. Chem.* **44**, 388–400 (1998).
71. Prasad, N. *et al.* Importance of dose intensity in treatment of advanced non-small cell lung cancer in the elderly. *South Asian J. Cancer* **1**, 9–15 (2012).
72. Chatelut, E. *et al.* A limited sampling strategy for determining carboplatin AUC and monitoring drug dosage. *Eur. J. Cancer Oxf. Engl. 1990* **36**, 264–269 (2000).
73. Reynolds, D. J. & Aronson, J. K. ABC of monitoring drug therapy. Making the most of plasma drug concentration measurements. *BMJ* **306**, 48–51 (1993).

74. FDA. Guidance for Industry Bioanalytical Method Validation DRAFT GUIDANCE. (2013).
75. EMA. Guideline on bioanalytical method validation EMA. (2011).
76. Arora, A. Role of Tyrosine Kinase Inhibitors in Cancer Therapy. *J. Pharmacol. Exp. Ther.* **315**, 971–979 (2005).
77. Faivre, S. Safety, Pharmacokinetic, and Antitumor Activity of SU11248, a Novel Oral Multitarget Tyrosine Kinase Inhibitor, in Patients With Cancer. *J. Clin. Oncol.* **24**, 25–35 (2006).
78. Atkins, M. B. *et al.* Innovations and challenges in renal cancer: consensus statement from the first international conference. *Clin. Cancer Res. Off. J. Am. Assoc. Cancer Res.* **10**, 6277S–81S (2004).
79. Bergers, G., Song, S., Meyer-Morse, N., Bergsland, E. & Hanahan, D. Benefits of targeting both pericytes and endothelial cells in the tumor vasculature with kinase inhibitors. *J. Clin. Invest.* **111**, 1287–1295 (2003).
80. Sangwan, S., Panda, T., Thiamattam, R., Dewan, S. & Thaper, R. Novel Salts of Sunitinib an Anticancer Drug with Improved Solubility. *Int. Res. J. Pure Appl. Chem.* **5**, 352–365 (2015).
81. Atkins, M., Jones, C. A. & Kirkpatrick, P. Sunitinib maleate. *Nat. Rev. Drug Discov.* **5**, 279–280 (2006).
82. Pawson, T. Regulation and targets of receptor tyrosine kinases. *Eur. J. Cancer Oxf. Engl. 1990 Suppl 5*, S3–10 (2002).
83. Schoffski, P. Emerging role of tyrosine kinase inhibitors in the treatment of advanced renal cell cancer: a review. *Ann. Oncol.* **17**, 1185–1196 (2006).
84. Adams, V. R. & Leggas, M. Sunitinib malate for the treatment of metastatic renal cell carcinoma and gastrointestinal stromal tumors. *Clin. Ther.* **29**, 1338–1353 (2007).
85. Demetri, G. D. *et al.* Efficacy and safety of sunitinib in patients with advanced gastrointestinal stromal tumour after failure of imatinib: a randomised controlled trial. *Lancet Lond. Engl.* **368**, 1329–1338 (2006).
86. Saleem, M., Dimeski, G., Kirkpatrick, C. M., Taylor, P. J. & Martin, J. H. Target concentration intervention in oncology: where are we at? *Ther. Drug Monit.* **34**, 257–265 (2012).
87. Beumer, J. H. Without Therapeutic Drug Monitoring, There Is No Personalized Cancer Care. *Clin. Pharmacol. Ther.* **93**, 228–230 (2013).

88. Houk, B. E., Bello, C. L., Kang, D. & Amantea, M. A Population Pharmacokinetic Meta-analysis of Sunitinib Malate (SU11248) and Its Primary Metabolite (SU12662) in Healthy Volunteers and Oncology Patients. *Clin. Cancer Res.* **15**, 2497–2506 (2009).
89. Khosravan, R. A retrospective analysis of data from two trials of sunitinib in patients with advanced renal cell carcinoma (RCC): Pitfalls of efficacy subgroup analyses based on dose-reduction status. (2012). at <<http://meetinglibrary.asco.org/print/569354>>
90. Houk, B. E. *et al.* Relationship between exposure to sunitinib and efficacy and tolerability endpoints in patients with cancer: results of a pharmacokinetic/pharmacodynamic meta-analysis. *Cancer Chemother. Pharmacol.* **66**, 357–371 (2010).
91. Turro, N. J. Mechanisms of sensitized photochemical cis-trans-isomerization in solution. *Photochem. Photobiol.* **9**, 555–563 (1969).
92. Zhang, L., Borysenko, C. W., Albright, T. A., Bittner, E. R. & Lee, T. R. The cis-trans isomerization of 1,2,5,6-tetrasilacycloocta-3,7-dienes: analysis by mechanistic probes and density functional theory. *J. Org. Chem.* **66**, 5275–5283 (2001).
93. Sistla, A. & Shenoy, N. Reversible Z-E Isomerism and Pharmaceutical Implications for SU5416. *Drug Dev. Ind. Pharm.* **31**, 1001–1007 (2005).
94. Lu, C.-Y. *et al.* FOLFIRI and regorafenib combination therapy with dose escalation of irinotecan as fourth-line treatment for patients with metastatic colon cancer according to UGT1A1 genotyping. *OncoTargets Ther.* **7**, 2143–2146 (2014).
95. Cecchin, E. *et al.* Predictive role of the UGT1A1, UGT1A7, and UGT1A9 genetic variants and their haplotypes on the outcome of metastatic colorectal cancer patients treated with fluorouracil, leucovorin, and irinotecan. *J. Clin. Oncol. Off. J. Am. Soc. Clin. Oncol.* **27**, 2457–2465 (2009).
96. Peter J. Russell. *iGenetics: A Molecular Approach.* (2002).
97. Hopfgartner, G. & Bourgogne, E. Quantitative high-throughput analysis of drugs in biological matrices by mass spectrometry. *Mass Spectrom. Rev.* **22**, 195–214 (2003).
98. Geoffrey Taylor. Disintegration of Water Drops in an Electric Field. (1964).
99. Lord Rayleigh. On the equilibrium of liquid conducting masses charged with electricity. (1882).

100. Booth, B. *et al.* Workshop Report: Crystal City V—Quantitative Bioanalytical Method Validation and Implementation: The 2013 Revised FDA Guidance. *AAPS J.* **17**, 277–288 (2015).
101. Shah, V. P. *et al.* Analytical methods validation: bioavailability, bioequivalence and pharmacokinetic studies. Conference report. *Eur. J. Drug Metab. Pharmacokinet.* **16**, 249–255 (1991).
102. Canadian Minister of Health. GUIDANCE FOR INDUSTRY Conduct and Analysis of Bioavailability and Bioequivalence Studies - Part A: Oral Dosage Formulations Used for Systemic Effects. *J. Comput. Assist. Tomogr.* **15**, 621–628 (1991).
103. FDA. Bioanalytical method validation for studies on pharmacokinetics, bioavailability and bioequivalence: Highlights of the FDA's Guidance. **4**, 5–13 (2001).
104. Fast, D. M. *et al.* Workshop report and follow-up--AAPS Workshop on current topics in GLP bioanalysis: Assay reproducibility for incurred samples--implications of Crystal City recommendations. *AAPS J.* **11**, 238–241 (2009).
105. González, O. *et al.* Bioanalytical chromatographic method validation according to current regulations, with a special focus on the non-well defined parameters limit of quantification, robustness and matrix effect. *J. Chromatogr. A* **1353**, 10–27 (2014).
106. Mei, H. *et al.* Investigation of matrix effects in bioanalytical high-performance liquid chromatography/tandem mass spectrometric assays: application to drug discovery. *Rapid Commun. Mass Spectrom. RCM* **17**, 97–103 (2003).
107. Bonfiglio, null, King, null, Olah, null & Merkle, null. The effects of sample preparation methods on the variability of the electrospray ionization response for model drug compounds. *Rapid Commun. Mass Spectrom. RCM* **13**, 1175–1185 (1999).
108. Eisenhauer, E. A., O'Dwyer, P. J., Christian, M. & Humphrey, J. S. Phase I clinical trial design in cancer drug development. *J. Clin. Oncol.* **18**, 684–684 (2000).
109. Ivy, S. P., Siu, L. L., Garrett-Mayer, E. & Rubinstein, L. Approaches to Phase 1 Clinical Trial Design Focused on Safety, Efficiency, and Selected Patient Populations: A Report from the Clinical Trial Design Task Force of the National Cancer Institute Investigational Drug Steering Committee. *Clin. Cancer Res.* **16**, 1726–1736 (2010).

110. Marangon, E., Posocco, B., Mazzega, E. & Toffoli, G. Development and validation of a high-performance liquid chromatography-tandem mass spectrometry method for the simultaneous determination of irinotecan and its main metabolites in human plasma and its application in a clinical pharmacokinetic study. *PLoS One* **10**, e0118194 (2015).
111. AIOM & SIAPEC-IAP. AIOM and SIAPEC-IAP recommendation for the evaluation of RAS mutations in colon rectum cancer. (2015).
112. Wei, X., McLeod, H. L., McMurrough, J., Gonzalez, F. J. & Fernandez-Salguero, P. Molecular basis of the human dihydropyrimidine dehydrogenase deficiency and 5-fluorouracil toxicity. *J. Clin. Invest.* **98**, 610–615 (1996).
113. van Kuilenburg, A. B. P. *et al.* Dihydropyrimidinase deficiency and severe 5-fluorouracil toxicity. *Clin. Cancer Res. Off. J. Am. Assoc. Cancer Res.* **9**, 4363–4367 (2003).
114. Meulendijks, D. *et al.* Clinical relevance of DPYD variants c. 1679T>G, c. 1236G>A/HapB3, and c. 1601G>A as predictors of severe fluoropyrimidine-associated toxicity: a systematic review and meta-analysis of individual patient data. *Lancet Oncol.* **16**, 1639–1650 (2015).
115. Innocenti, F. DPYD variants to predict 5-FU toxicity: the ultimate proof. *J. Natl. Cancer Inst.* **106**, (2014).
116. Boisdrone-Celle Michele. Prevention of 5-FU-induced health-threatening toxicity by pretherapeutic DPD deficiency screening: Medical and economic assessment of a multiparametric approach. (2013). at <http://meetinglibrary.asco.org/print/1158501>
117. Van Cutsem, E. *et al.* Cetuximab and chemotherapy as initial treatment for metastatic colorectal cancer. *N. Engl. J. Med.* **360**, 1408–1417 (2009).
118. Johnson, M. R., Wang, K. & Diasio, R. B. Profound dihydropyrimidine dehydrogenase deficiency resulting from a novel compound heterozygote genotype. *Clin. Cancer Res. Off. J. Am. Assoc. Cancer Res.* **8**, 768–774 (2002).
119. de Gramont, A. *et al.* Leucovorin and fluorouracil with or without oxaliplatin as first-line treatment in advanced colorectal cancer. *J. Clin. Oncol. Off. J. Am. Soc. Clin. Oncol.* **18**, 2938–2947 (2000).

120. Falvella, F. *et al.* Undetected Toxicity Risk in Pharmacogenetic Testing for Dihydropyrimidine Dehydrogenase. *Int. J. Mol. Sci.* **16**, 8884–8895 (2015).
121. Deenen, M. J. *et al.* Upfront Genotyping of DPYD\*2A to Individualize Fluoropyrimidine Therapy: A Safety and Cost Analysis. *J. Clin. Oncol.* **34**, 227–234 (2016).
122. Aggarwal, S. Targeted cancer therapies. *Nat. Rev. Drug Discov.* **9**, 427–428 (2010).
123. Niraula, S. *et al.* The price we pay for progress: a meta-analysis of harms of newly approved anticancer drugs. *J. Clin. Oncol. Off. J. Am. Soc. Clin. Oncol.* **30**, 3012–3019 (2012).
124. Funakoshi, T., Latif, A. & Galsky, M. D. Safety and efficacy of addition of VEGFR and EGFR-family oral small-molecule tyrosine kinase inhibitors to cytotoxic chemotherapy in solid cancers: a systematic review and meta-analysis of randomized controlled trials. *Cancer Treat. Rev.* **40**, 636–647 (2014).
125. Klümpen, H.-J., Samer, C. F., Mathijssen, R. H. J., Schellens, J. H. M. & Gurney, H. Moving towards dose individualization of tyrosine kinase inhibitors. *Cancer Treat. Rev.* **37**, 251–260 (2011).
126. Gao, B. *et al.* Evidence for therapeutic drug monitoring of targeted anticancer therapies. *J. Clin. Oncol. Off. J. Am. Soc. Clin. Oncol.* **30**, 4017–4025 (2012).
127. Giamas, G. *et al.* Kinases as targets in the treatment of solid tumors. *Cell. Signal.* **22**, 984–1002 (2010).
128. Mendel, D. B. *et al.* In vivo antitumor activity of SU11248, a novel tyrosine kinase inhibitor targeting vascular endothelial growth factor and platelet-derived growth factor receptors: determination of a pharmacokinetic/pharmacodynamic relationship. *Clin. Cancer Res. Off. J. Am. Assoc. Cancer Res.* **9**, 327–337 (2003).
129. Qiu, F., Bian, W., Li, J. & Ge, Z. Simultaneous determination of sunitinib and its two metabolites in plasma of Chinese patients with metastatic renal cell carcinoma by liquid chromatography-tandem mass spectrometry: Determination of sunitinib and its metabolites in plasma by LC-MS/MS. *Biomed. Chromatogr.* **27**, 615–621 (2013).
130. Lankheet, N. A. G. *et al.* Method development and validation for the quantification of dasatinib, erlotinib, gefitinib, imatinib, lapatinib, nilotinib, sorafenib and sunitinib in human plasma by liquid chromatography coupled with tandem mass spectrometry: Simultaneous determination of eight tyrosine kinase inhibitors for TDM. *Biomed. Chromatogr.* **27**, 466–476 (2013).

131. Musijowski, J., Piórkowska, E. & Rudzki, P. J. Determination of sunitinib in human plasma using liquid chromatography coupled with mass spectrometry: Liquid Chromatography. *J. Sep. Sci.* **37**, 2652–2658 (2014).
132. de Bruijn, P. *et al.* Bioanalytical method for the quantification of sunitinib and its n-desethyl metabolite SU12662 in human plasma by ultra performance liquid chromatography/tandem triple-quadrupole mass spectrometry. *J. Pharm. Biomed. Anal.* **51**, 934–941 (2010).
133. Lankheet, N. A. G. *et al.* Quantification of Sunitinib and N-Desethyl Sunitinib in Human EDTA Plasma by Liquid Chromatography Coupled With Electrospray Ionization Tandem Mass Spectrometry: Validation and Application in Routine Therapeutic Drug Monitoring. *Ther. Drug Monit.* **35**, 168–176 (2013).
134. Heinemann, V. *et al.* FOLFIRI plus cetuximab versus FOLFIRI plus bevacizumab as first-line treatment for patients with metastatic colorectal cancer (FIRE-3): a randomised, open-label, phase 3 trial. *Lancet Oncol.* **15**, 1065–1075 (2014).
135. Pietrantonio, F., Iacovelli, R., Di Bartolomeo, M. & de Braud, F. FOLFIRI with cetuximab or bevacizumab: FIRE-3. *Lancet Oncol.* **15**, e581 (2014).

# APPENDIX 1.

## FORM 1

### PATIENT REGISTRATION FORM

To be forwarded via fax to: 0434 XXXXX  
or via e-mail to the following address: XXXXXX@cro.it

<b>Patient information</b>	<b>Clinical file No.:</b> _____
<b>Initials</b> <input type="text"/>	<b>Date of birth</b> <input type="text"/> <input type="text"/> <input type="text"/>
<b>Center</b>	
<b>Physician's name</b> _____	<b>Fax</b> <input type="text"/> <input type="text"/> <input type="text"/> <input type="text"/> <input type="text"/> <input type="text"/>
<b>Physician's signature:</b>	<b>Tel</b> <input type="text"/> <input type="text"/> <input type="text"/> <input type="text"/> <input type="text"/> <input type="text"/>

## FORM 2

<b>PRIMITIVE TUMOR FORM</b>	<b>Center</b> [      ]	<b>Patient code</b> <input type="text"/> <input type="text"/> <input type="text"/>
-----------------------------	---------------------------	---

<b>Disease sites upon recruitment</b>		
Diagnosed disease stage (TNM- Tumor Node Metastasis)		
<b>Primitive tumor surgery</b>	[ YES ]	[ NO ]
<b>Neo-adjuvant treatment</b>	[ YES ]	[ NO ]
<b>Adjuvant treatment</b>	[ YES ]	[ NO ]
<b>Metastatic (1°line)</b>	[ YES ]	[ NO ]
<b>Metastatic (2°line)</b>	[ YES ]	[ NO ]

**FORM 3**

<b>CHEMOTHERAPY (cicle 1)</b>	<b>Center</b> [ ]	<b>Patient code</b> <input type="checkbox"/> <input type="checkbox"/> <input type="checkbox"/>
<b>WEIGHT (Kg)</b>	_____	
<b>HEIGHT (cm)</b>	_____	
<b>BSA (m<sup>2</sup>)</b>	_____	
<b>PS (Karnowsky)</b>	_____	
<b>Date of start of therapy</b> _____ / _____ / _____		
<b>Drug</b>	<b>Administered dose (mg/ m<sup>2</sup>)</b>	<b>Total Dose (mg)</b>
_____	_____	_____
_____	_____	_____
_____	_____	_____
_____	_____	_____
_____	_____	_____
_____	_____	_____

## **FORM 4**

<b>CHEMOTHERAPY (TOXIC EVENT)</b>	Center [      ]	Patient code □□□
-----------------------------------	--------------------	---------------------

<b>Administration setting</b>	_____
<b>Regimen</b>	_____
<b>Radiotherapy</b>	[ YES ] [ NO ]
<b>Reason for interruption of the treatment</b>	[ 1 ] end of the scheduled cycles [ 2 ] progression of the disease [ 3 ] toxicity [ 4 ] death during treatment [ 5 ] rejection by the patient
<b>The developed toxicity causes:</b>	[ 1 ] therapy delay [ 2 ] dose reduction [ 3 ] treatment interruption [ 4 ] hospitalization [ 5 ] death
<b>Precedent fluoropyrimidine assumption</b>	[ YES ] [ NO ]
REGIMEN _____	
<b>If [ YES ] specify:</b>	

## FORM 5

<b>SEVERE TOXICITY</b> <i>(see protocol appendix II for NCIC-CTC criteria)</i>	Center [ ]	Patient code □□□
<i>Specify all the toxicities developed in the cycle concern the severe toxic event</i>		

<i>Administration n°:</i>	<i>date:</i>	<i>Grade</i>	<i>Days (n°)</i>	<i>To:</i>	<i>From:</i>
Anemia	Hgb Value _____				
	Trasfuse units _____				
Leukopenia	Value _____				
Neutropenia	Value _____				
	Fever _____				
	Temperature _____				
Infection without neutropenia	Description _____				
Piastrenopenia	Value _____				
Plates trasfusion					
Nausea	Description _____				
Vomiting	Episodes n° _____				
Diarrhea	Episodes n° _____				
Stomatitis	Description _____				
Stipsi	Description _____				
Anorexia	Description _____				
Epatic (transaminase level)	Value _____				
Epatic (bilirubin level)	Value _____				
Renal (creatine level)	Value _____				
Cardiac (rhythm alteration)	Description _____				
Cardiac (ischemia)	Description _____				
Alopecia	Description _____				
Skin (Hand-foot syndrome)	Description _____				
Skin (hot flushing)	Description _____				
Astenia	Description _____				
Hospitalization					
*Other(.....)	Description _____				

### OUTCOME OF THE TOXIC EVENT

- |                                |              |
|--------------------------------|--------------|
| 1. Complete resolution         | 4. Unchanged |
| 2. Resolution with Consequence | 5. Worsen    |
| 3. Persistent                  | 6. Fatal     |

## APPENDIX 2

EudraCT n. 2013-005618-37  
 CRO-2014-01  
 Protocol Version n. 1  
 17 September 2013

**A genotype-guided phase I study of irinotecan administered in combination with 5-fluorouracil/leucovorin (FOLFI) and cetuximab as first-line therapy in metastatic colorectal cancer patients**

### SAMPLING FOR THE PK OF CPT-11

Date of start of the therapy: \_\_\_\_\_

Protocol n°\_CRO-2014-01\_\_\_\_\_ Medical record n° \_\_\_\_\_ Paz.n° \_\_\_\_\_

First name and last name \_\_\_\_\_ Sigla \_\_\_\_\_

Date of birth\_\_\_\_\_ PS(Kamowsky) \_\_\_\_\_ BSA (m<sup>2</sup>) \_\_\_\_\_

Weight (kg) \_\_\_\_\_ Height (cm) \_\_\_\_\_

Center \_\_\_\_\_

#### Scheduled Therapy

CPT-11	LV	5-FU	CTX
1 mg/m <sup>2</sup> 2h i.v. (day 1 and day 15)	200 mg/m <sup>2</sup> 2h i.v. (day 1 and day 15)	400 mg /m <sup>2</sup> bolus (day 1 and day 15) 2.4 gr/m <sup>2</sup> 46h i.v. (day 1 and day 15)	500 mg /m <sup>2</sup>

Therapy cycle n° \_\_\_\_\_ Date and time of the therapy\_\_\_\_\_

CPT-11 dose (mg/m<sup>2</sup>) \_\_\_\_\_ Total CPT-11 dose (mg) \_\_\_\_\_

N°	Aliquote	Time	Scheduled time	Actual time	Administration	Note
<u>1</u>		<u>0'</u>			Before CPT-11 infusion (IV)	
<u>2</u>		<u>1.0 h</u>			1h after start of IV	
<u>3</u>		<u>2.0 h</u>			End of the IV	
<u>4</u>		<u>2.25 h</u>			15min after the end of IV	
<u>5</u>		<u>2.50 h</u>			30min after the end of IV	
<u>6</u>		<u>3.0 h</u>			1h after the end of IV	
<u>7</u>		<u>4.0 h</u>			2h after the end of IV	
<u>8</u>		<u>6.0 h</u>			4h after the end of IV	
<u>9</u>		<u>8.0 h</u>			6h after the end of IV	
<u>10</u>		<u>10.0 h</u>			8h after the end of IV	
<u>12</u>		<u>26.0 h</u>			24h after the end of IV	
<u>13</u>		<u>50.0 h</u>			48h after the end of IV	

